



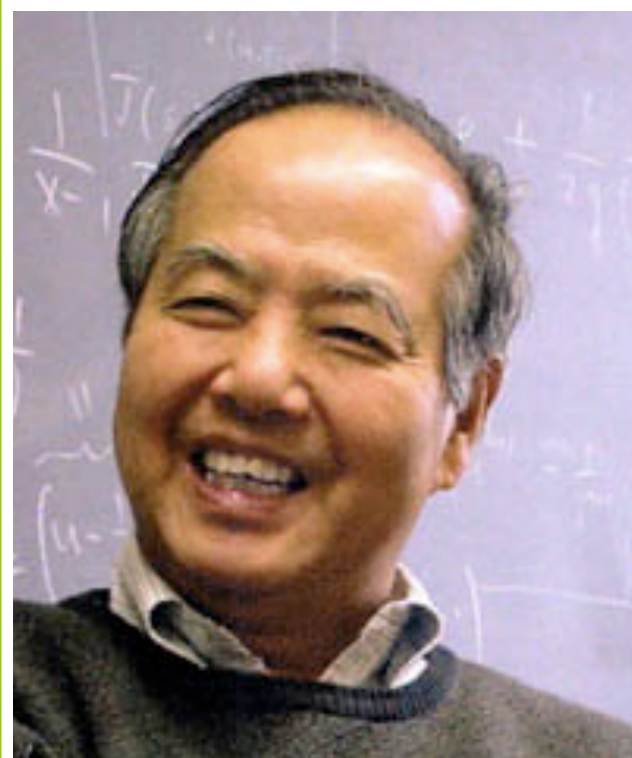
多粒子碰撞系统中集体流效应

马国亮



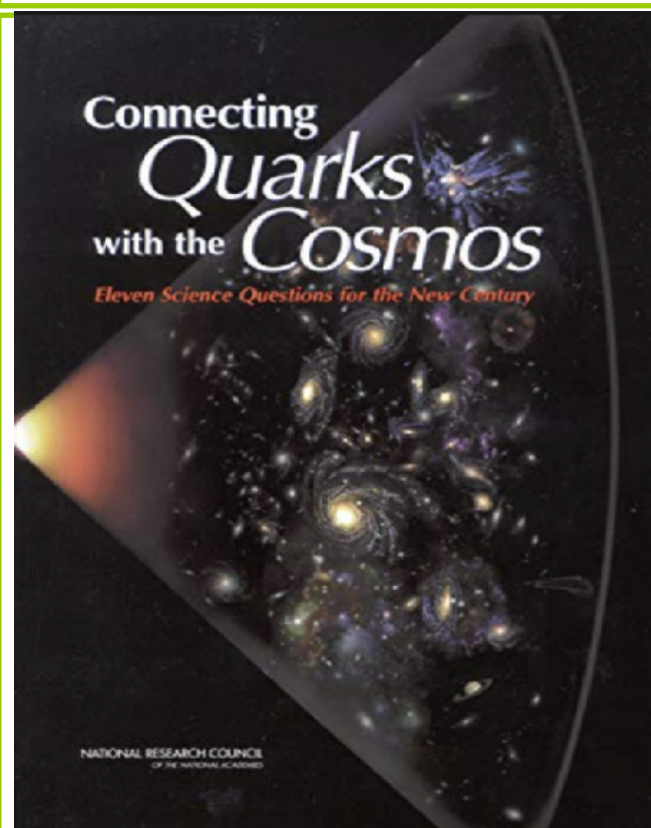
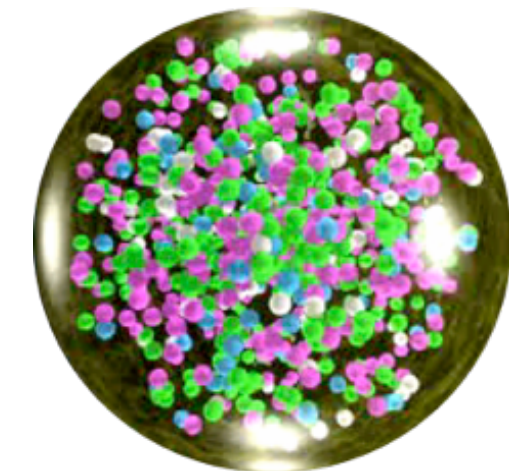
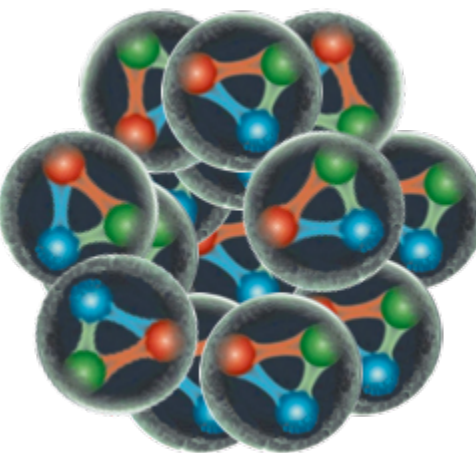
现代物理研究所
理论物理专款上海核物理研究中心

21世纪基础物理的最重要科学问题



1999年，李政道先生说21世纪物理学的“四朵乌云”

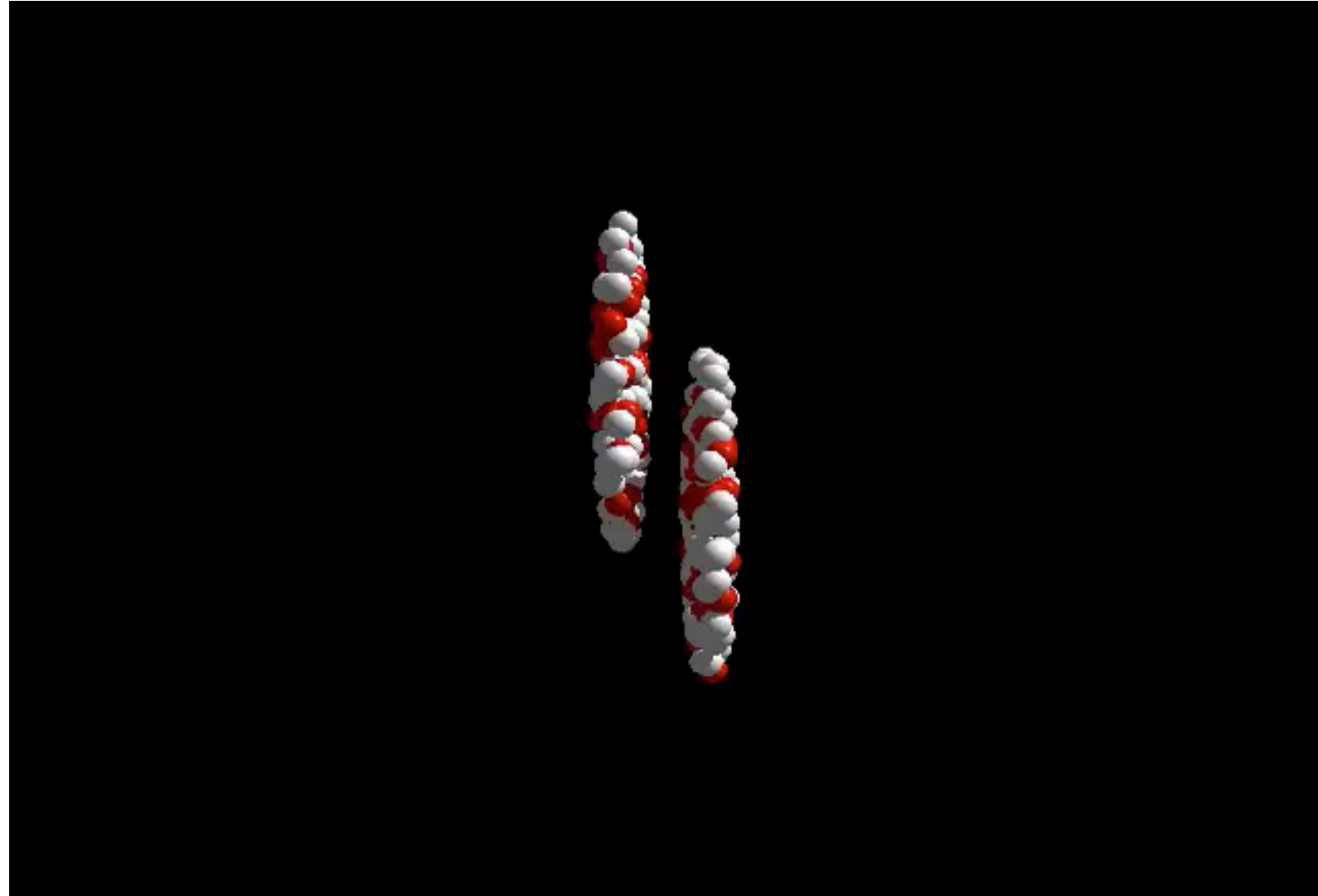
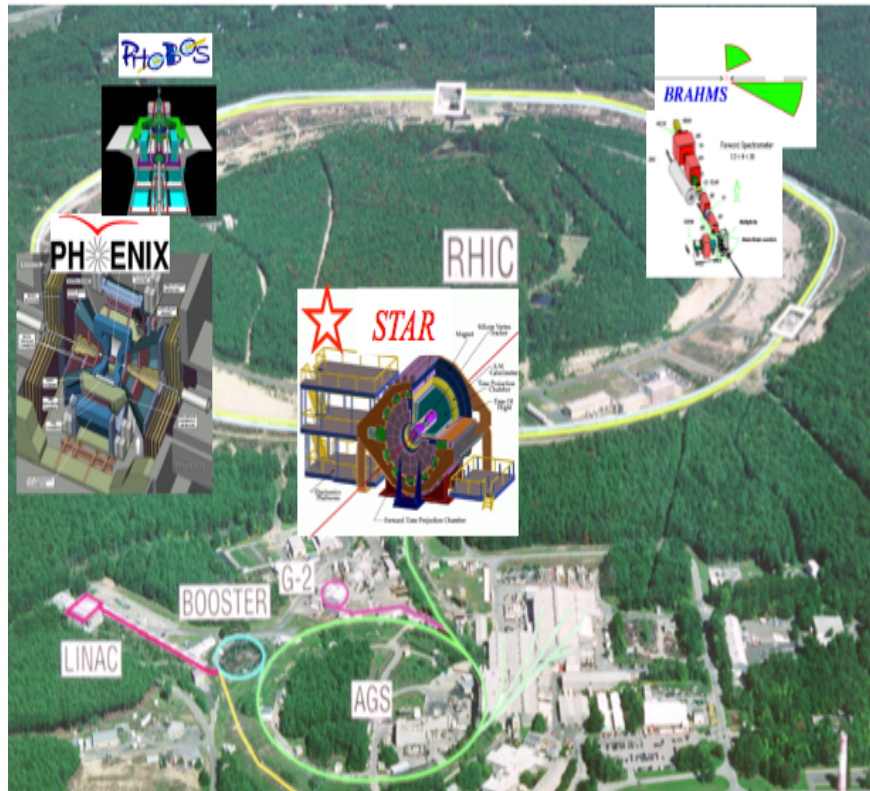
- 一是看不见的夸克
- 二是缺失的对称性
- 三是类星体的能源
- 四是暗物质暗能量



THE ELEVEN QUESTIONS IN 21st CENTURY

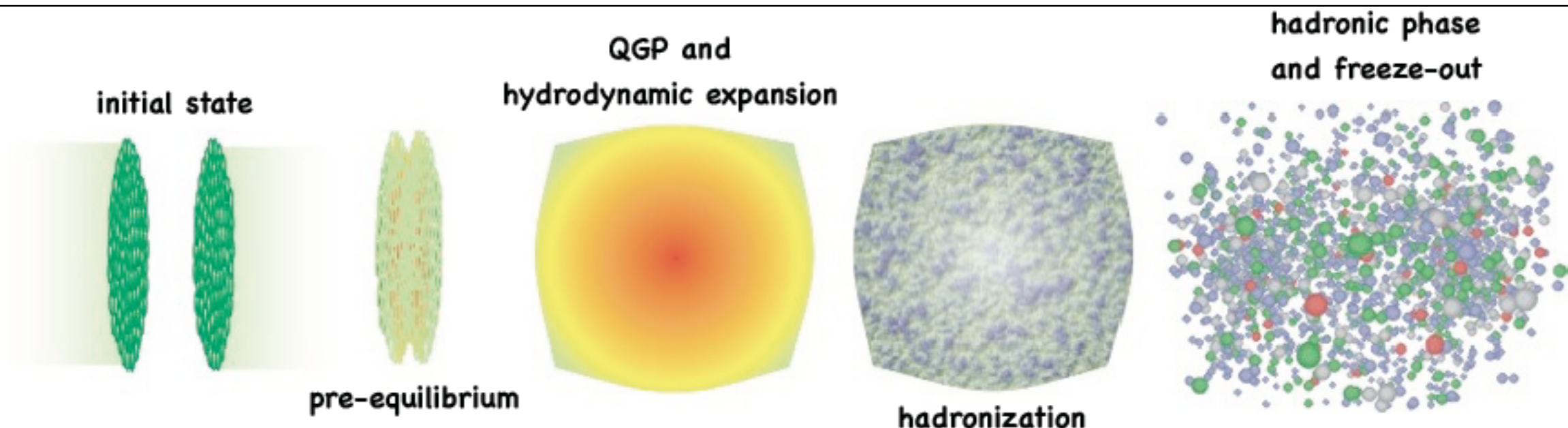
- What Is Dark Matter?
- What Is the Nature of the Dark Energy?
- How Did the Universe Begin?
- Did Einstein Have the Last Word on Gravity?
- What Are the Masses of the Neutrinos and How Have They Shaped the Evolution of the Universe?
- How Do Cosmic Accelerators Work and What Are They Accelerating?
- Are Protons Unstable?
- What Are the New States of Matter at Exceedingly High Density and Temperature?**
- Are There Additional Space-Time Dimensions?
- How Were the Elements from Iron to Uranium Made?
- Is a New Theory of Matter and Light Needed at the Highest Energies?

相对论重离子碰撞



- Little bangs @ RHIC and LHC.
Au+Au at $\sqrt{s_{NN}}=200 \text{ GeV}$
Pb+Pb at $\sqrt{s_{NN}}=5.02 \text{ TeV}$

相对论重离子碰撞图像



• Initial State:

- fluctuates event-by-event
- classical color-field dynamics

• QGP and hydrodynamic expansion:

- proceeds via 3D viscous RFD
- EoS from Lattice QCD

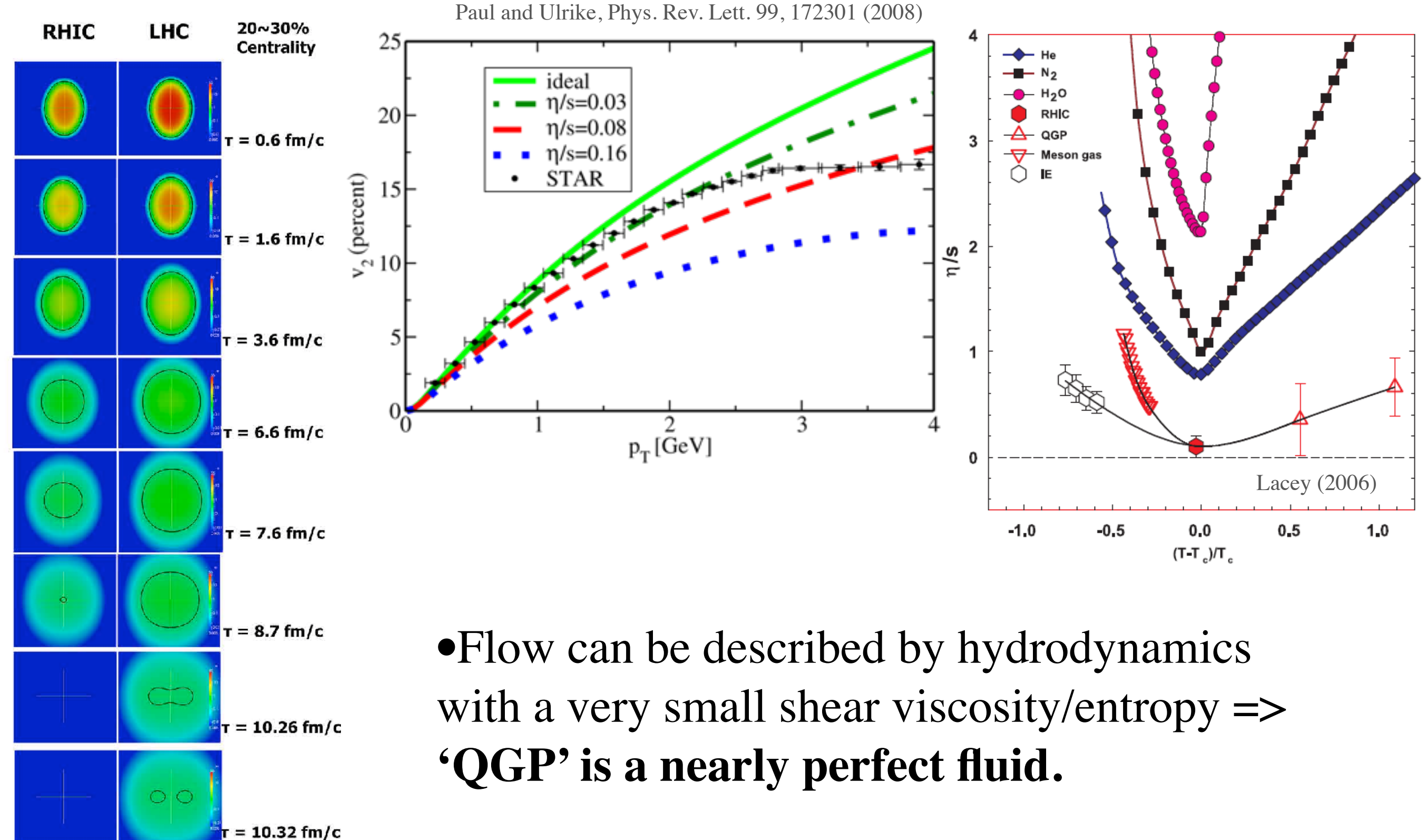
• Pre-equilibrium:

- rapid change-over from glue-field dominated initial state to thermalized QGP
- time scale: 0.15 to 2 fm/c in duration
- build-up of transverse velocity fields?

• hadronic phase & freeze-out

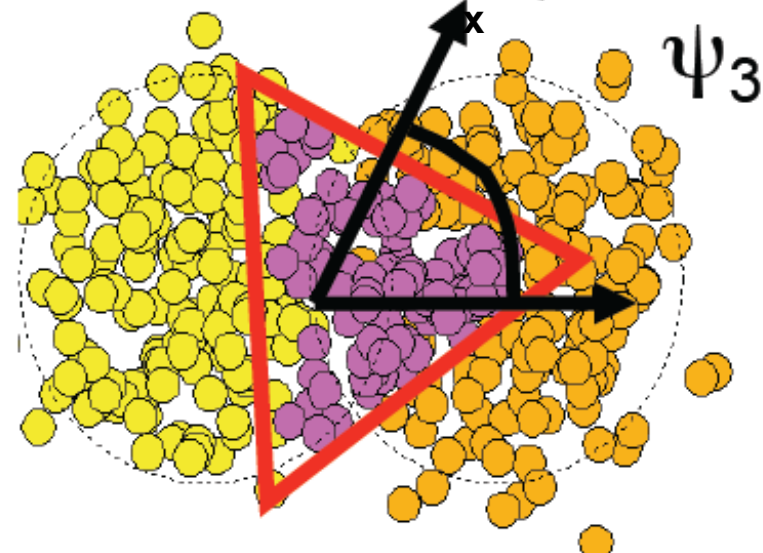
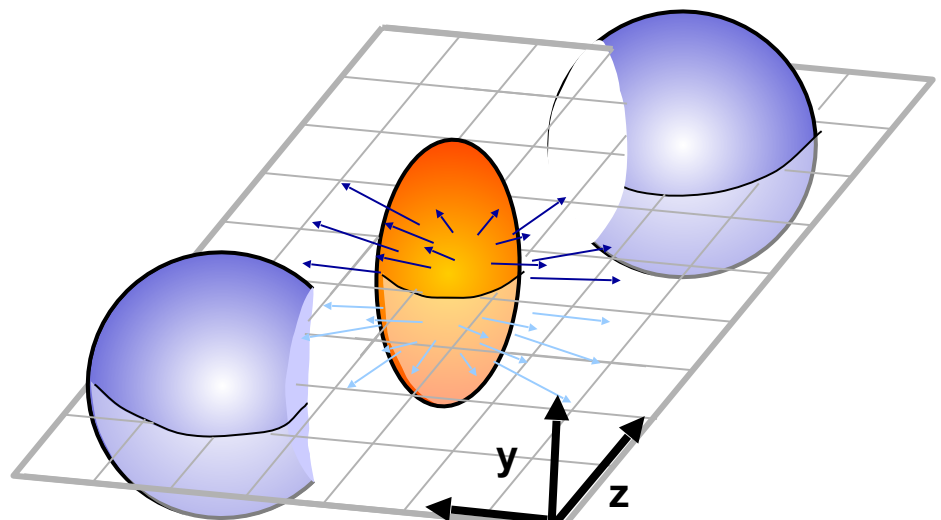
- interacting hadron gas
- separation of chemical and kinetic freeze-out

Perfect fluid with smallest viscosity/entropy



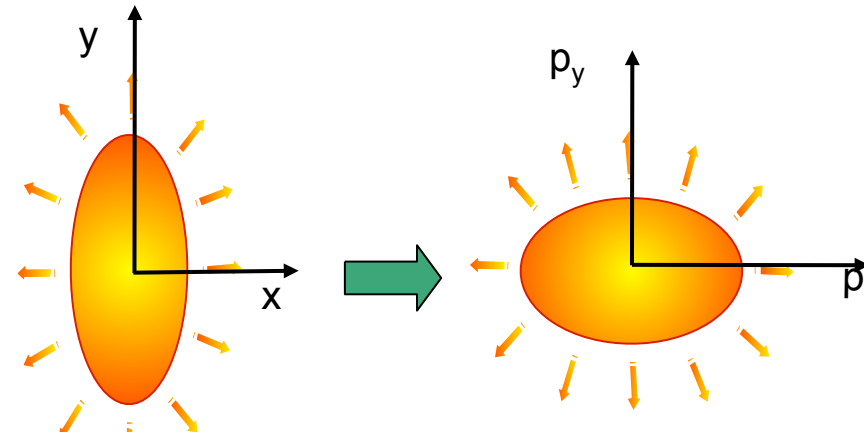
- Flow can be described by hydrodynamics with a very small shear viscosity/entropy => ‘QGP’ is a nearly perfect fluid.

实验观测量: collective flow



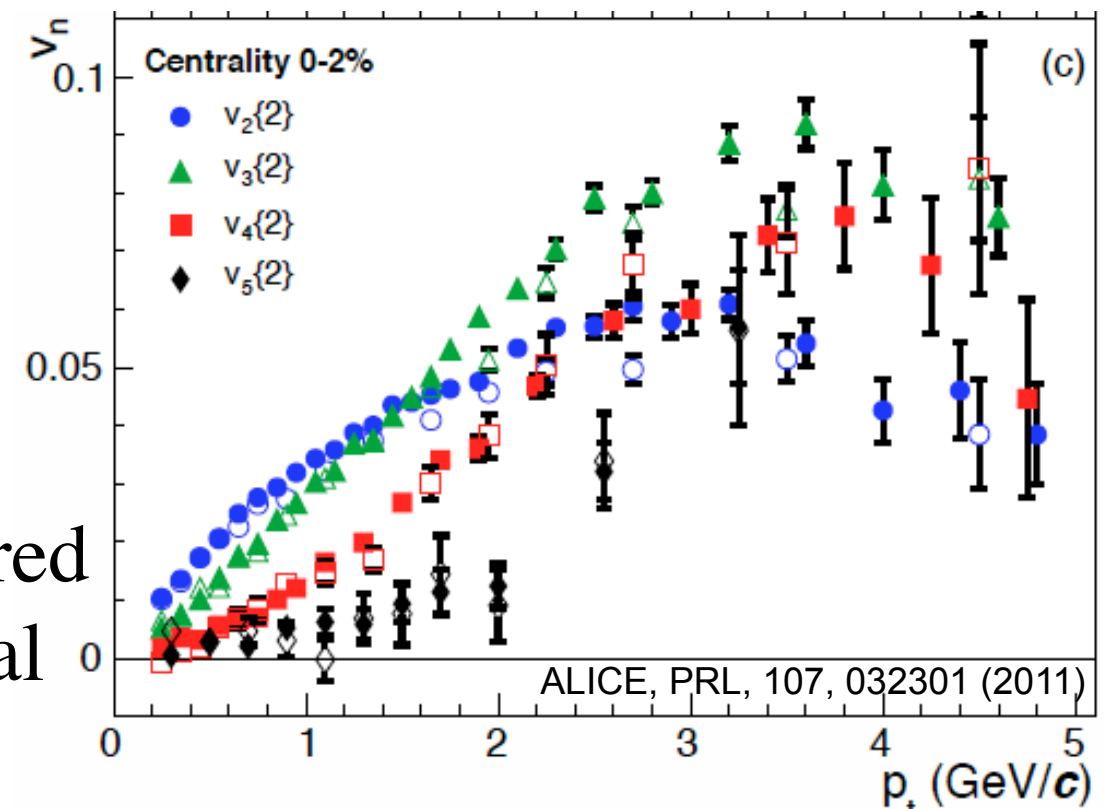
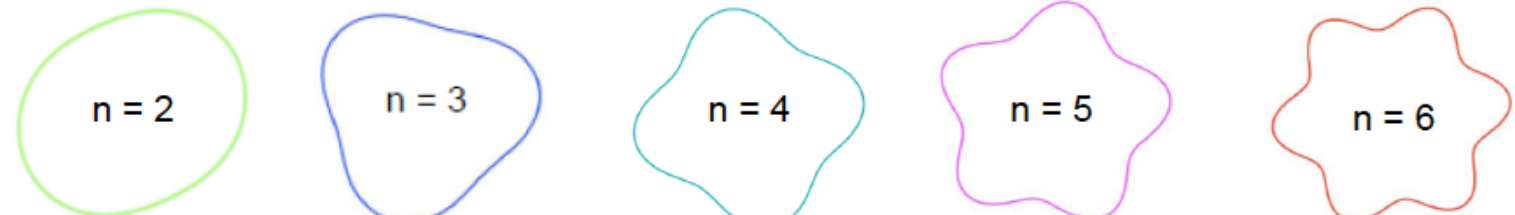
$$\frac{dN}{dp_T dy d\phi} = \frac{1}{2\pi} \frac{d^2 N}{dp_T dy} (1 + 2v_1 \cos(\phi) + 2v_2 \cos(2\phi) + \dots)$$

$$v_2 = \langle \cos(2\phi) \rangle$$



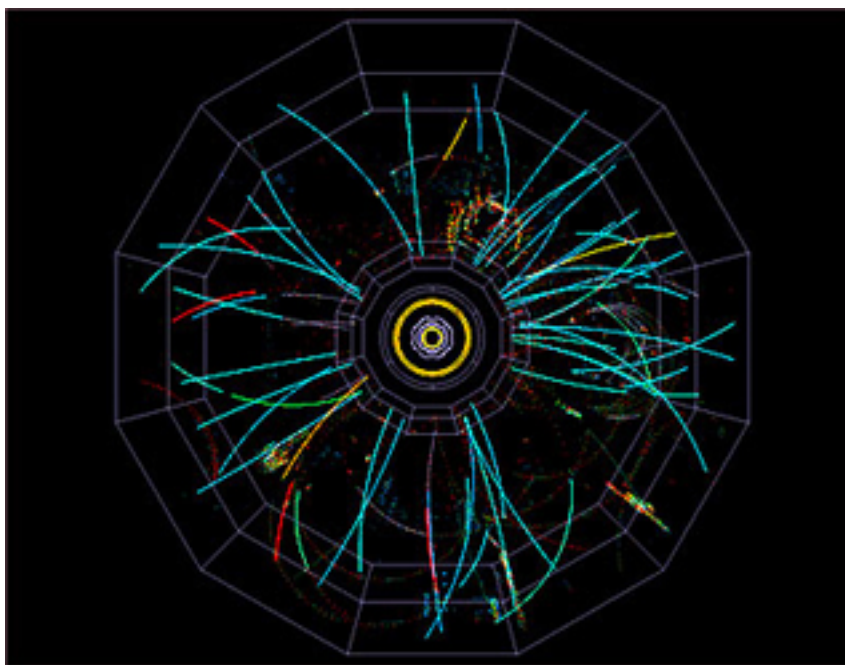
$$\epsilon = \frac{\langle y^2 - x^2 \rangle}{\langle y^2 + x^2 \rangle}$$

$$v_2 = \langle \cos 2\varphi \rangle, \quad \varphi = \tan^{-1}\left(\frac{p_y}{p_x}\right)$$



- Initial geometry shape can be transferred into final momentum space through final interactions \rightarrow collective flow

flow and Fourier Series



$f(\theta)$ be a periodic function with period 2π

The function can be represented by a trigonometric series as:

$$f(\theta) = a_0 + \sum_{n=1}^{\infty} a_n \cos n\theta + \sum_{n=1}^{\infty} b_n \sin n\theta$$

The coefficients are:

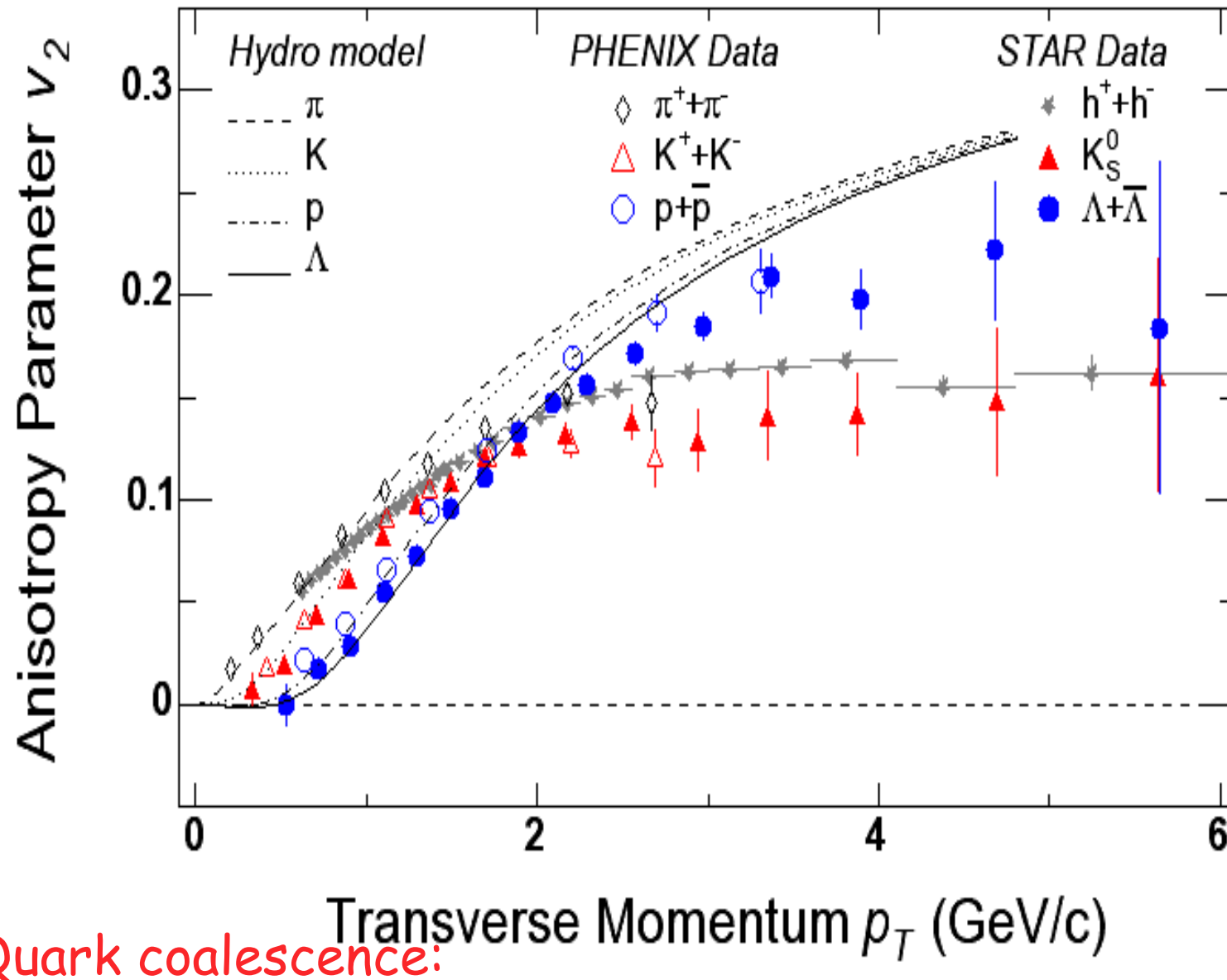
$$a_0 = \frac{1}{2\pi} \int_{-\pi}^{\pi} f(\theta) d\theta$$

$$a_m = \frac{1}{\pi} \int_{-\pi}^{\pi} f(\theta) \cos m\theta d\theta \quad m = 1, 2, \dots$$

$$b_m = \frac{1}{\pi} \int_{-\pi}^{\pi} f(\theta) \sin m\theta d\theta \quad m = 1, 2, \dots$$

- Measuring collective flow v_n is nothing but a Fourier analysis on the exp. data.
- $v_n = a_m$

Mass ordering and NCQ scaling of v2



$$v_2^{\text{hadron}}(p_T) \approx n v_2^{\text{quark}}(p_T/n)$$

- Partonic flow is followed by coalescence to form hadrons, indicating the existence of deconfined QGP phase

Multi-particle cumulant flow

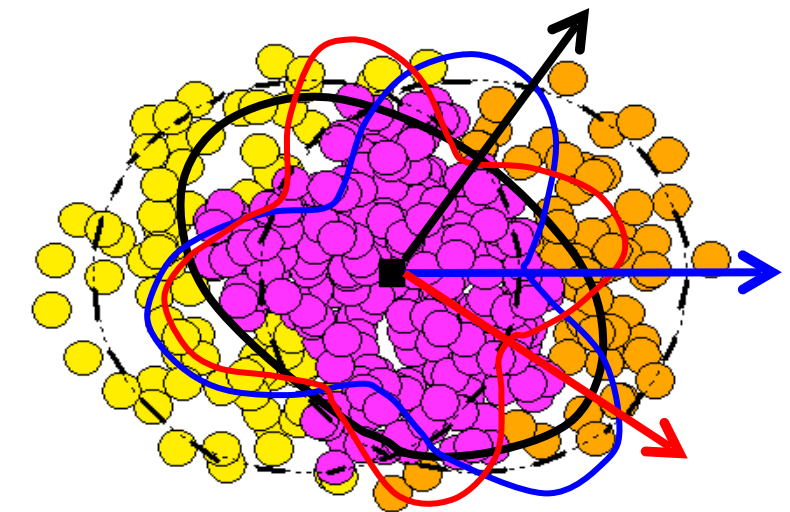
$$\frac{dN}{d\varphi} \propto 1 + 2 \sum_n v_n \cos n(\varphi - \Psi_r)$$

$$v_n = \langle \cos n(\varphi - \Psi_r) \rangle = \langle e^{in(\varphi - \Psi_r)} \rangle$$

$$c_n\{2\} = \langle e^{in(\varphi_1 - \varphi_2)} \rangle = \langle e^{in(\varphi_1 - \psi_r)} e^{in(\psi_r - \varphi_2)} \rangle \approx \langle e^{in(\varphi_1 - \psi_r)} \rangle \langle e^{in(\psi_r - \varphi_2)} \rangle = (v_n\{2\})^2$$

$$c_2\{4\} = \langle e^{in(\varphi_1 + \varphi_2 - \varphi_3 - \varphi_4)} \rangle - \langle e^{in(\varphi_1 - \varphi_2)} \rangle \langle e^{in(\varphi_3 - \varphi_4)} \rangle - \langle e^{in(\varphi_1 - \varphi_4)} \rangle \langle e^{in(\varphi_3 - \varphi_2)} \rangle \approx -(v_n\{4\})^4$$

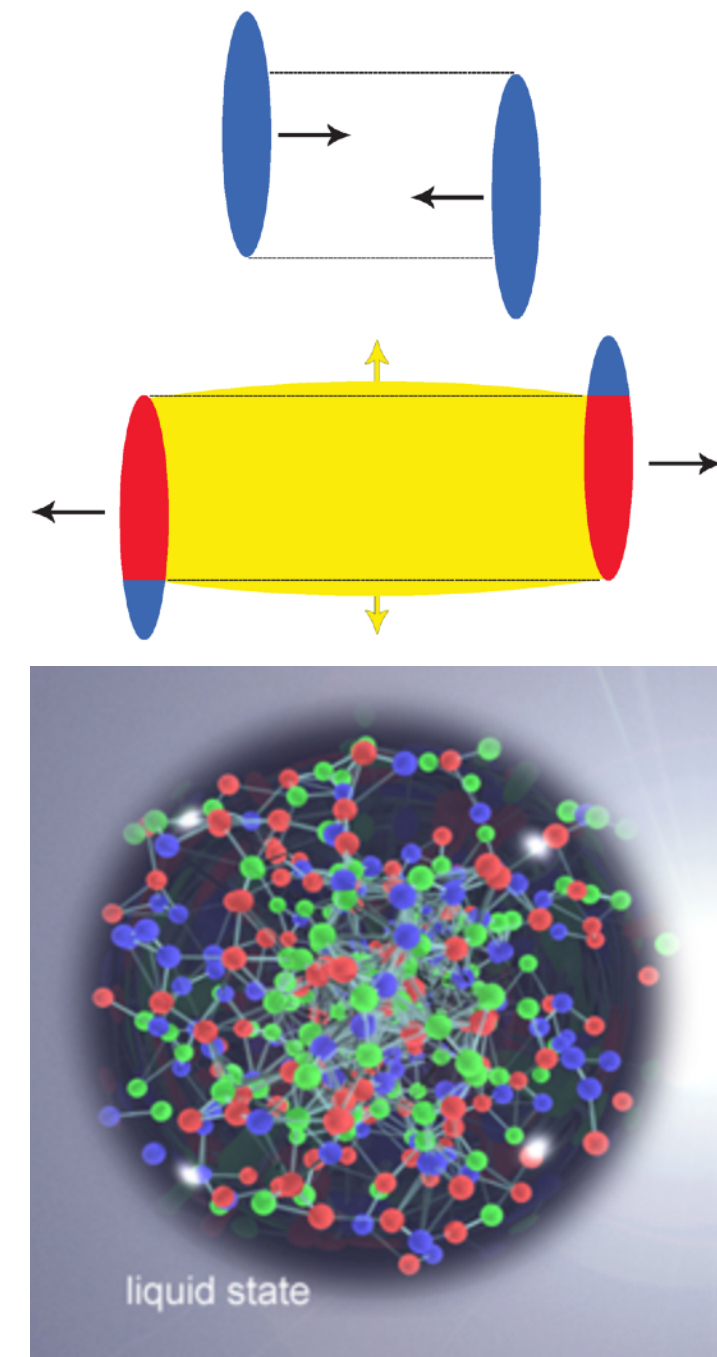
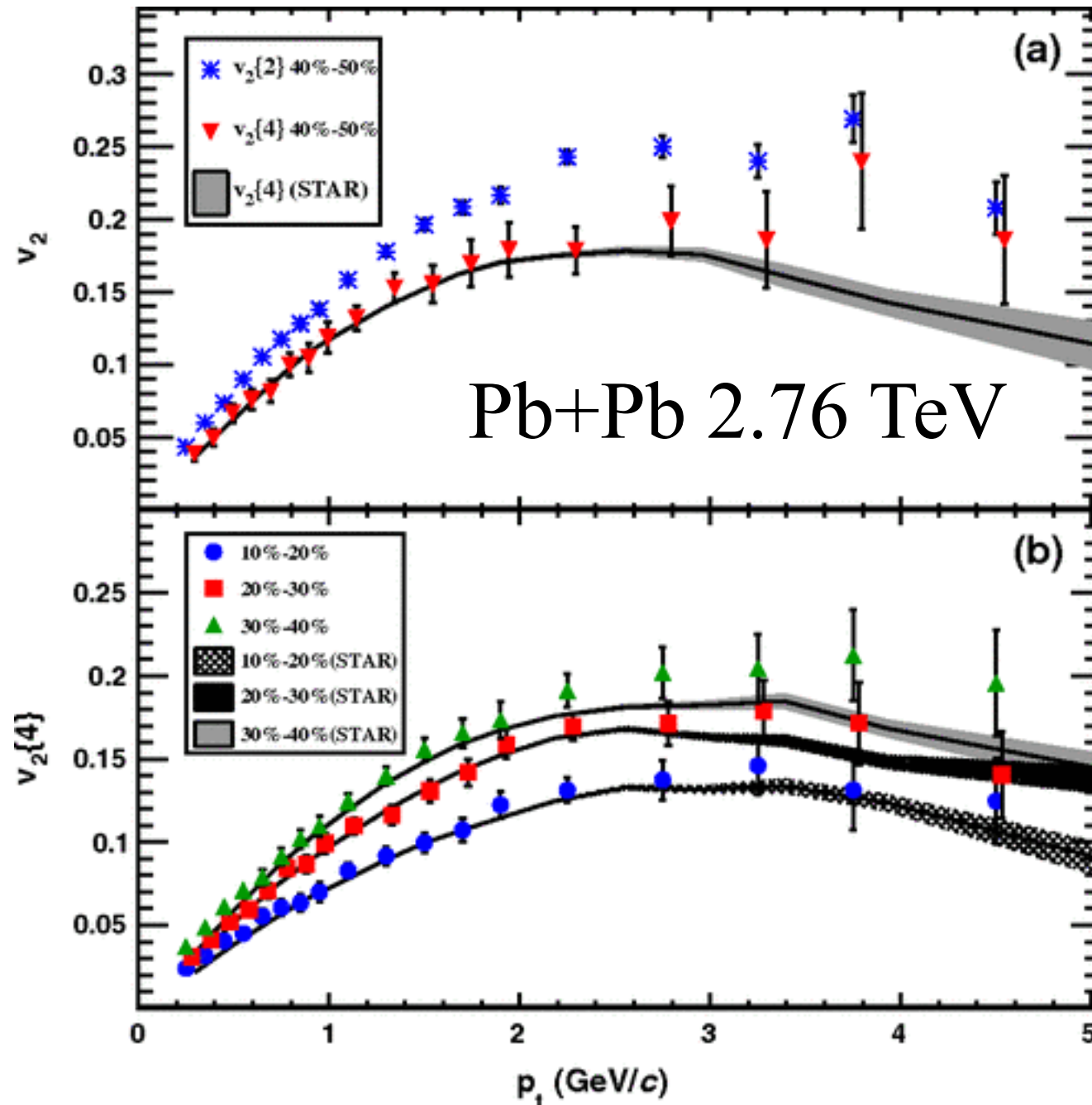
N. Borghini, P.M. Dinh and J.-Y Ollitrault, Phys. Rev. C63 (2001) 054906



- Multi-particle cumulant v_n was designed to measure the *real* flow by reducing non-flow effects.

Multi-particle cumulant flow in A+A

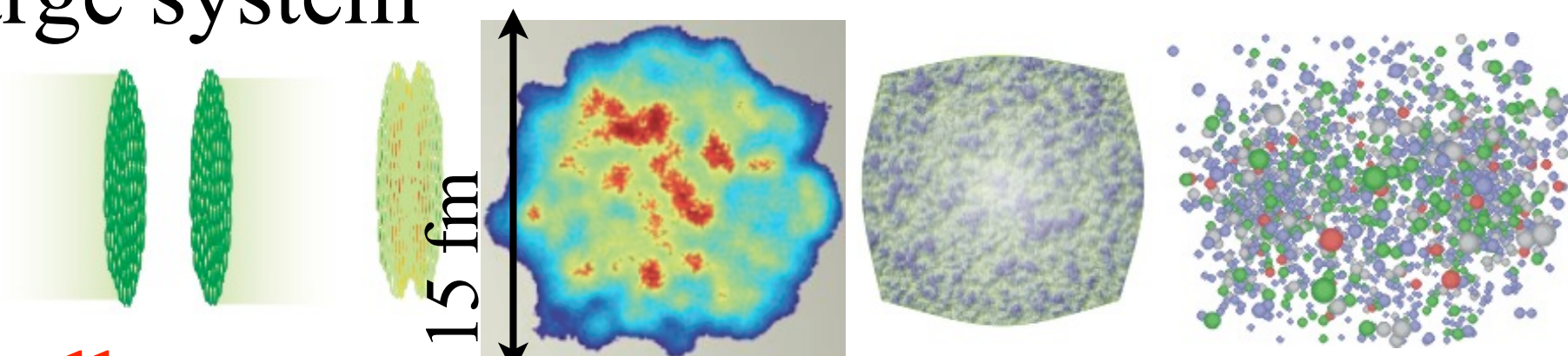
Phys. Rev. Lett. 105, 252302



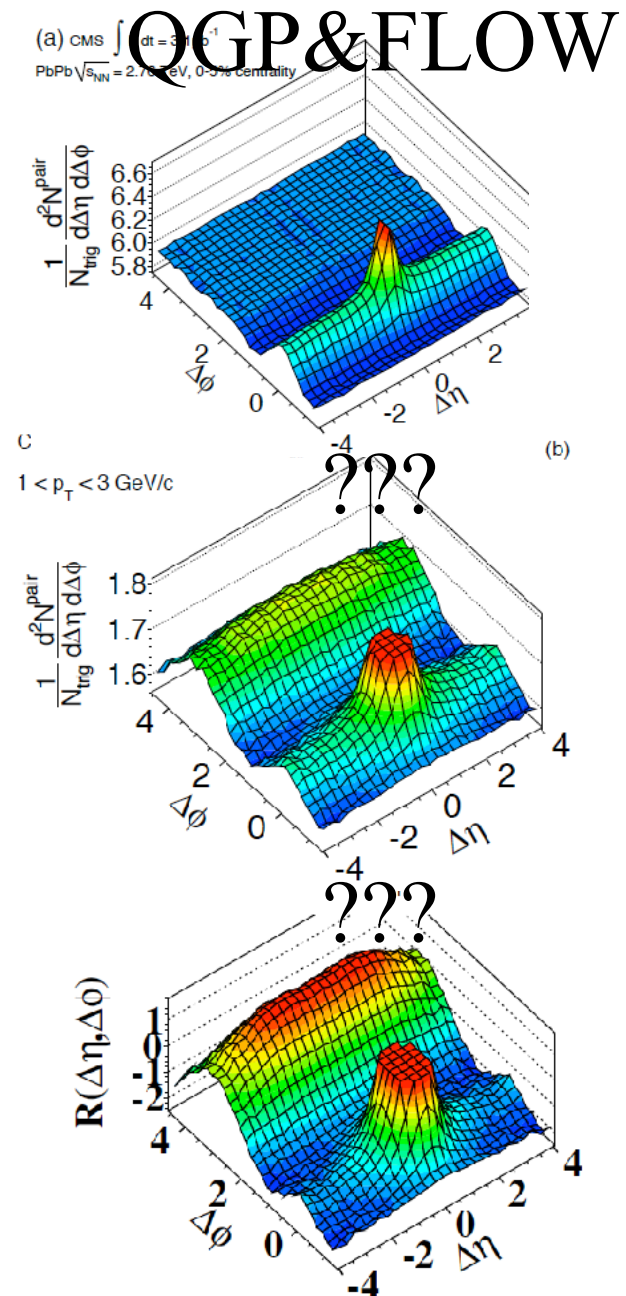
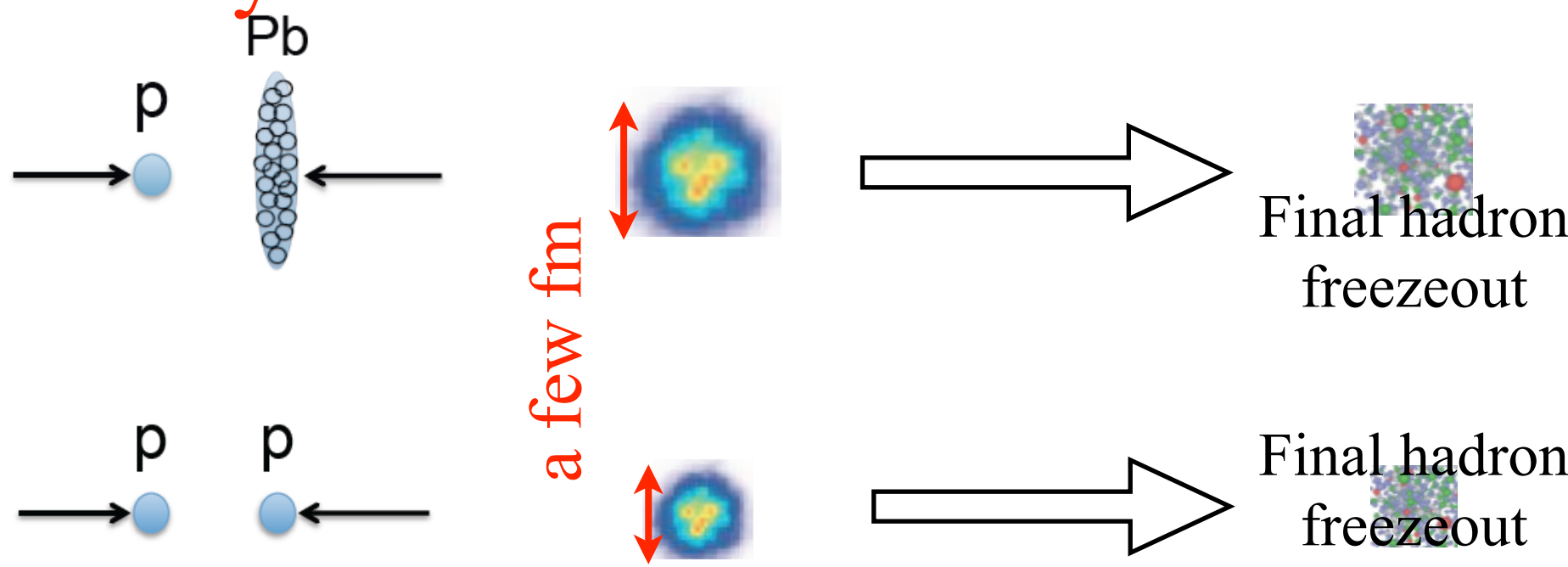
- $v_2\{4\}$ is smaller than $v_2\{2\}$ because of reduction of non-flow effect.
- Similar flow between LHC and RHIC, indicating the formation of QGP in A+A.

Long-range correlation in large and small systems

Large system



Small systems

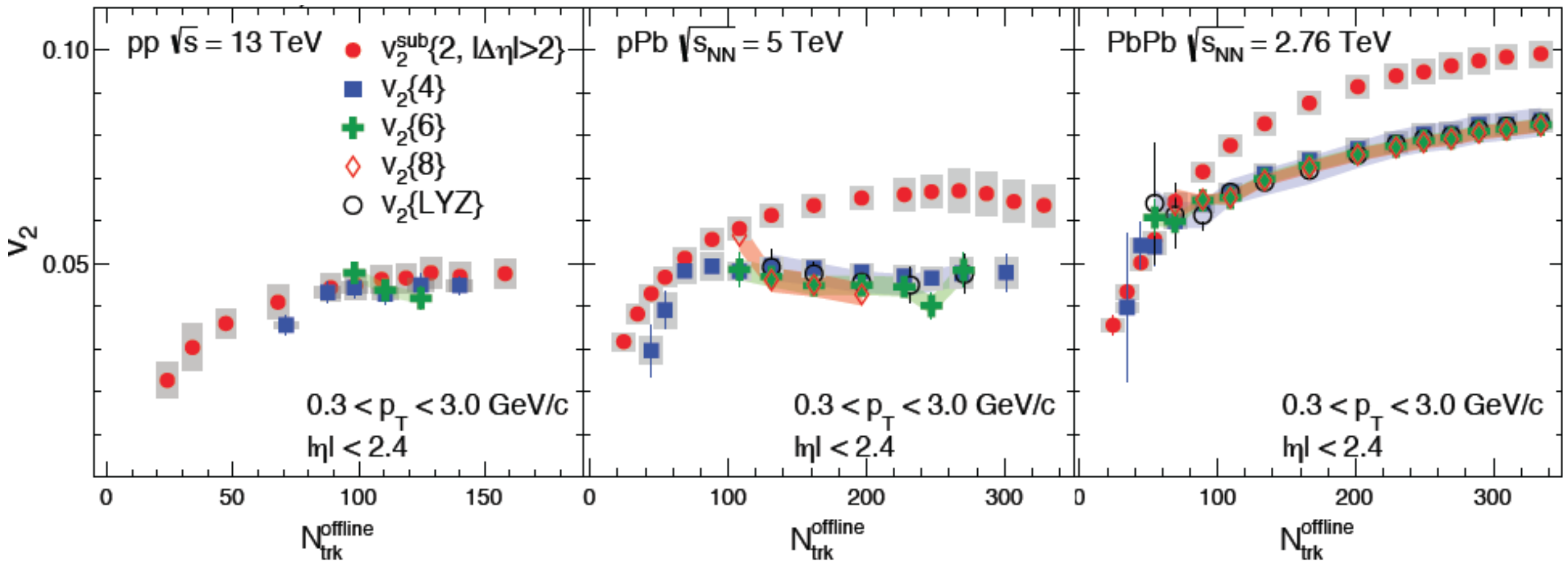


- Do long-range correlations in small and large systems have the same physical origin? Can QGP be formed in small systems?

v_2 in large and small systems

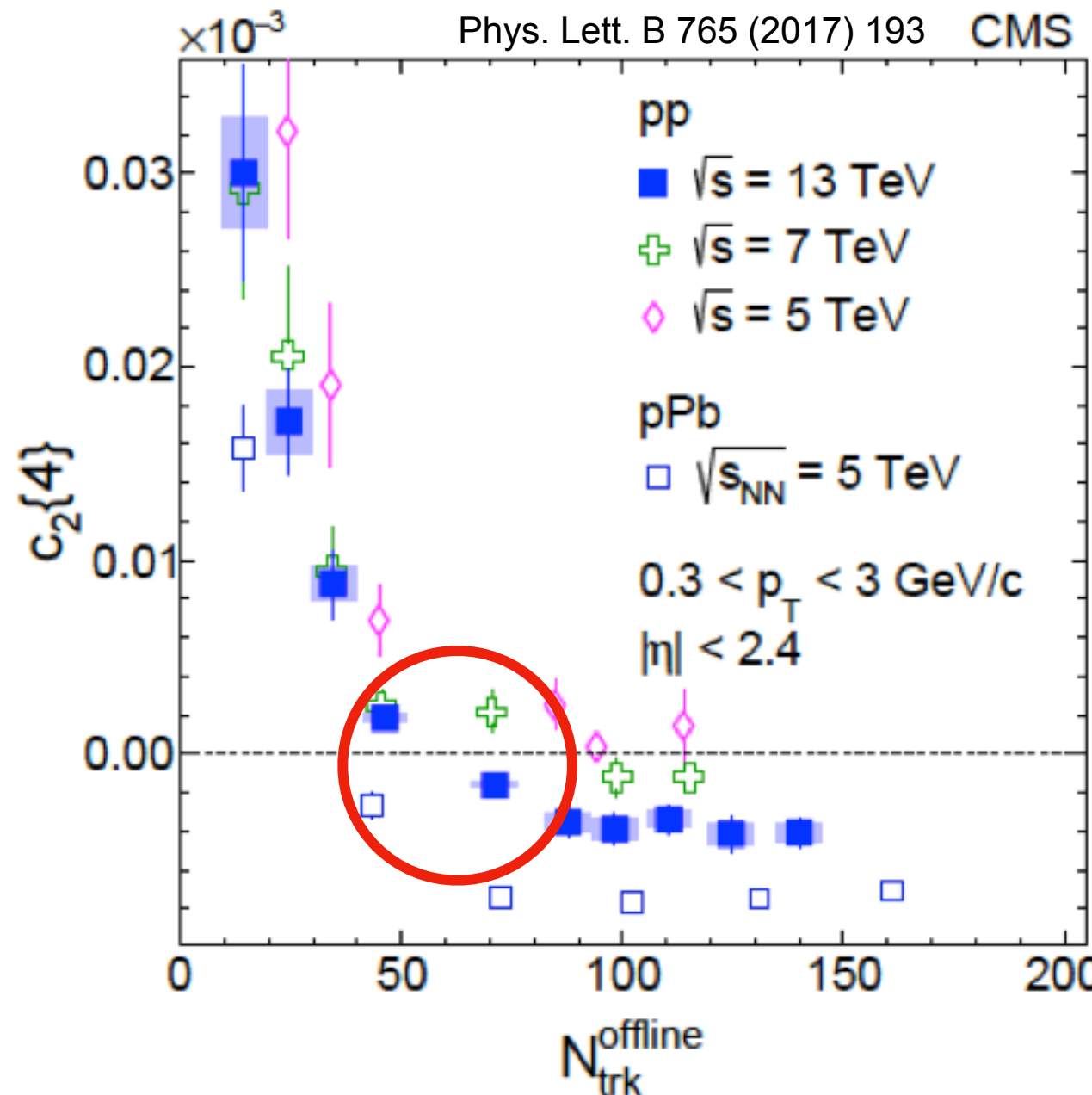
Small systems → Large system

CMS, Phys.Rev.Lett. 115 (2015) no.1, 012301



- Multi-particle cumulant v_2 are less than 2-particle $v_2 \Rightarrow$ non-flow
- Similar v_2 for 4,6,8-particle cumulants $v_2\{k\} \Rightarrow$ multi-particle correlation/flow

Sign change of $c_2\{4\}$ in small systems



$$v_n\{4\} = \sqrt[4]{-c_n\{4\}}, \quad n=2$$

$$c_n\{4\} = \langle\langle 4 \rangle\rangle - 2 \times \langle\langle 2 \rangle\rangle^2,$$

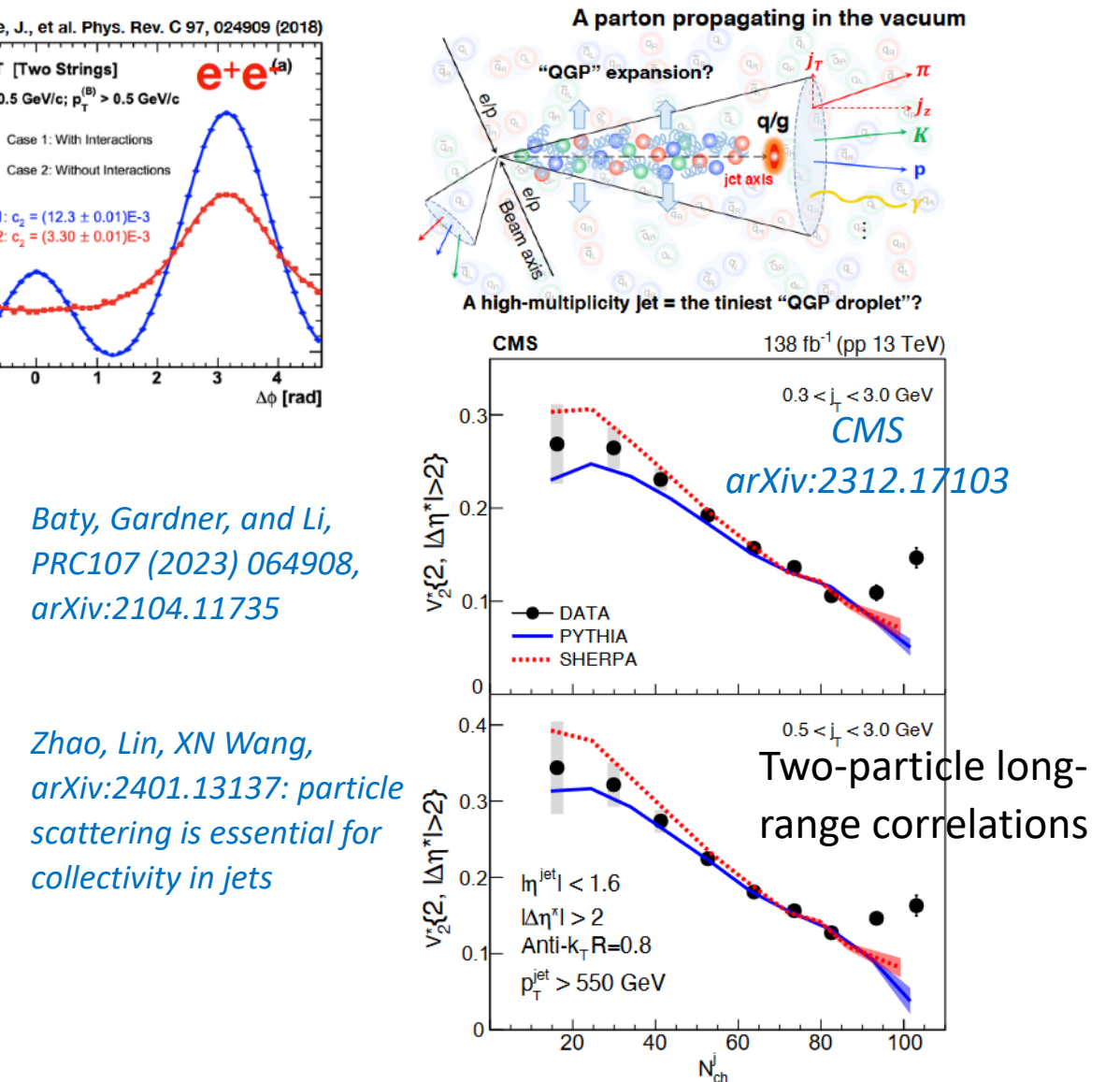
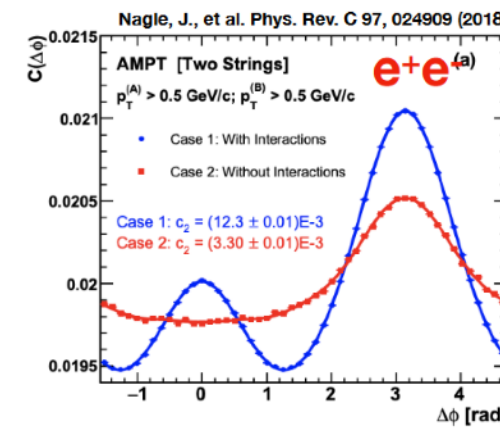
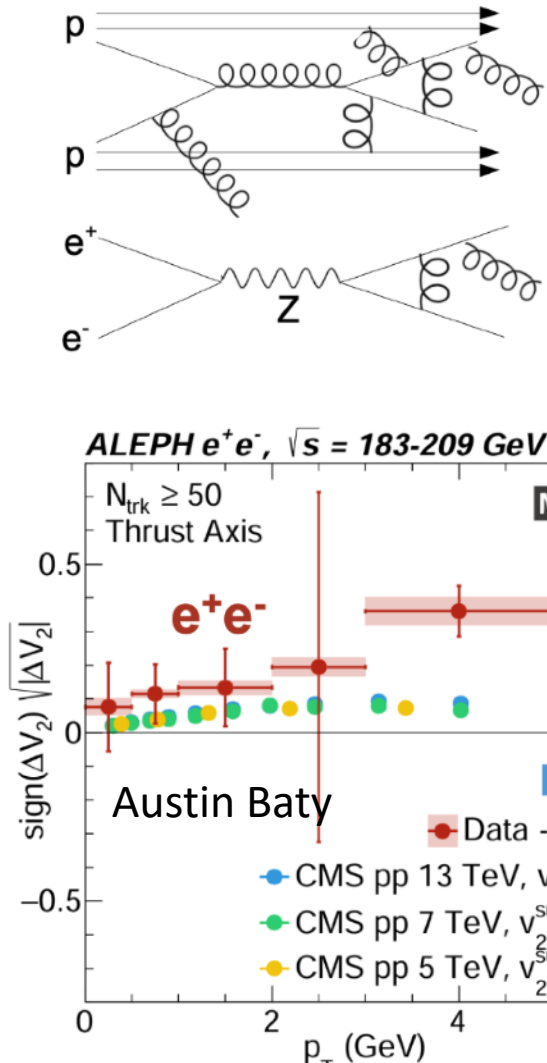
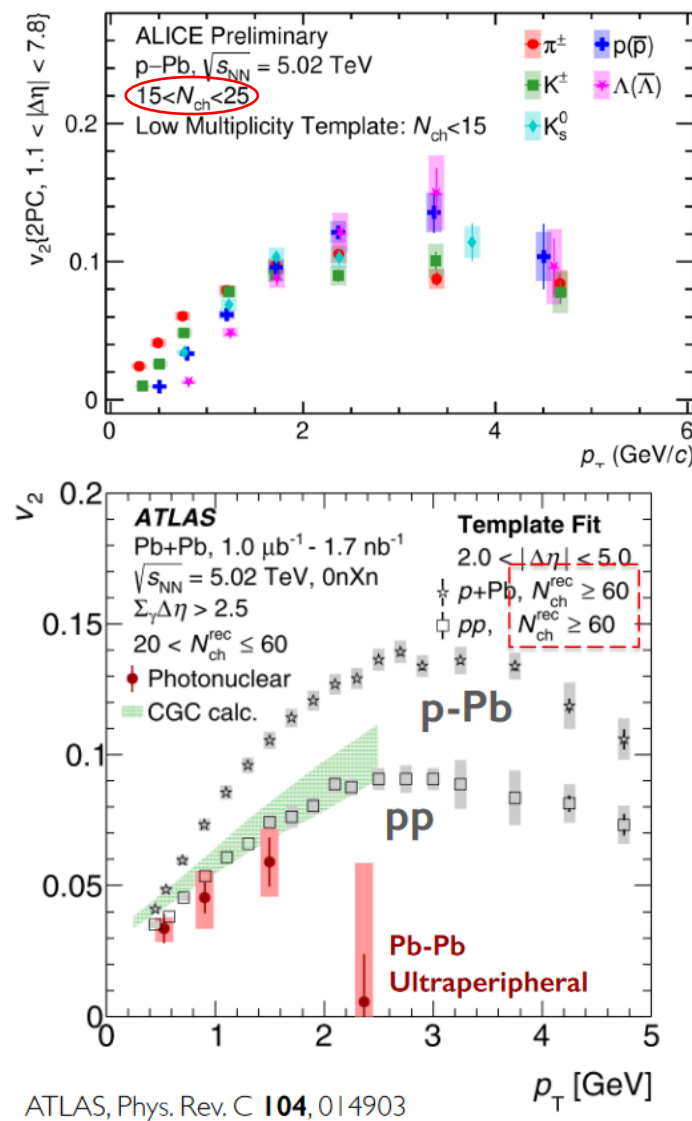
$$\langle\langle 2 \rangle\rangle \equiv \langle\langle e^{in(\phi_1-\phi_2)} \rangle\rangle,$$

$$\langle\langle 4 \rangle\rangle \equiv \langle\langle e^{in(\phi_1+\phi_2-\phi_3-\phi_4)} \rangle\rangle,$$

- $c_2\{4\}$ changes sign at a N_{trk} !

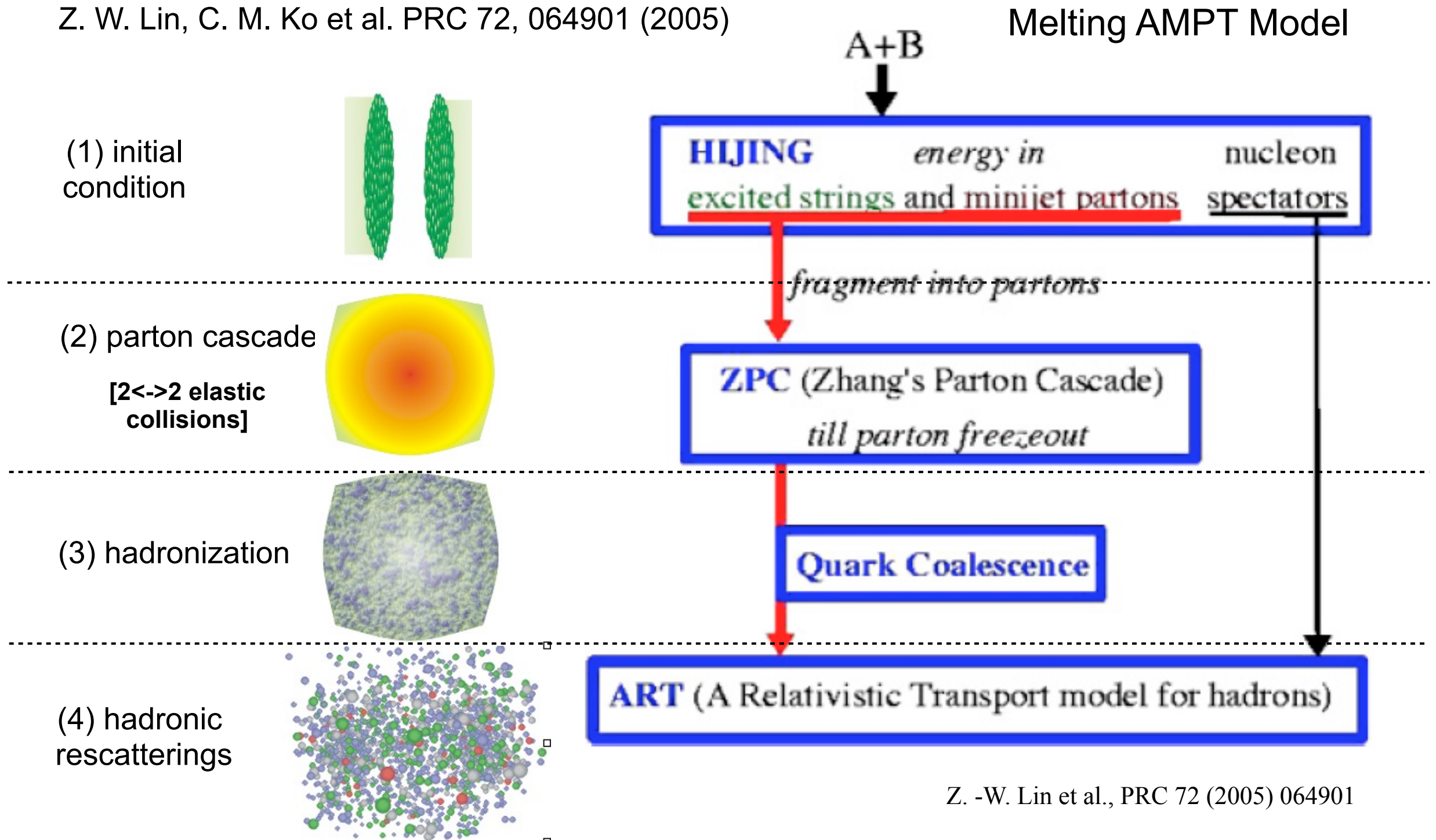
=> an onset of collectivity in small system?

ULTIMATE SMALL SYSTEMS

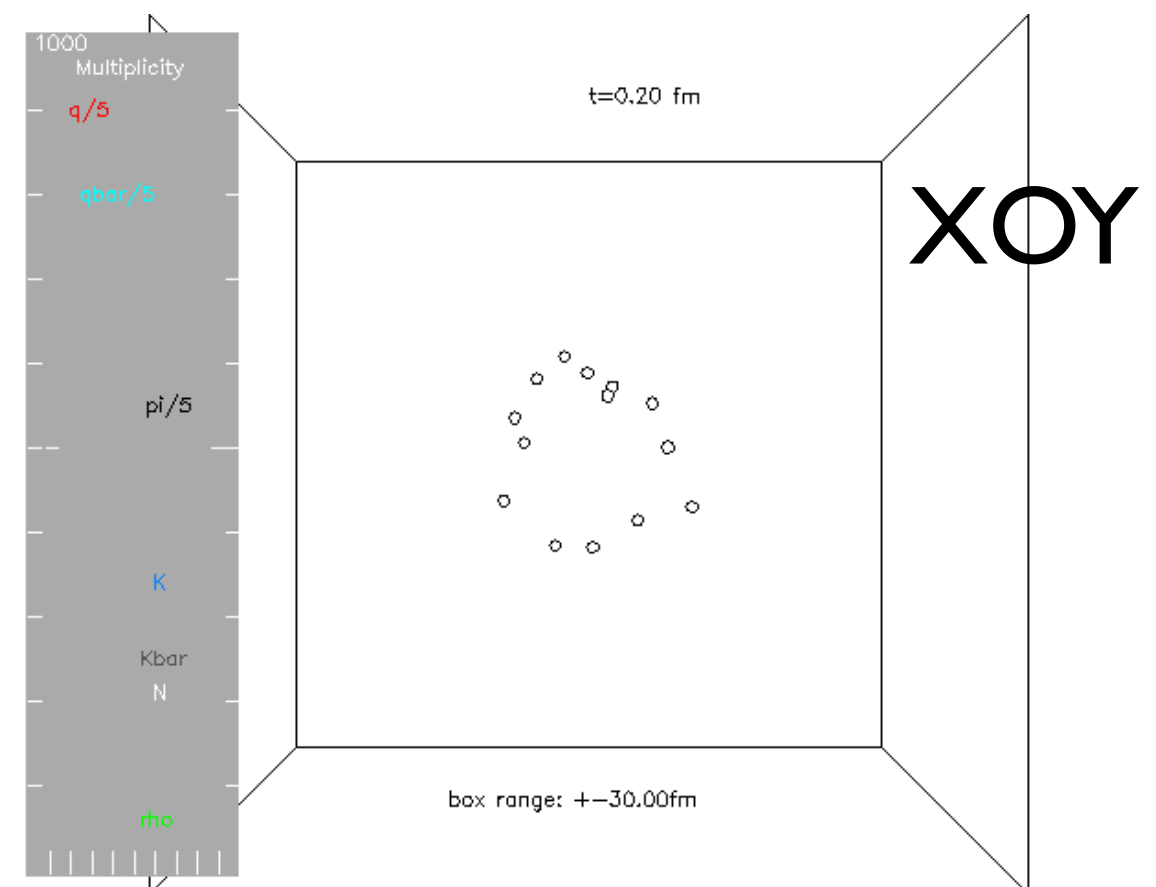
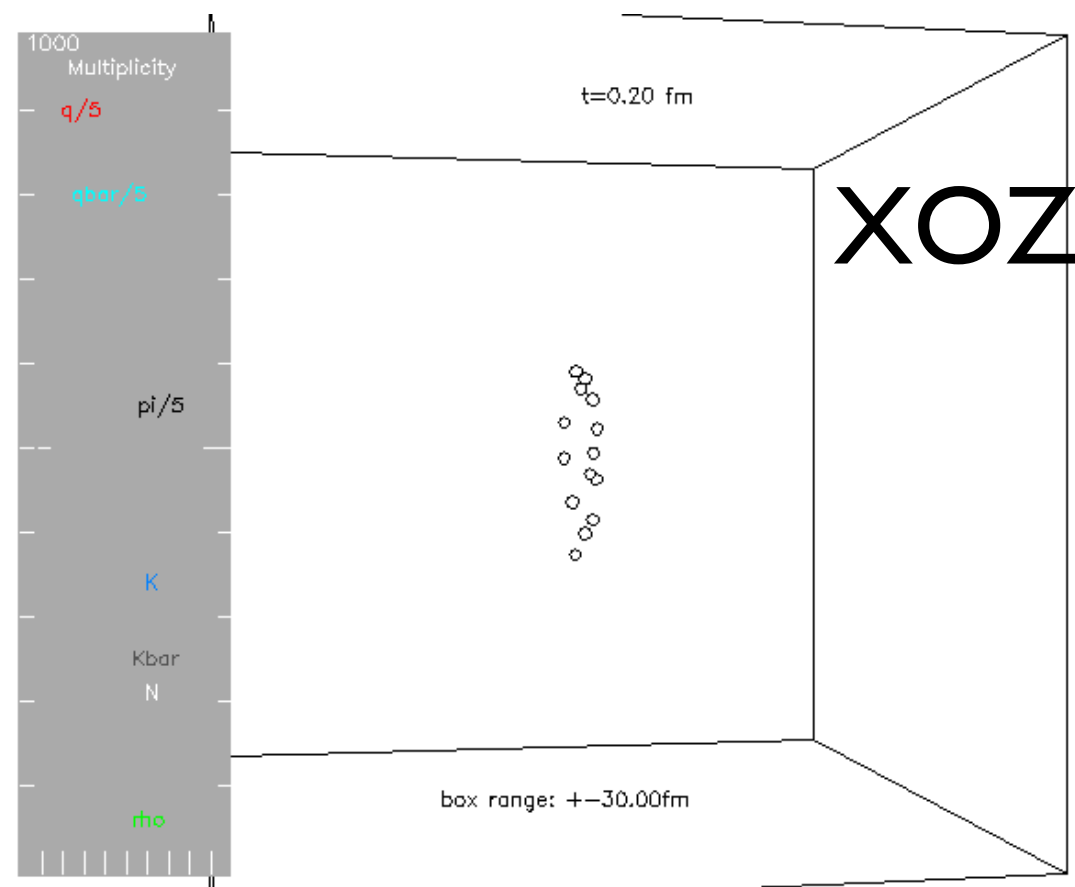
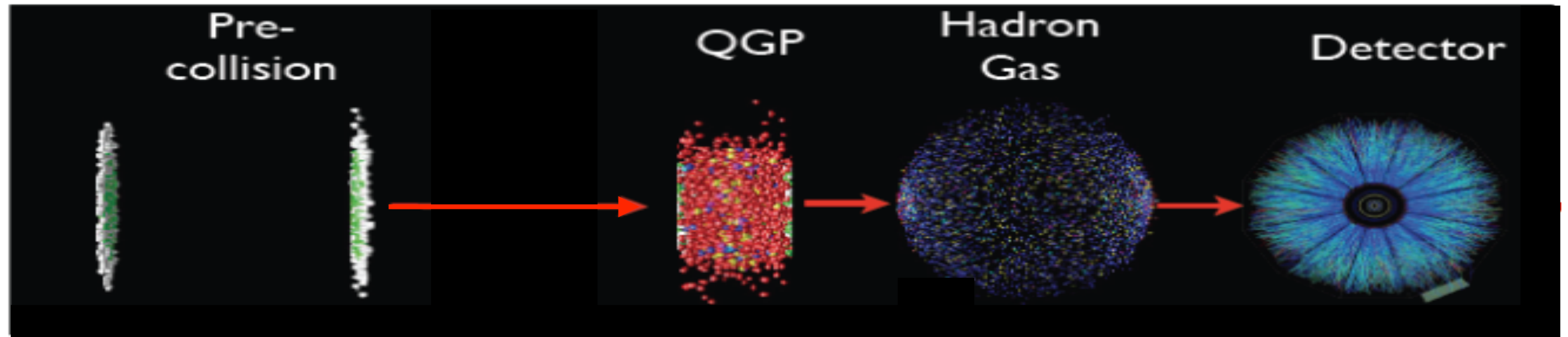


A multiphase transport (AMPT) model

Z. W. Lin, C. M. Ko et al. PRC 72, 064901 (2005)

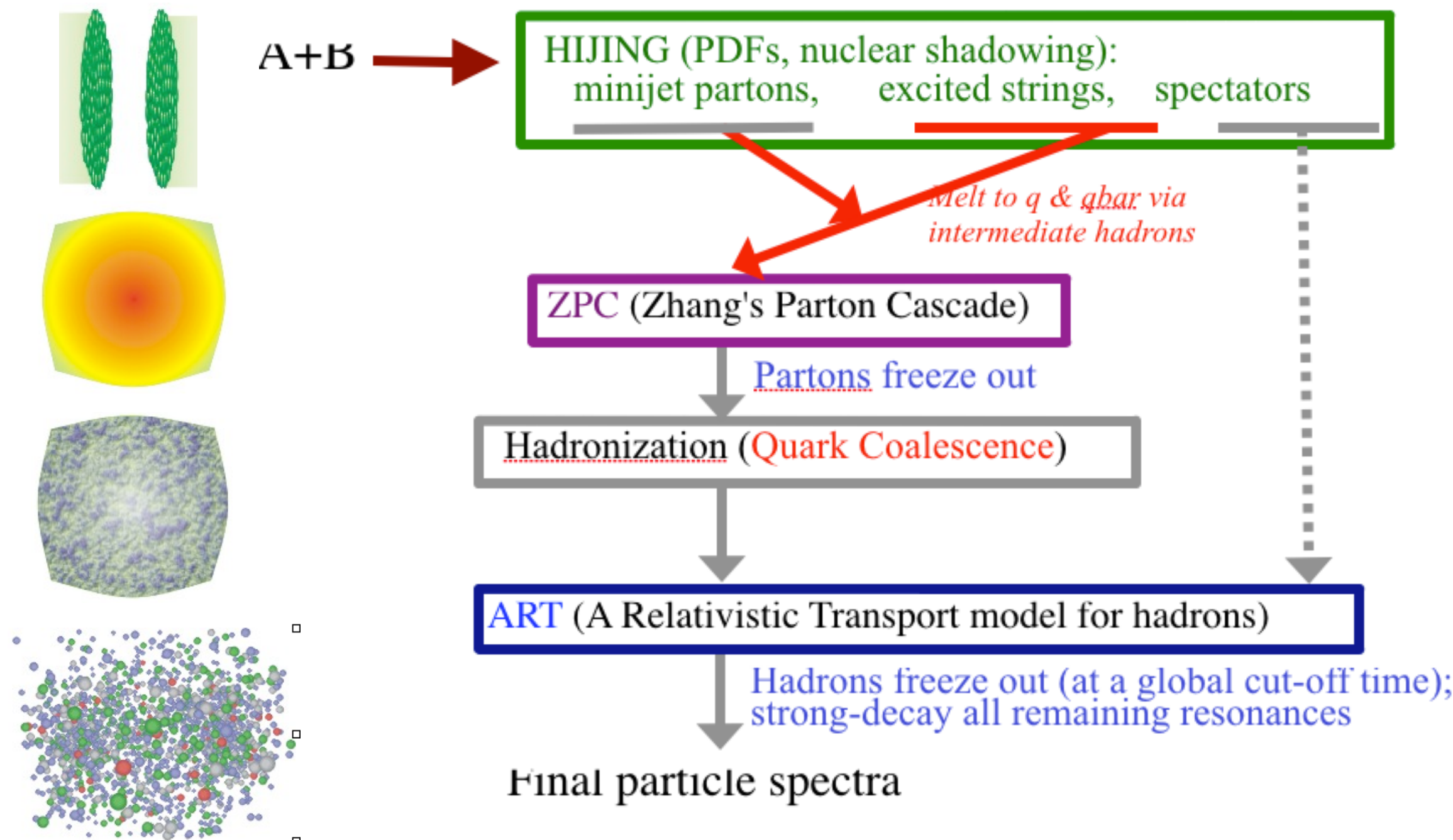


Time evolution of a central Au+Au collision from the AMPT model (string-melting version)



Studying flow` with AMPT model

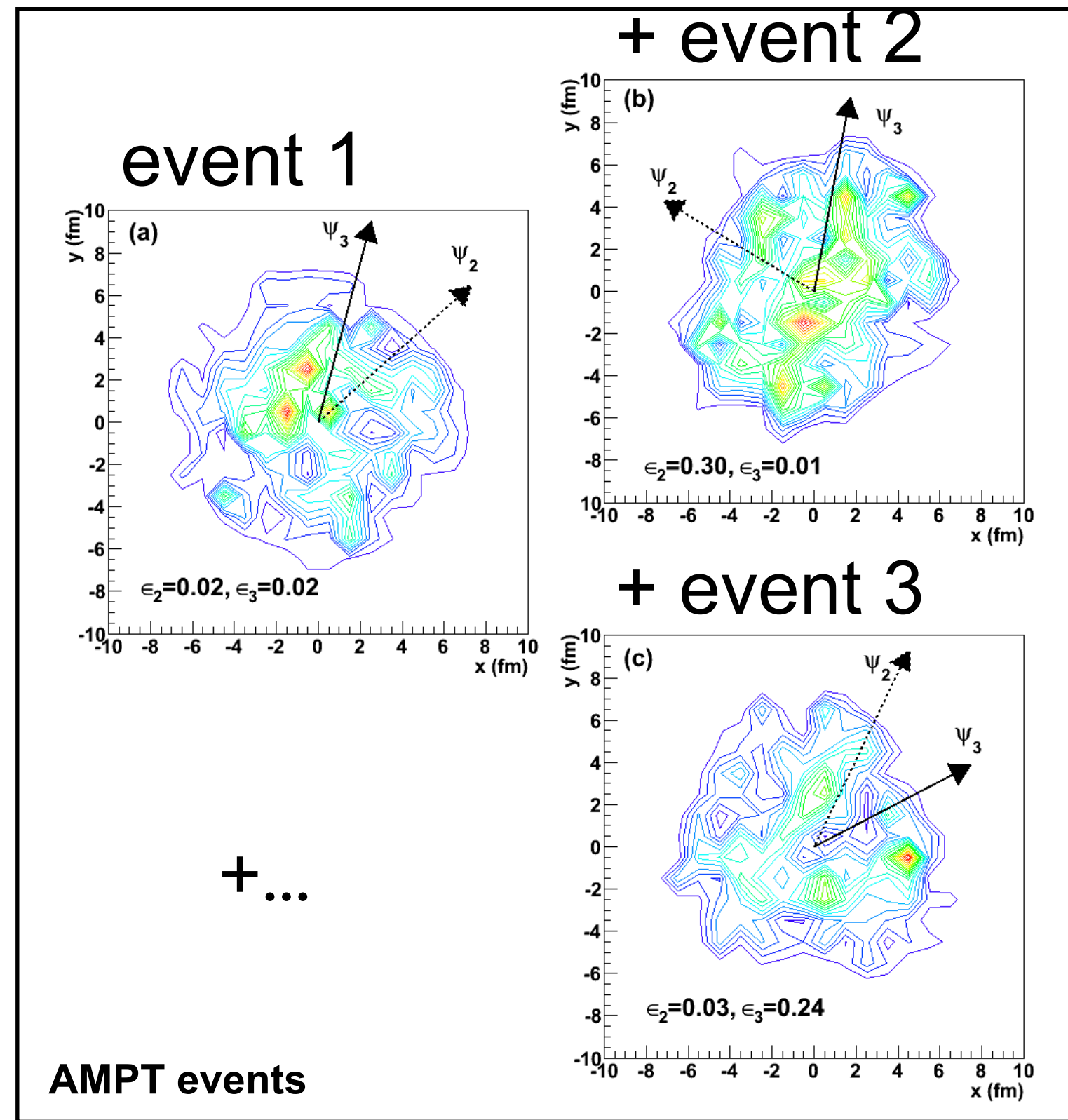
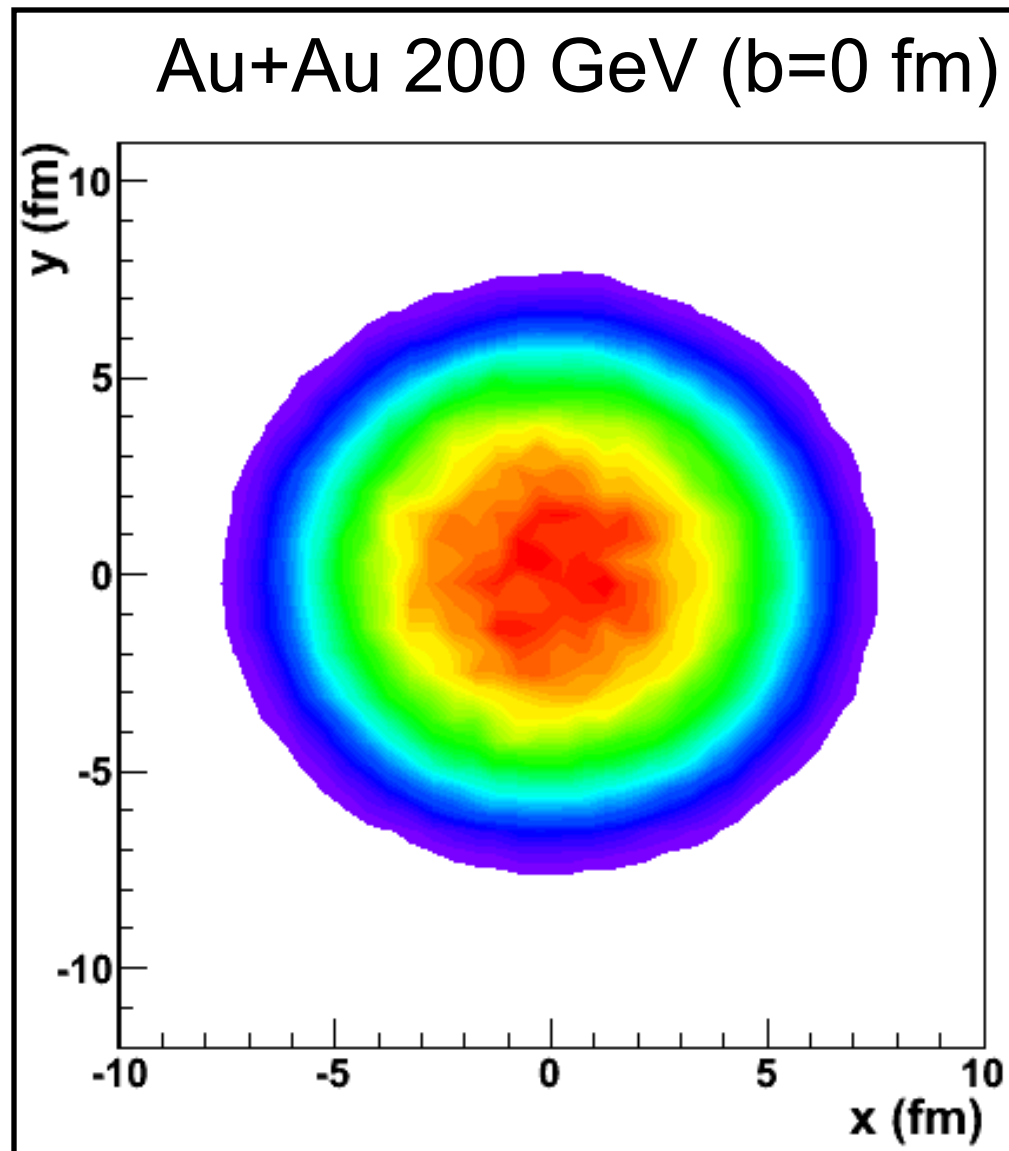
Z.-W.Lin et al., Phys. Rev C 72, 064901 (2005)



flow` = flow(escape \oplus hydro \oplus CGC) \oplus non-flow

初始几何涨落

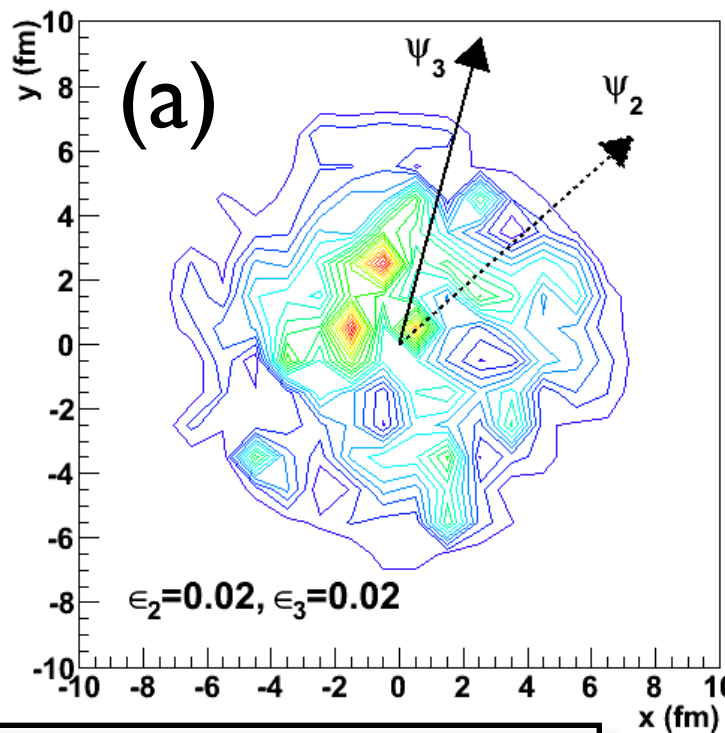
Ma et al. 2011



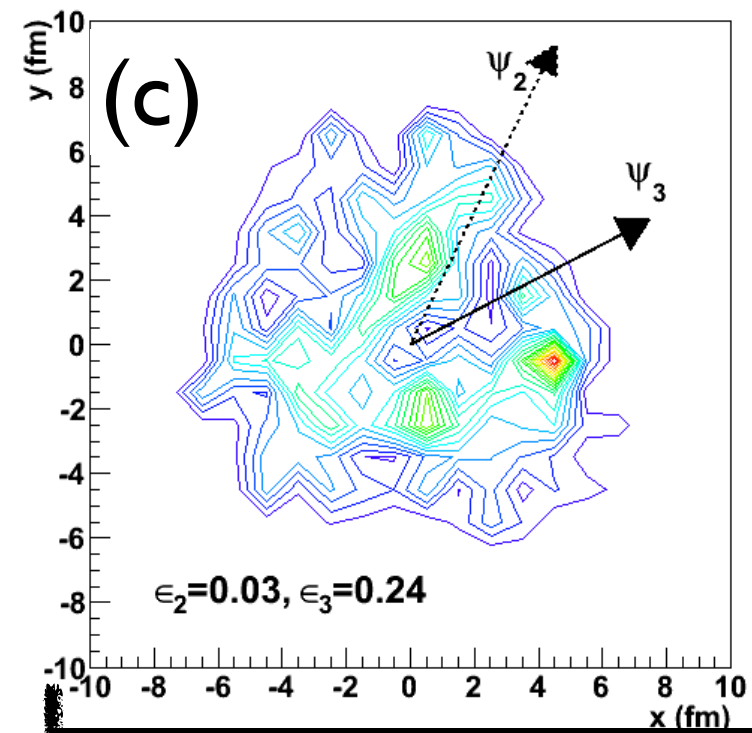
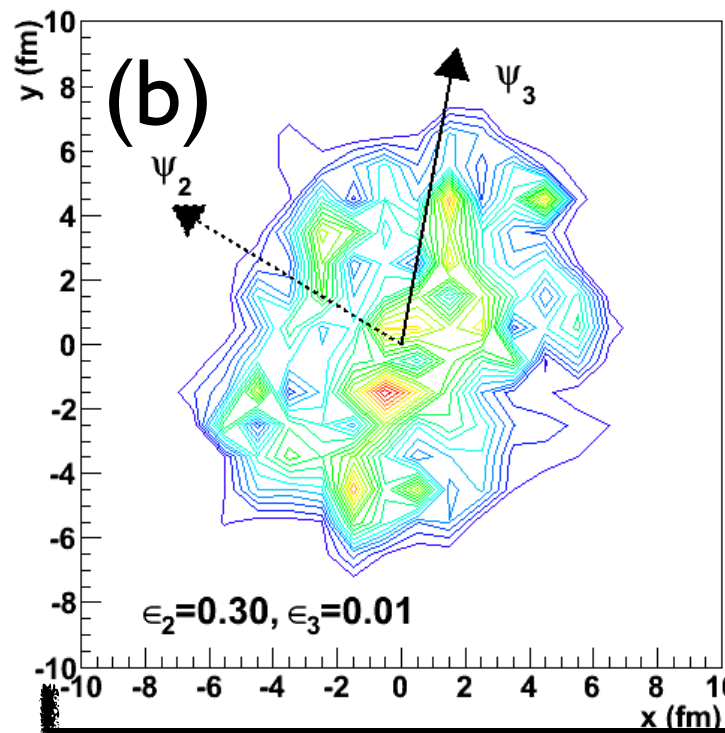
- 最中心的碰撞 ($b=0$) 由于初态几何空间的涨落存在，所以也不总是圆形对称分布

初始几何涨落 \Rightarrow 各种集体流

initial spacial space

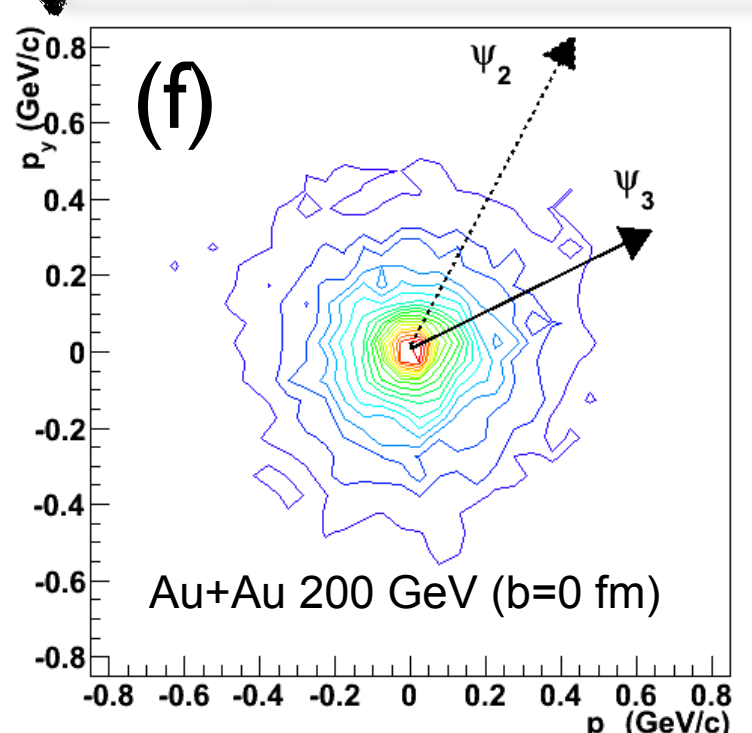
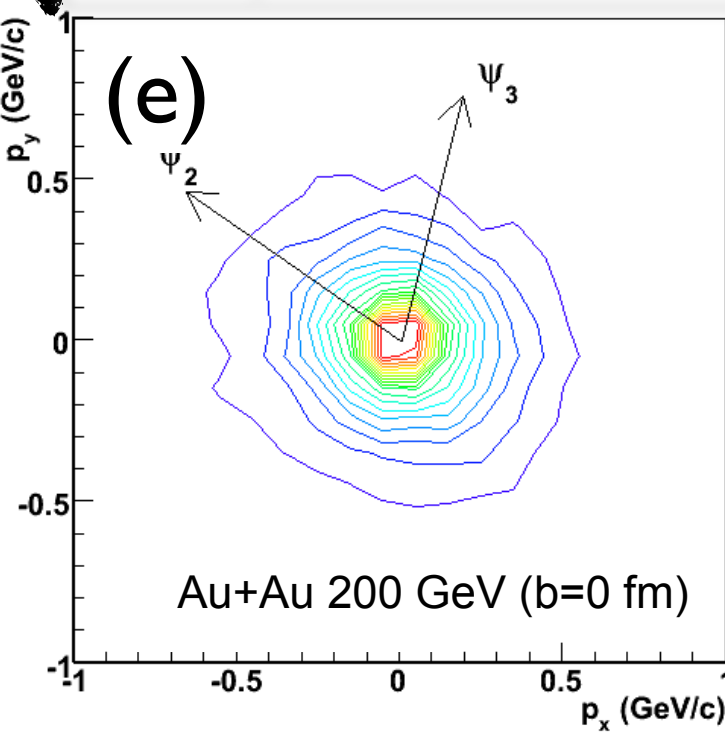
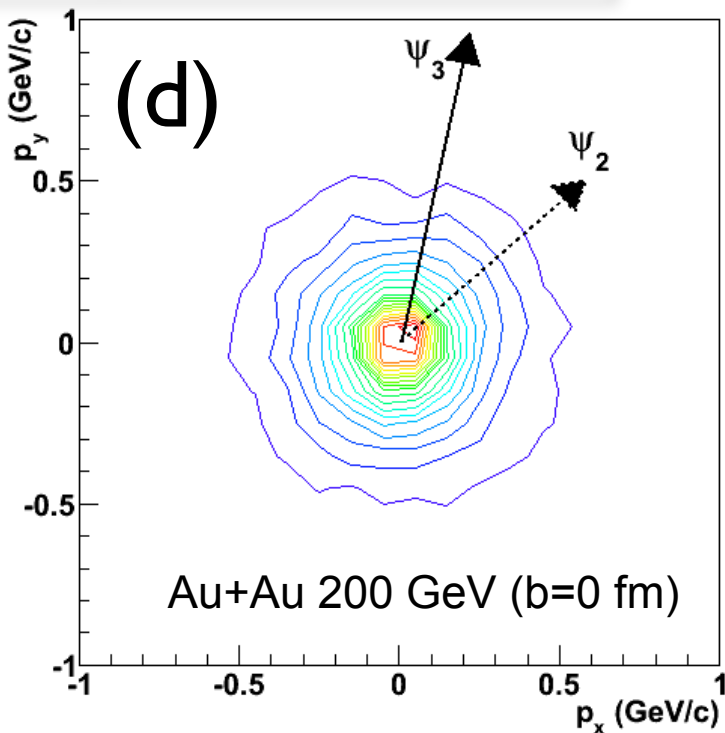


via parton cascade



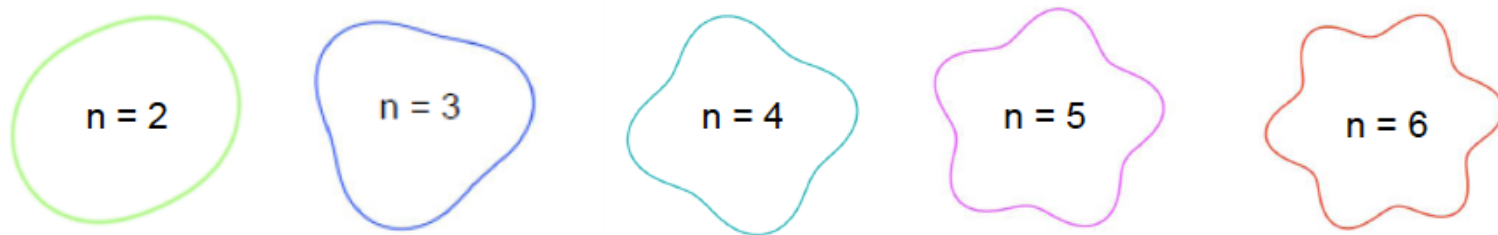
via parton cascade

final momentum space

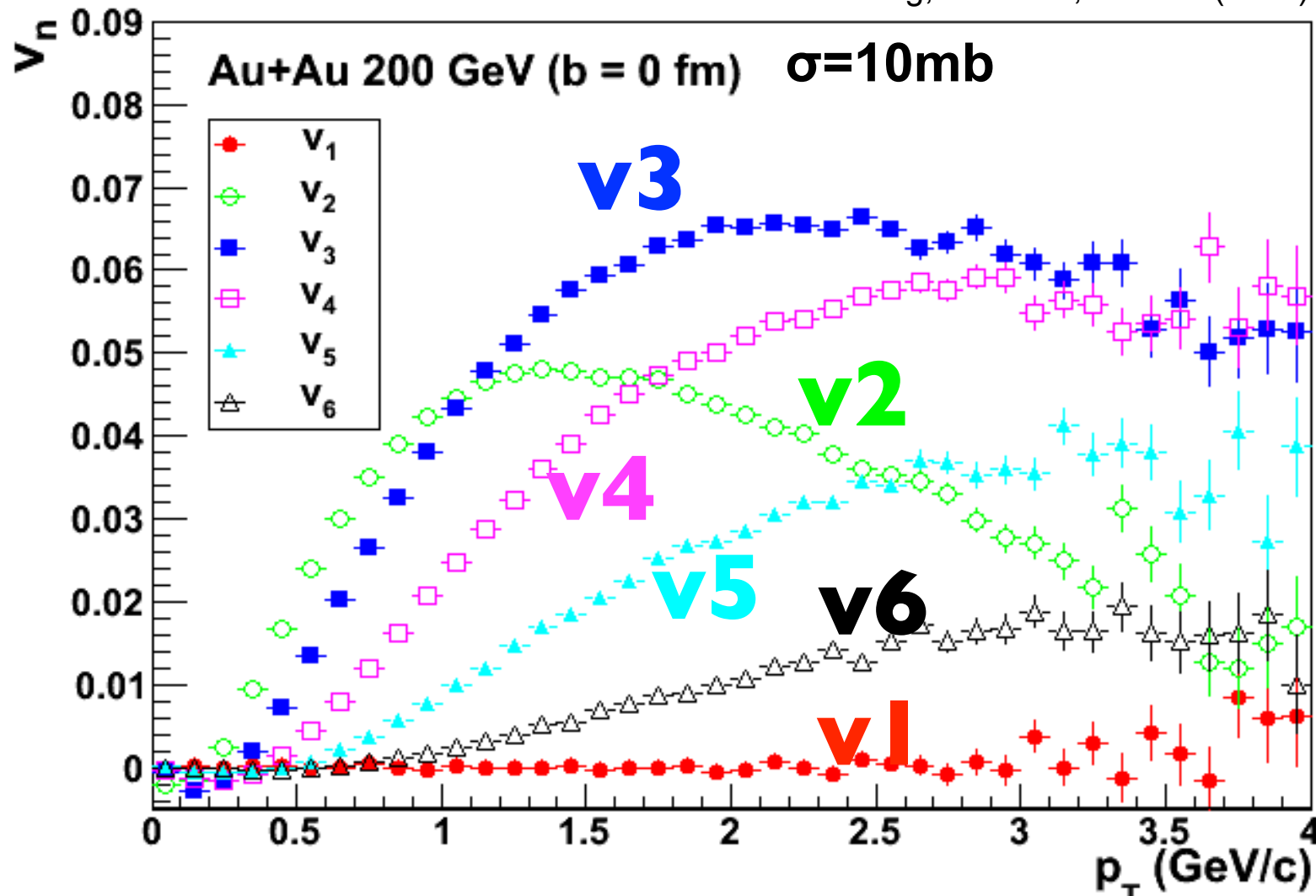


●部分子相互作用将初始的几何不对称分布转化为末态动量空间的各种集体流。

各种集体流



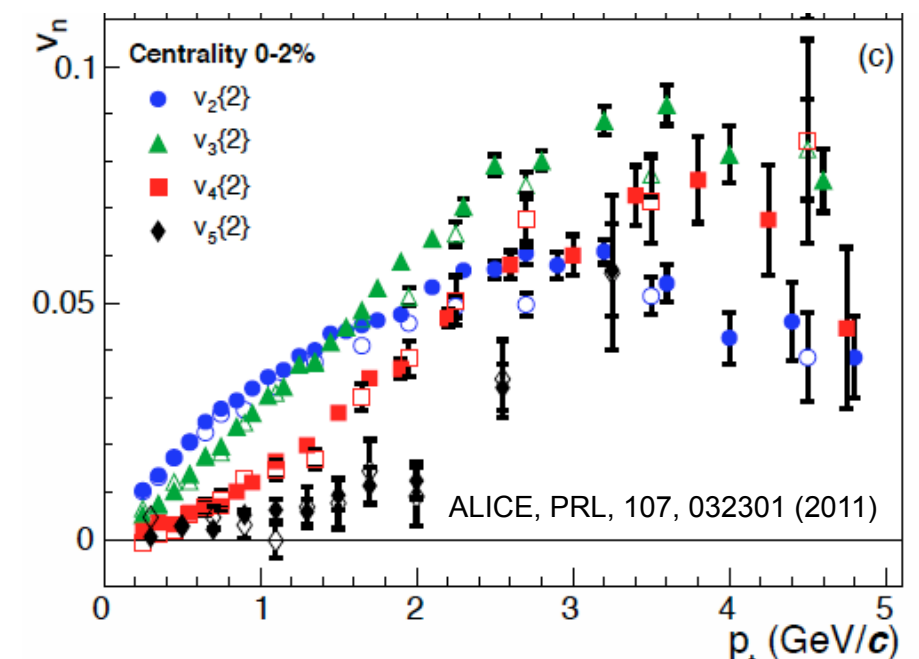
G. L. Ma and X.-N. Wang, PRL 106, 162301 (2011)



$$\psi_n = \frac{1}{n} \left[\arctan \frac{\langle r^2 \sin(n\varphi) \rangle}{\langle r^2 \cos(n\varphi) \rangle} + \pi \right].$$

$$v_n = \langle \cos n(\phi - \psi_n) \rangle$$

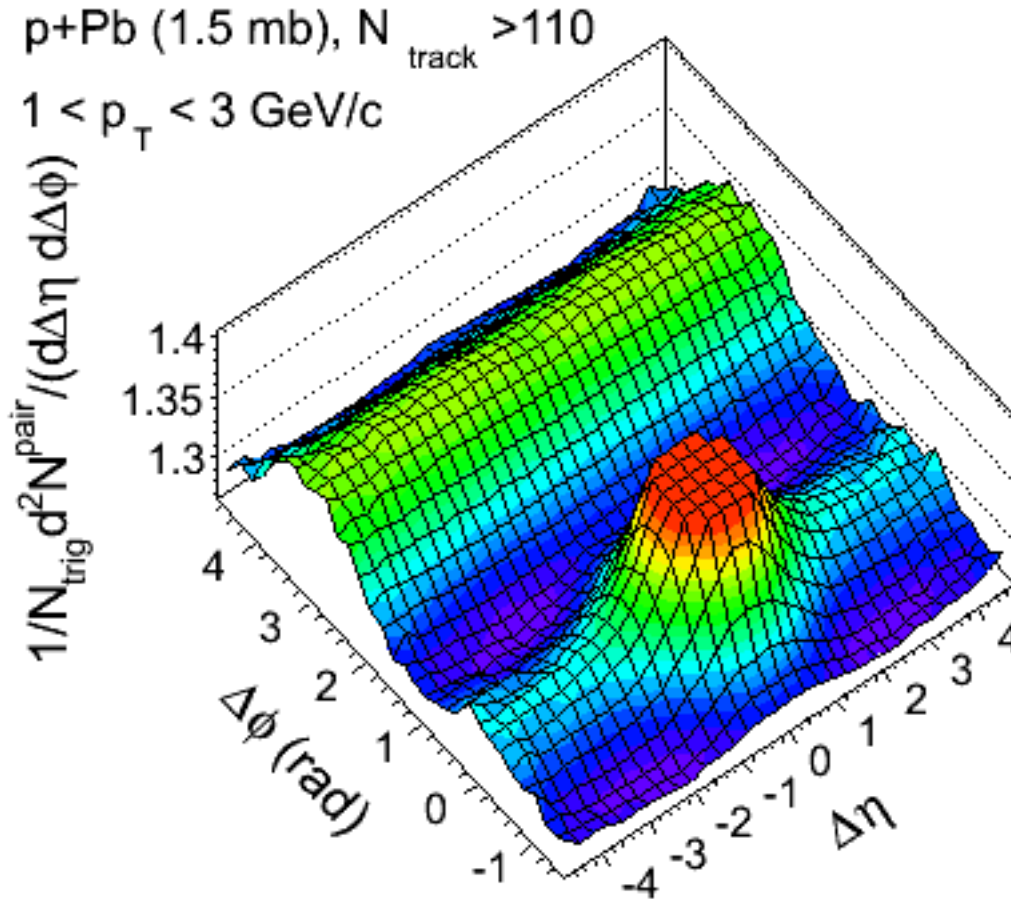
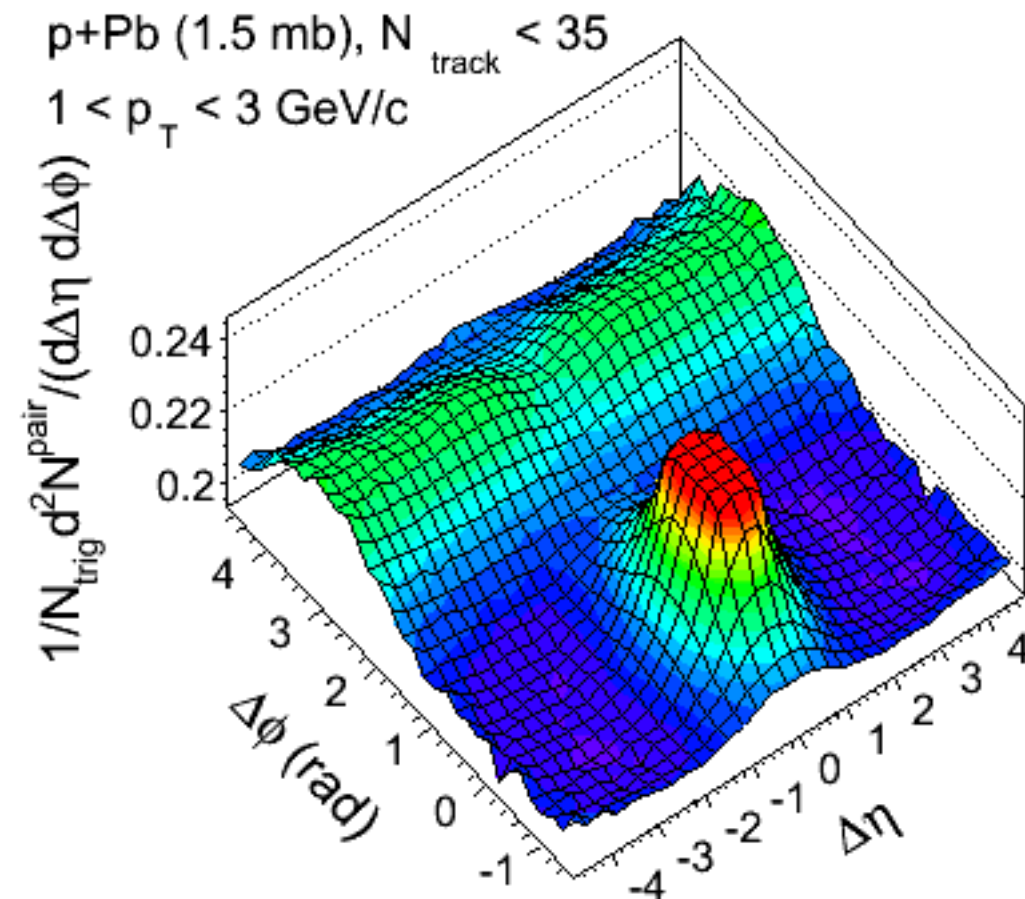
Note: ψ_n is the minor axis of initial geometry distribution.



- 我们在 $b=0$ 的中心碰撞中给出各个阶次的集体流，和实验结果非常相似。

AMPT results on long-range correlation in p+Pb

G.-L. Ma and A. Bzdak, PLB 739, 209 (2014)

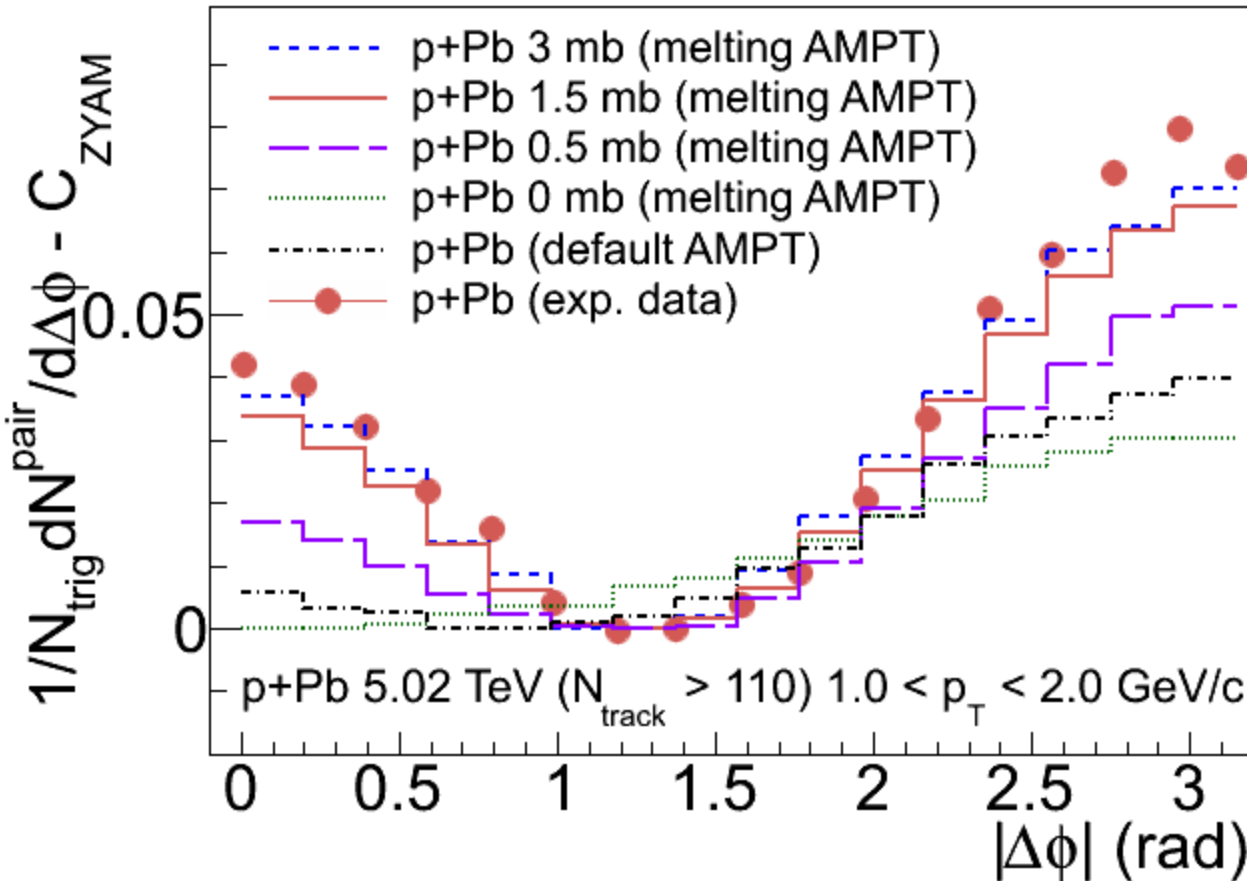


- No long-range correlation in low-multiplicity p+Pb.

- Clear long-range correlation in high-multiplicity p+Pb.

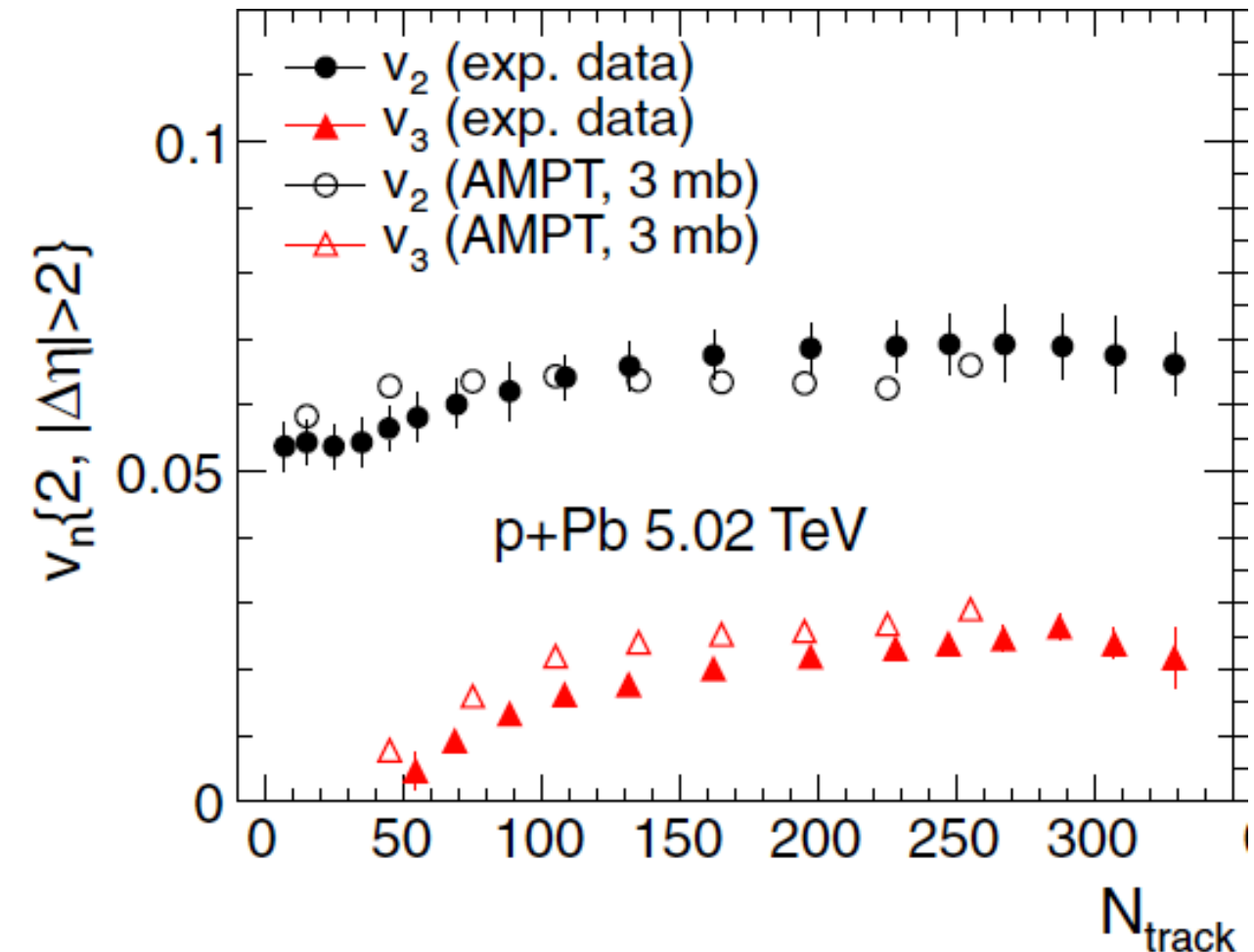
AMPT results on long-range correlation and v_n

G.-L. Ma and A. Bzdak, Phys.Lett. B 739 (2014) 209.



- The two-particle correlation in p+Pb can be well described by $\sigma=1.5-3$ mb.
- The signal strength increases with σ and vanishes for $\sigma = 0$ mb. \Rightarrow Long-range correlation is produced by parton cascade.

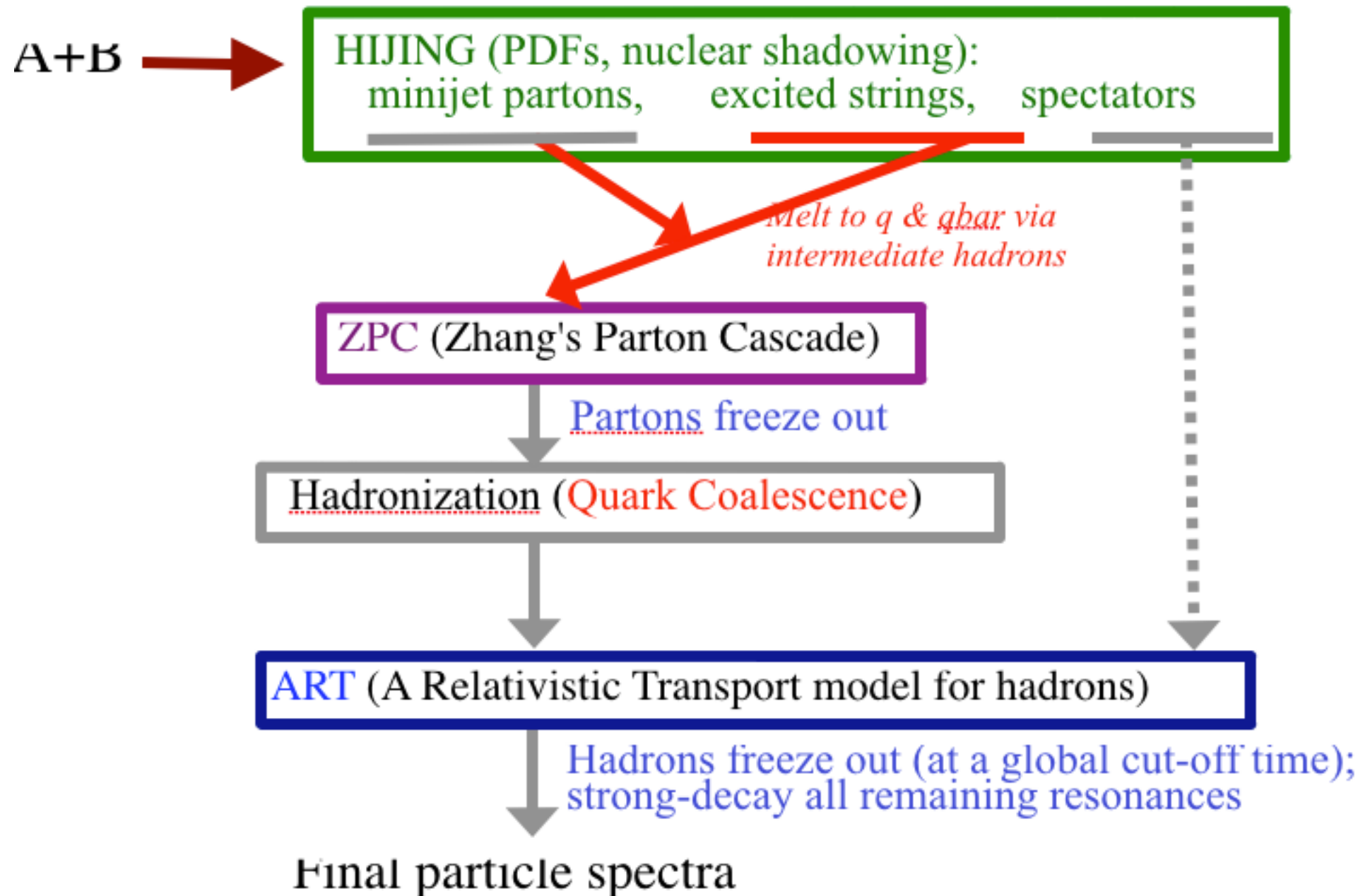
A. Bzdak and G.-L. Ma, Phys.Rev.Lett. 113, (2014) 252301.



- For p+Pb, AMPT ($\sigma=3$ mb) reproduces the integrated two-particle v_2 and v_3 .

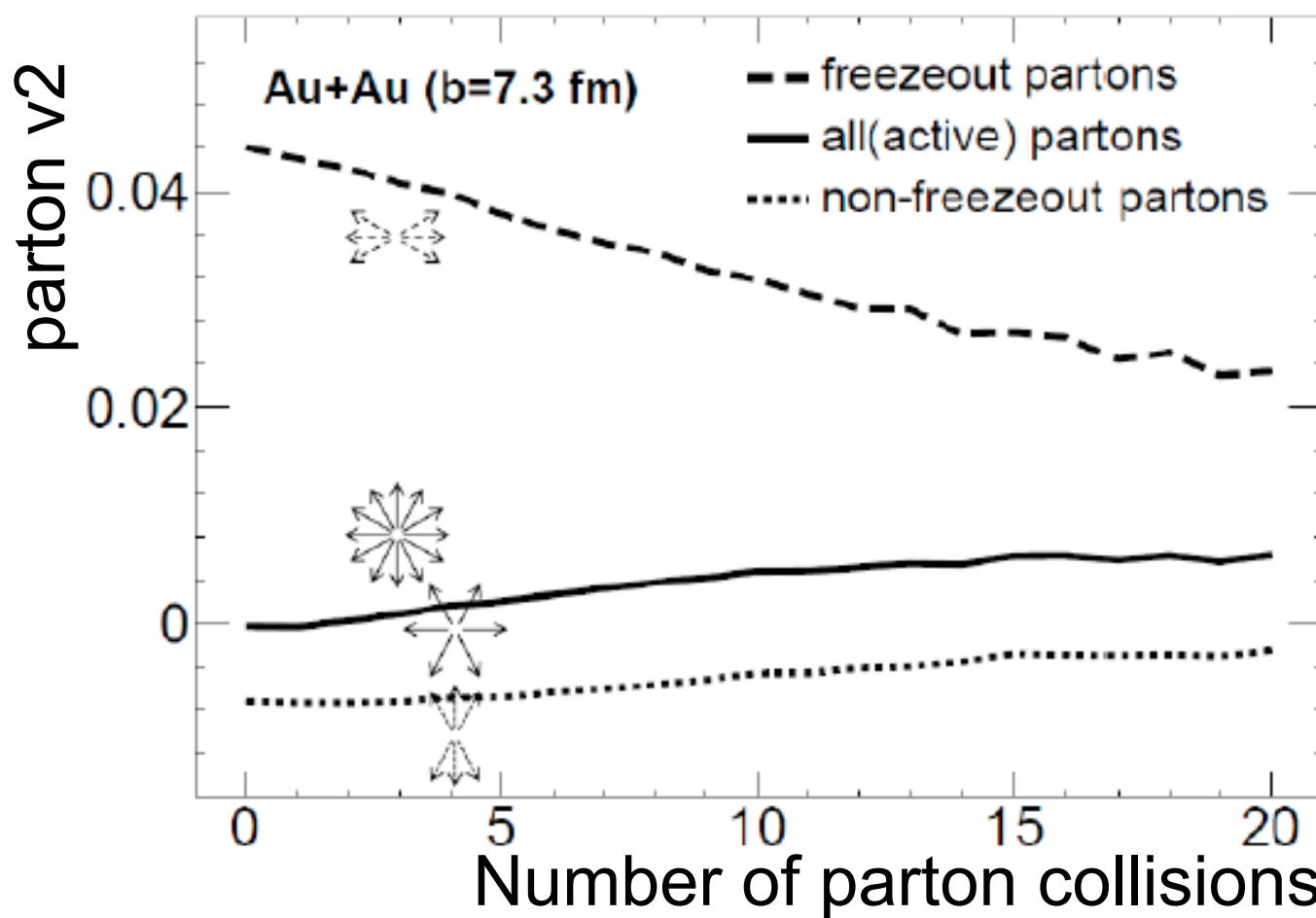
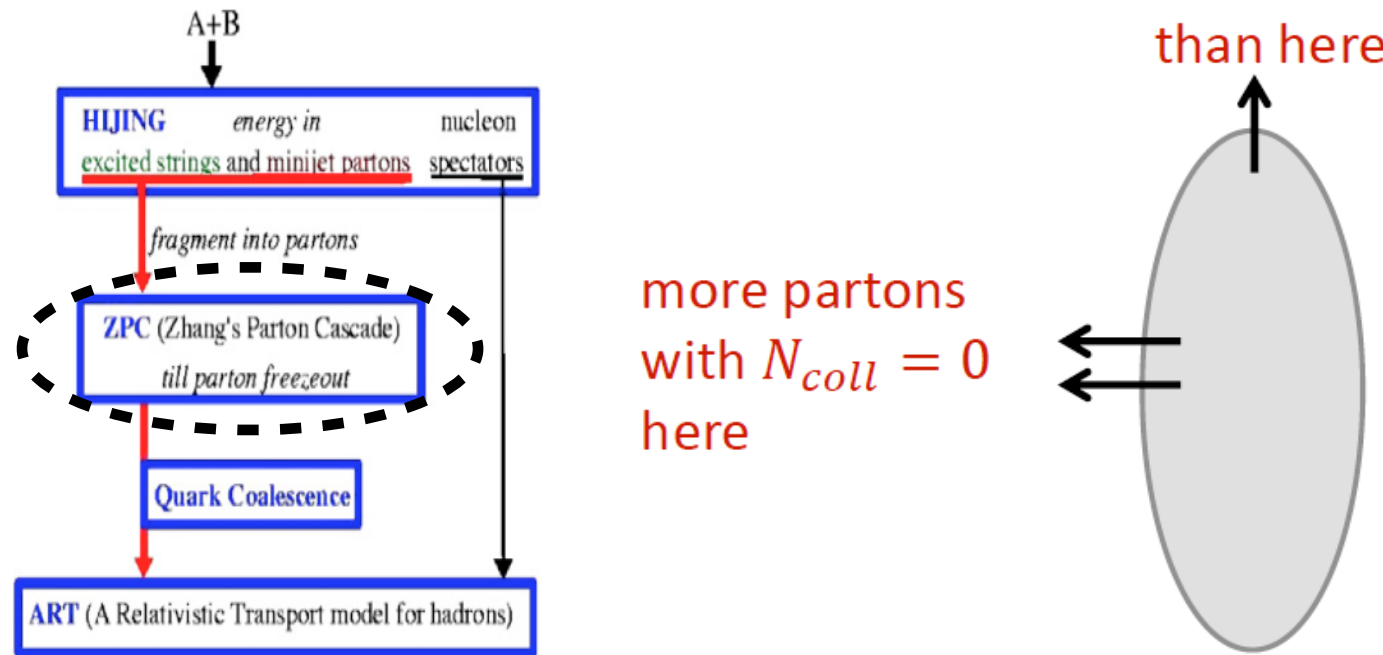
Studying flow` with AMPT model

Z.-W.Lin et al., Phys. Rev C 72, 064901 (2005)



flow` = flow(escape ⊕ hydro ⊕ CGC) ⊕ non-flow

Escape-type small systems?



L. He, T. Edmonds, Zi-Wei Lin, F. Liu, D. Molnar, Fuqiang Wang, Phys.Lett. B753 (2016) 506.

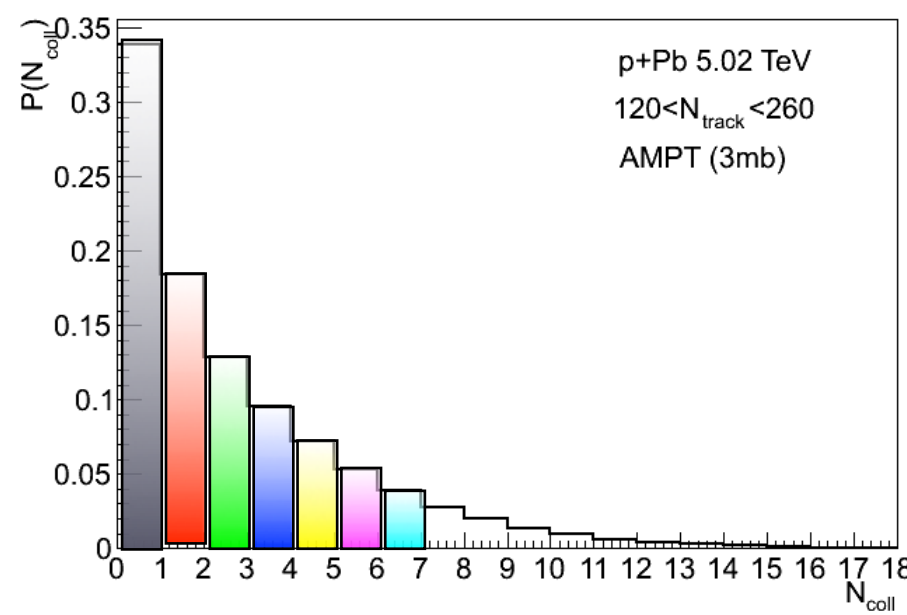
larger probability for partons to escape along the short axis

Features:

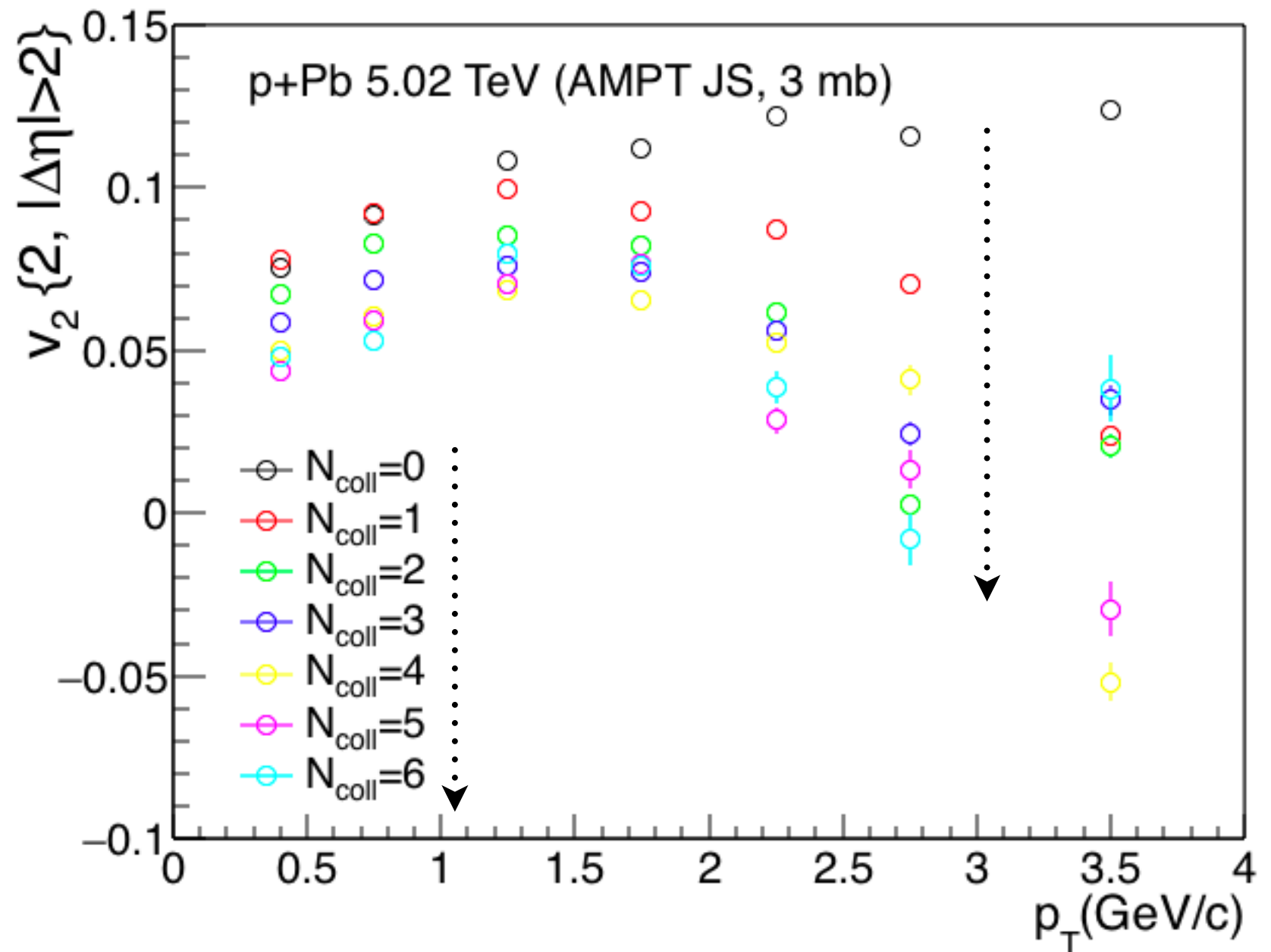
- All partons' v_2 increases with N_{coll}
- Freezeout partons' v_2 decreases with N_{coll} .
- Non-freezeout partons go from negative v_2 to small v_2 after collisions
- The escape contribution to total v_2 is large ($\sim 70\%$) in mid-central $Au+Au$; larger for $d+Au$ ($\sim 90\%$)

Final partons' v2 with different Ncoll

Final freezeout partons

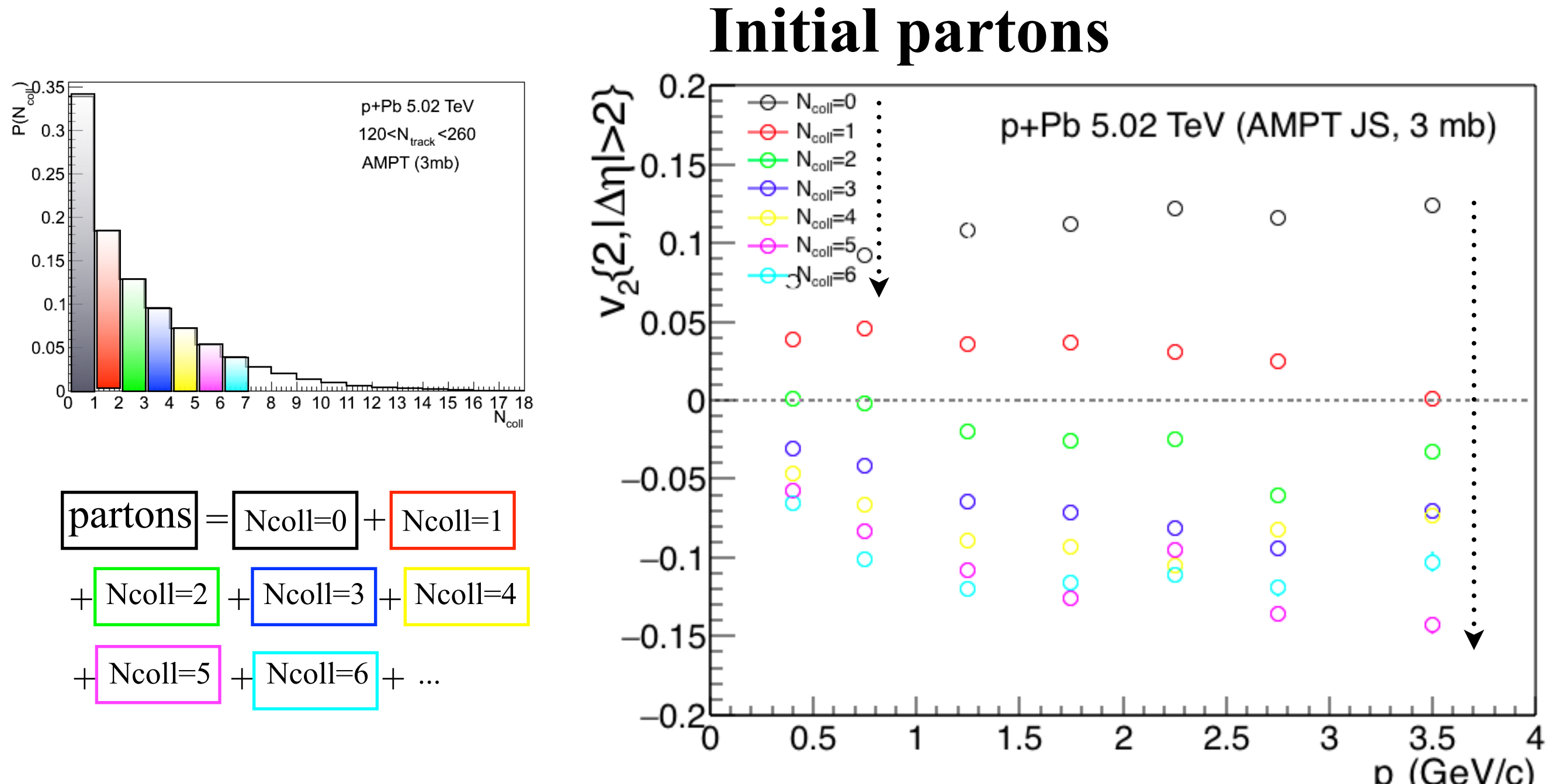


$$\begin{aligned} \text{partons} &= \boxed{N_{\text{coll}}=0} + \boxed{N_{\text{coll}}=1} \\ &+ \boxed{N_{\text{coll}}=2} + \boxed{N_{\text{coll}}=3} + \boxed{N_{\text{coll}}=4} \\ &+ \boxed{N_{\text{coll}}=5} + \boxed{N_{\text{coll}}=6} + \dots \end{aligned}$$



- Final partons' v2 decreases with Ncoll.

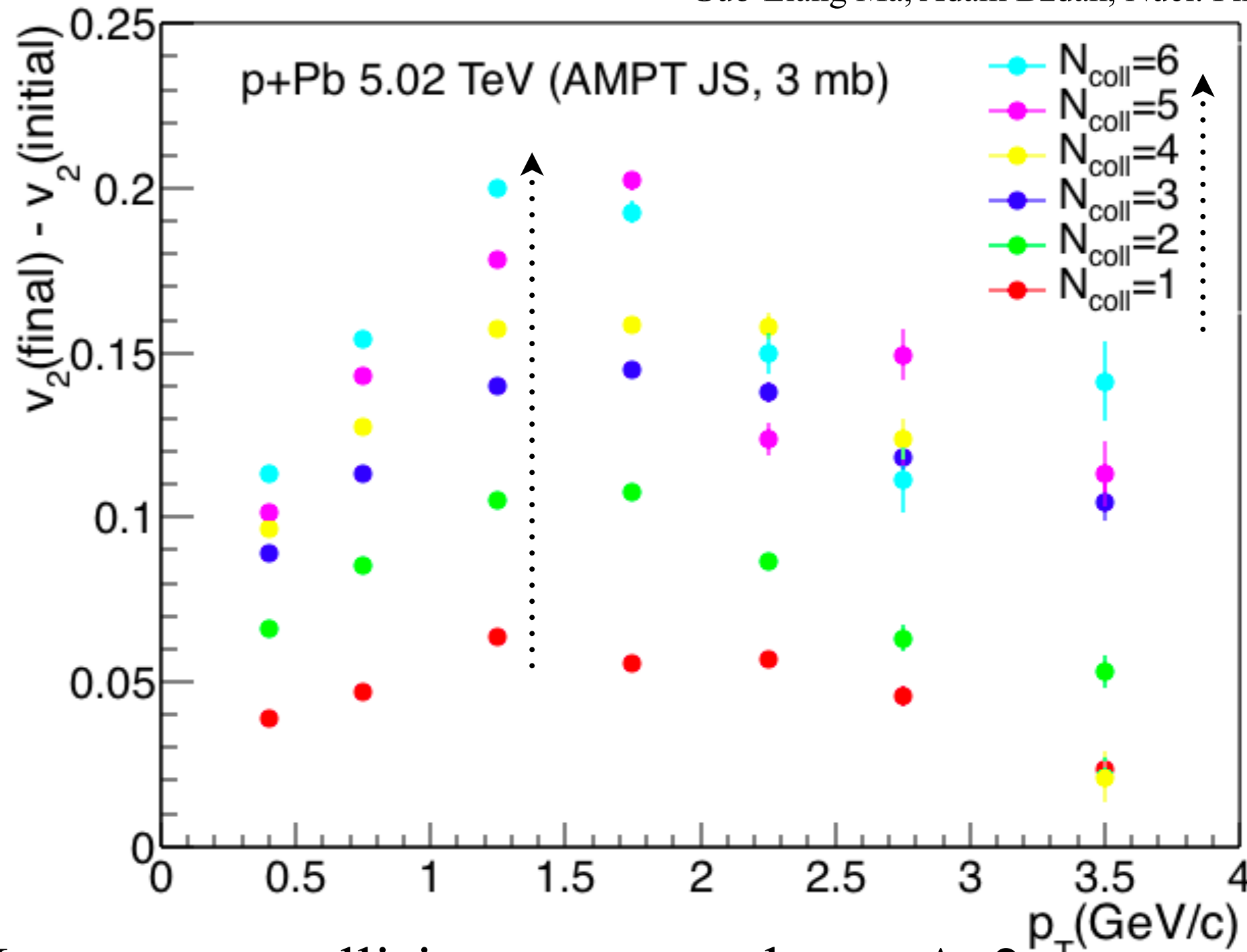
Initial partons' v2 with different Ncoll



- In the initial state, v_2 (small N_{coll}) >0 and v_2 (large N_{coll}) <0 since the average v_2 must be zero.

Partons' Δv_2 with different N_{coll}

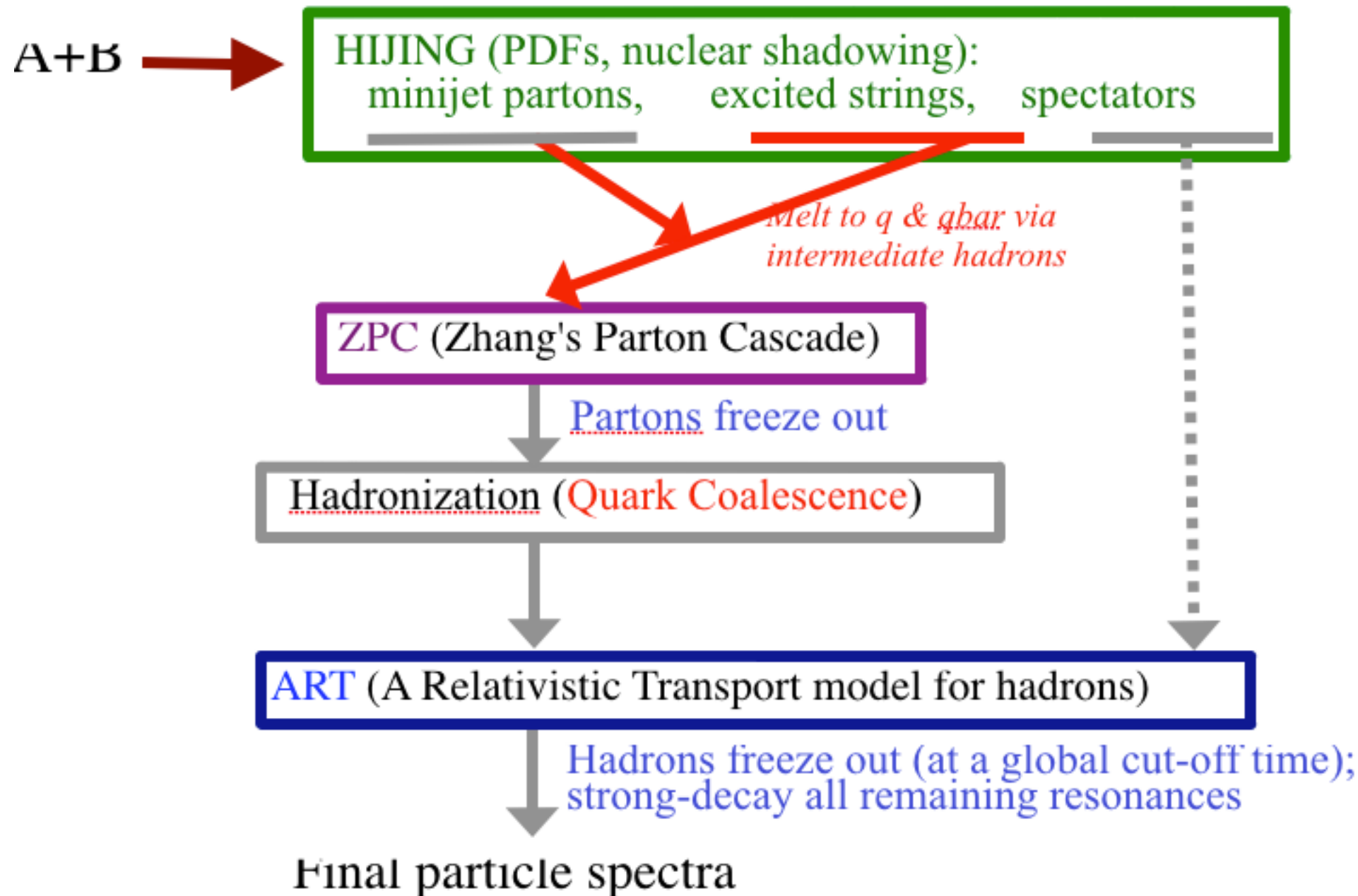
Guo-Liang Ma, Adam Bzdak, Nucl. Phys. A 956 (2016) 745.



- More parton collisions generate larger Δv_2 .
=>The escape mechanism needs collisions.

Studying flow` with AMPT model

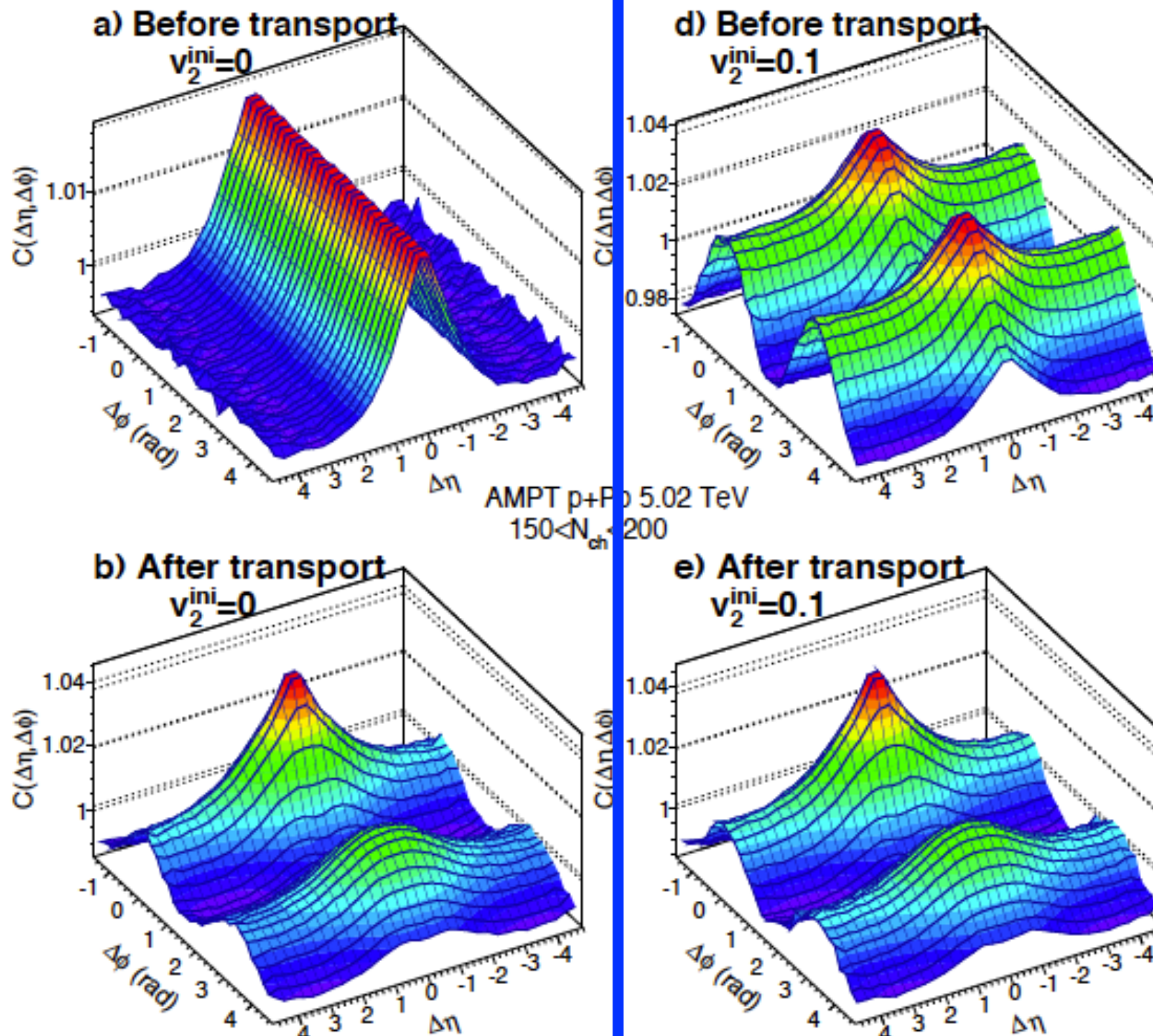
Z.-W.Lin et al., Phys. Rev C 72, 064901 (2005)



flow` = flow(escape ⊕ hydro ⊕ CGC) ⊕ non-flow

AMPT with introducing an initial ‘flow’

Initial flow $v_2=0$

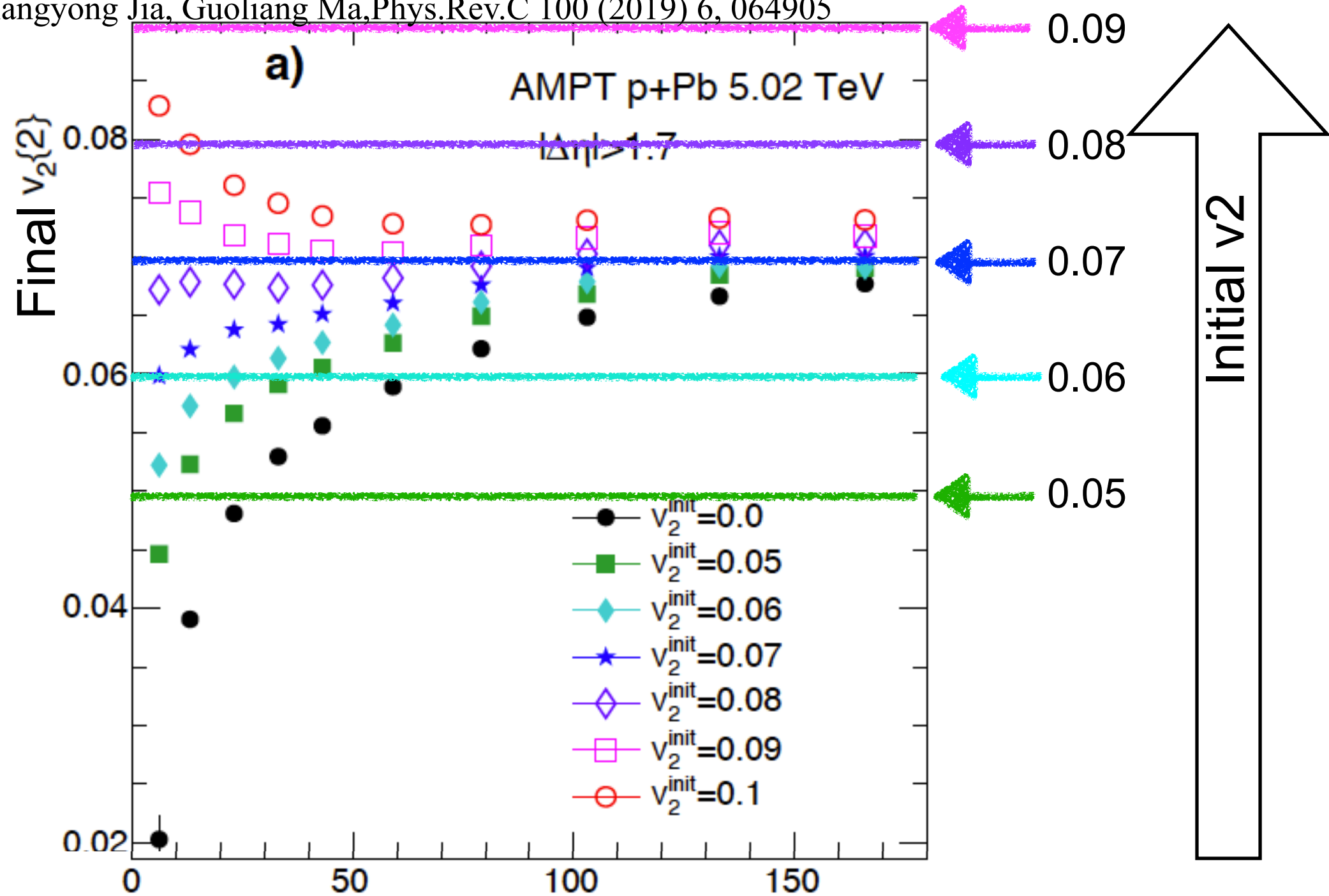


Initial flow $v_2=0.1$

- If an initial momentum anisotropy from CGC, how does the initial flow interplay with final flow? Can it survive?

AMPT results with different strengths of initial flow

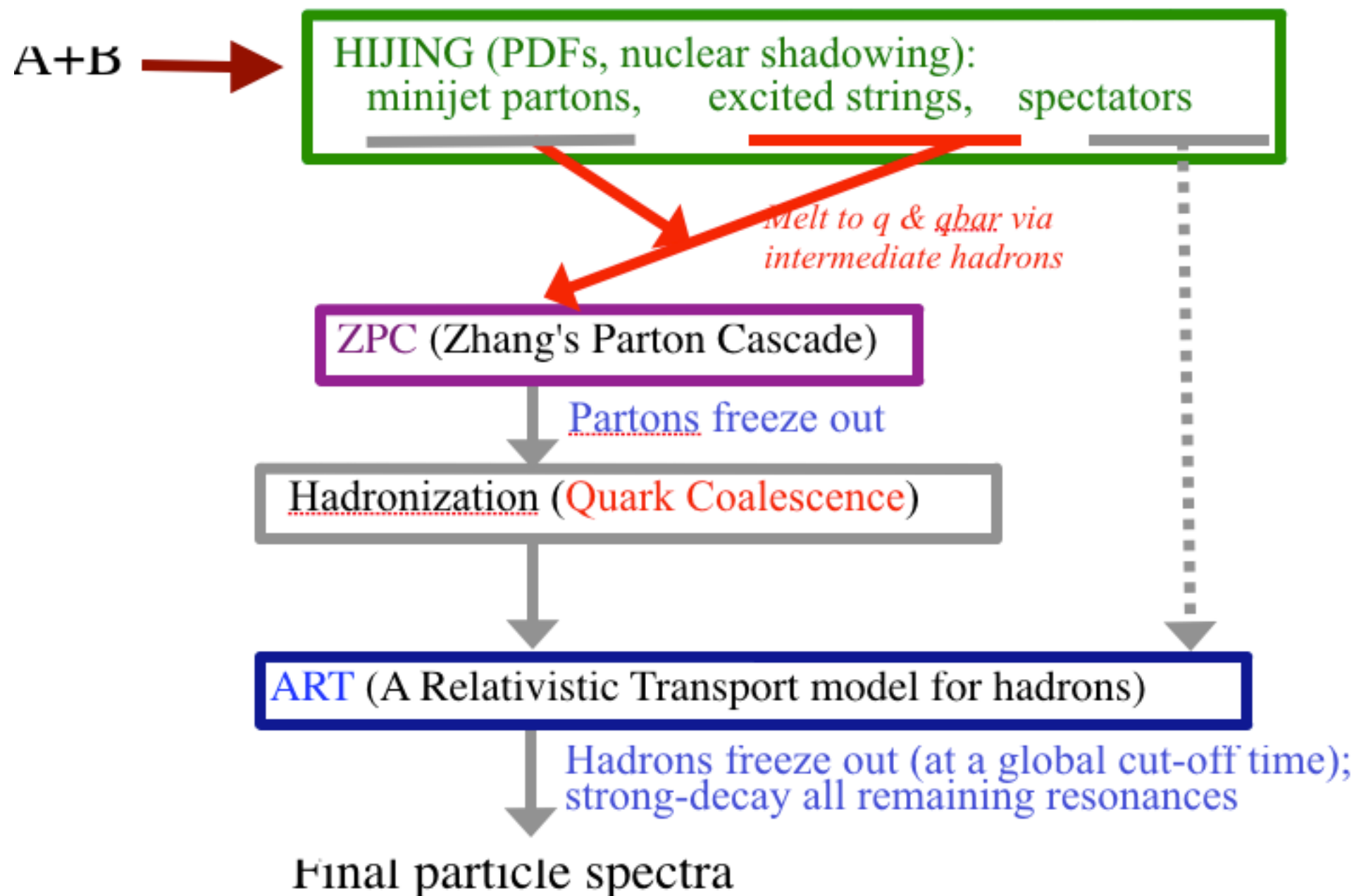
Maowu Nie, Li Yi, Jiangyong Jia, Guoliang Ma, Phys.Rev.C 100 (2019) 6, 064905



- The existence of initial flow affects final flow measurement. $\langle N_{\text{ch}} \rangle$
- At small N_{ch} , initial flow is basically dominant and easily survive.
- At large N_{ch} , final flow is dominant; initial flow but help increase final flow.

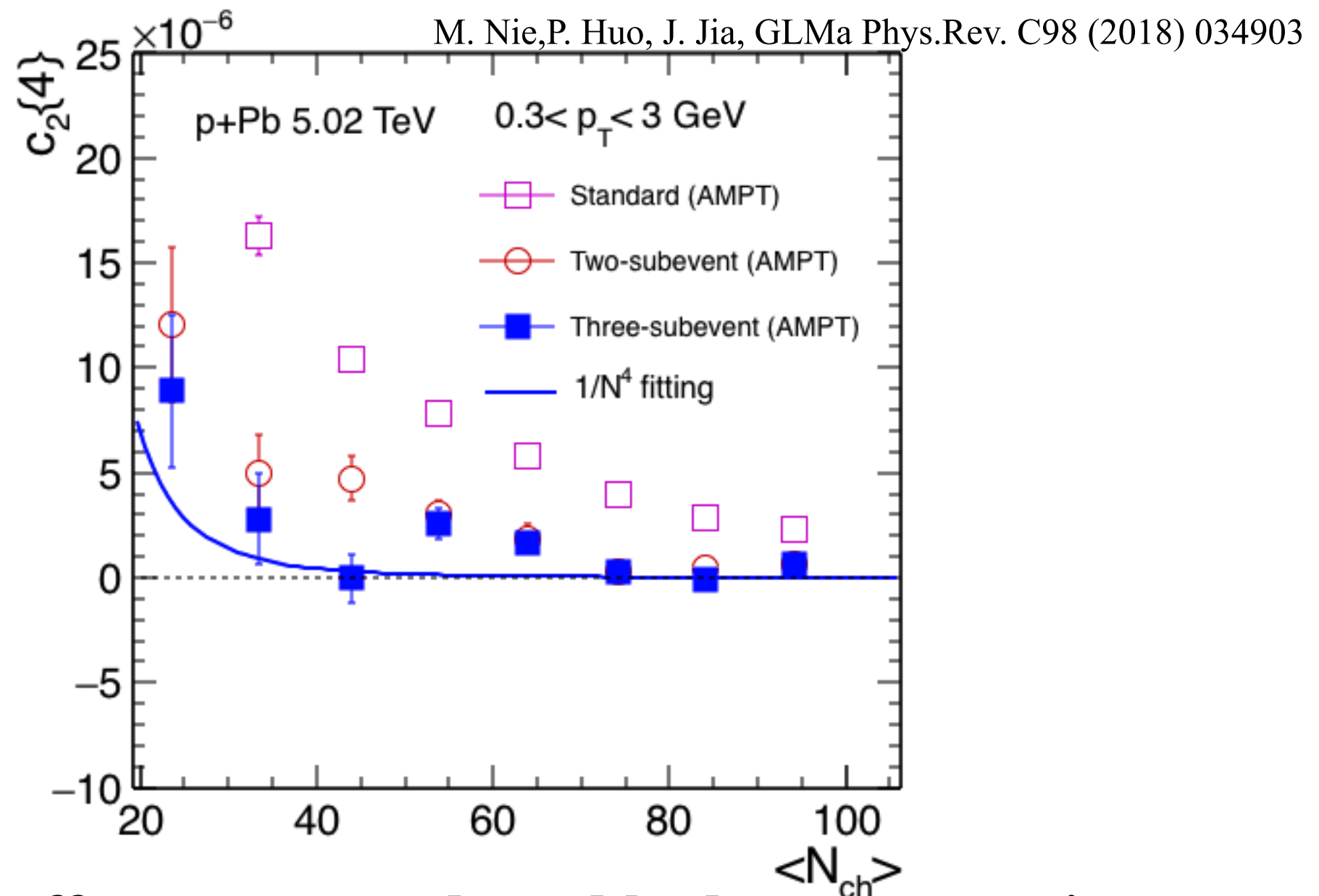
Studying flow` in small systems with AMPT model

Z.-W.Lin et al., Phys. Rev C 72, 064901 (2005)



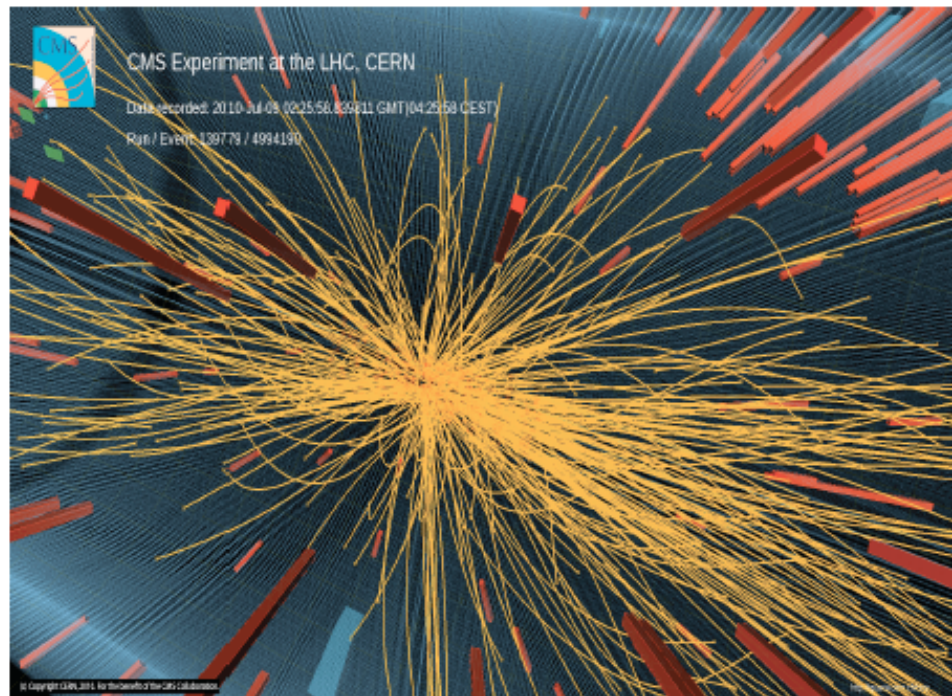
flow` = flow(escape ⊕ hydro ⊕ CGC) ⊕ non-flow

AMPT results on non-flow in p+A



- By turning off parton cascade and hadron rescatterings, we can study non-flow due to jets , resonance decays, TMC, etc..
- Subevent cumulant method suppresses jets and resonance decays.
- The three-subevent $c_2\{4\}$ obeys $\sim 1/N^4$. **<=TMC effect**

Particle production under TMC

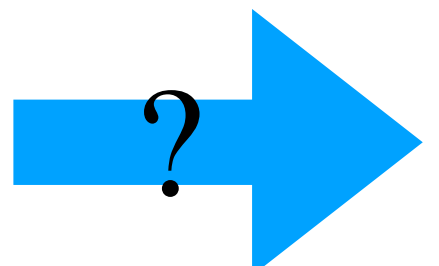


- All produced N particle must obey the transverse momentum conservation(TMC).
- But ones only can experimentally measure part of them, i.e. k particles ($k < N$), due to the limits of acceptance and resolution.

N-particle momentum probability distribution:

$$f_N(\vec{p}_1, \dots, \vec{p}_N) = \frac{1}{A} \delta^2(\vec{p}_1 + \dots + \vec{p}_N) f(\vec{p}_1) \cdots f(\vec{p}_N),$$

$$A = \int_F \delta^2(\vec{p}_1 + \dots + \vec{p}_N) f(\vec{p}_1) \cdots f(\vec{p}_N) d^2\vec{p}_1 \cdots d^2\vec{p}_N,$$

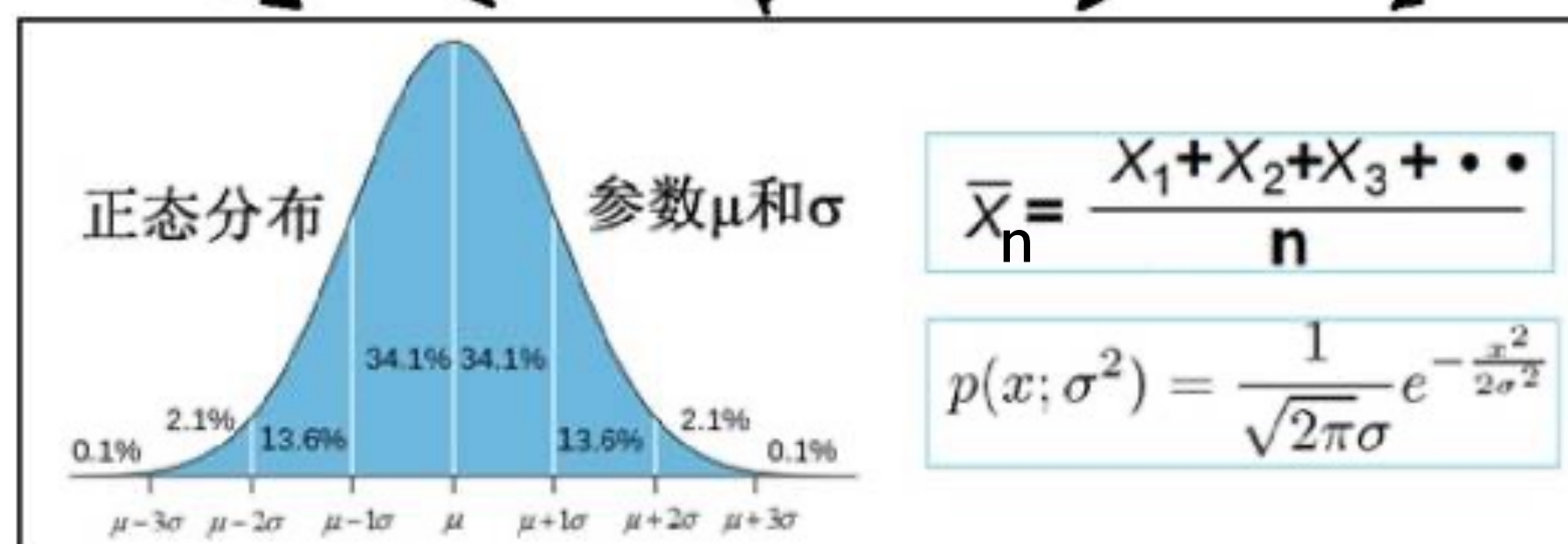
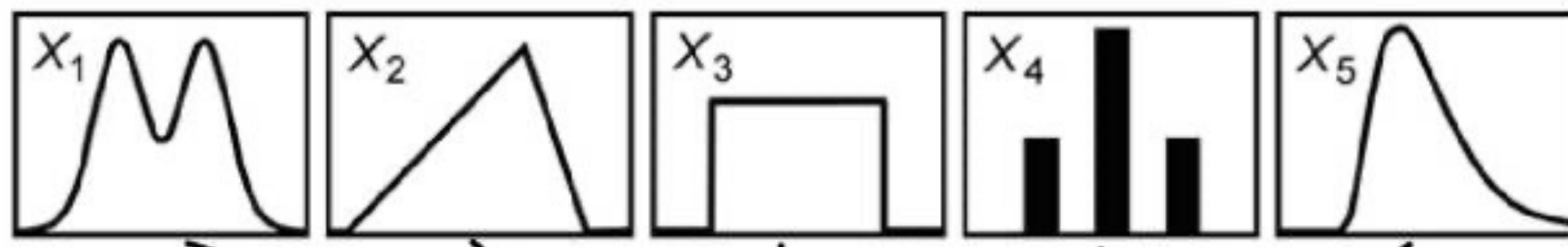


k-particle momentum probability distribution:

$$f_k(\vec{p}_1, \dots, \vec{p}_k) = \frac{1}{A} f(\vec{p}_1) \cdots f(\vec{p}_k) \int_F \delta^2(\vec{p}_1 + \dots + \vec{p}_N) f(\vec{p}_{k+1}) \cdots f(\vec{p}_N) d^2\vec{p}_{k+1} \cdots d^2\vec{p}_N$$

Central limit theorem

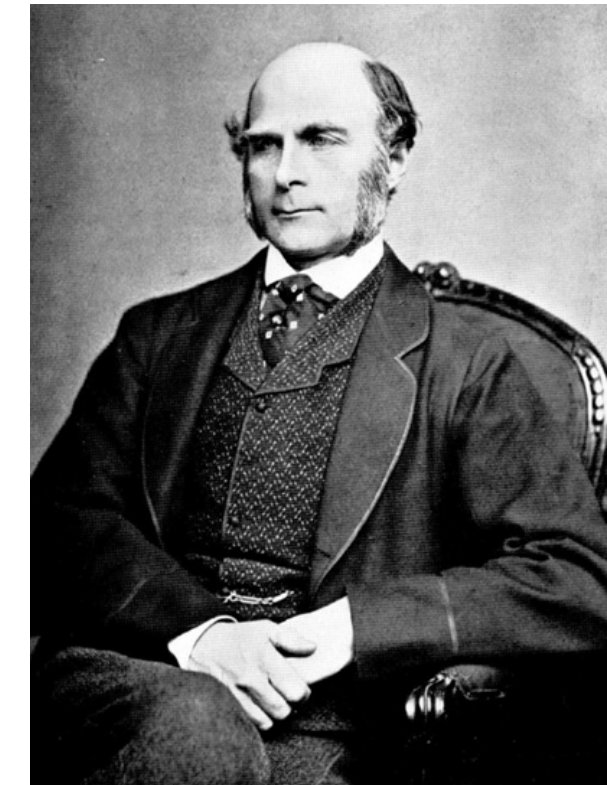
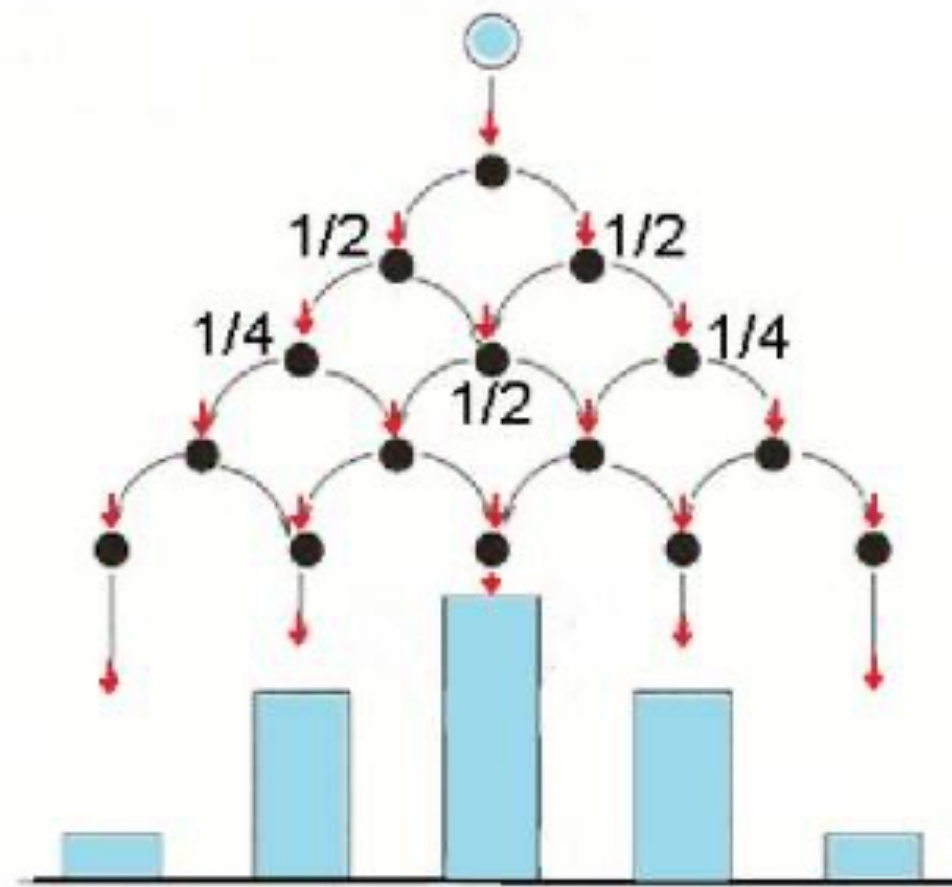
Why always normal distribution?



Abraham de Moivre
法国数学家棣莫佛
(1667-1754)

- For large enough n , the distribution of \bar{X}_n is close to the normal distribution with mean μ and variance σ^2/n .

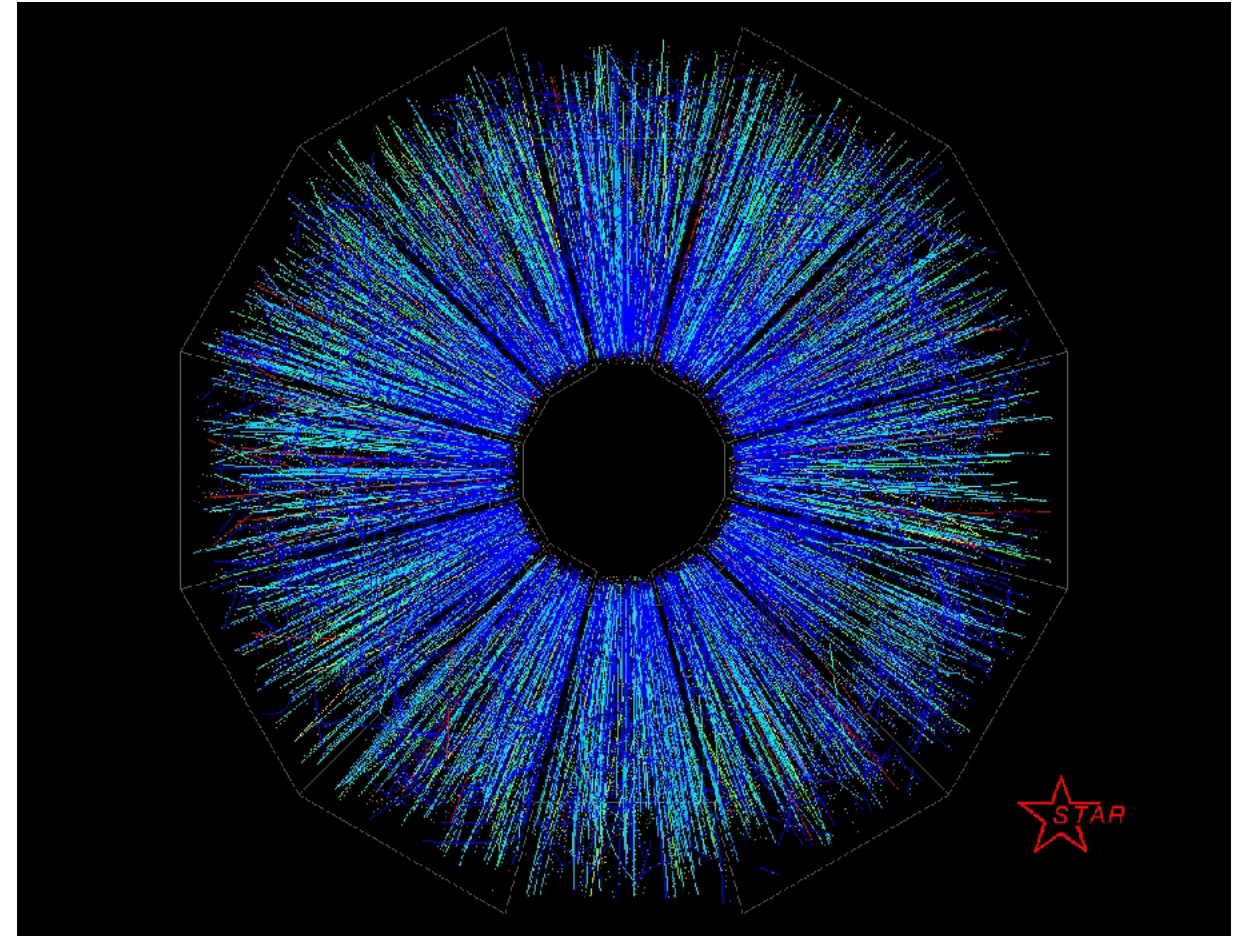
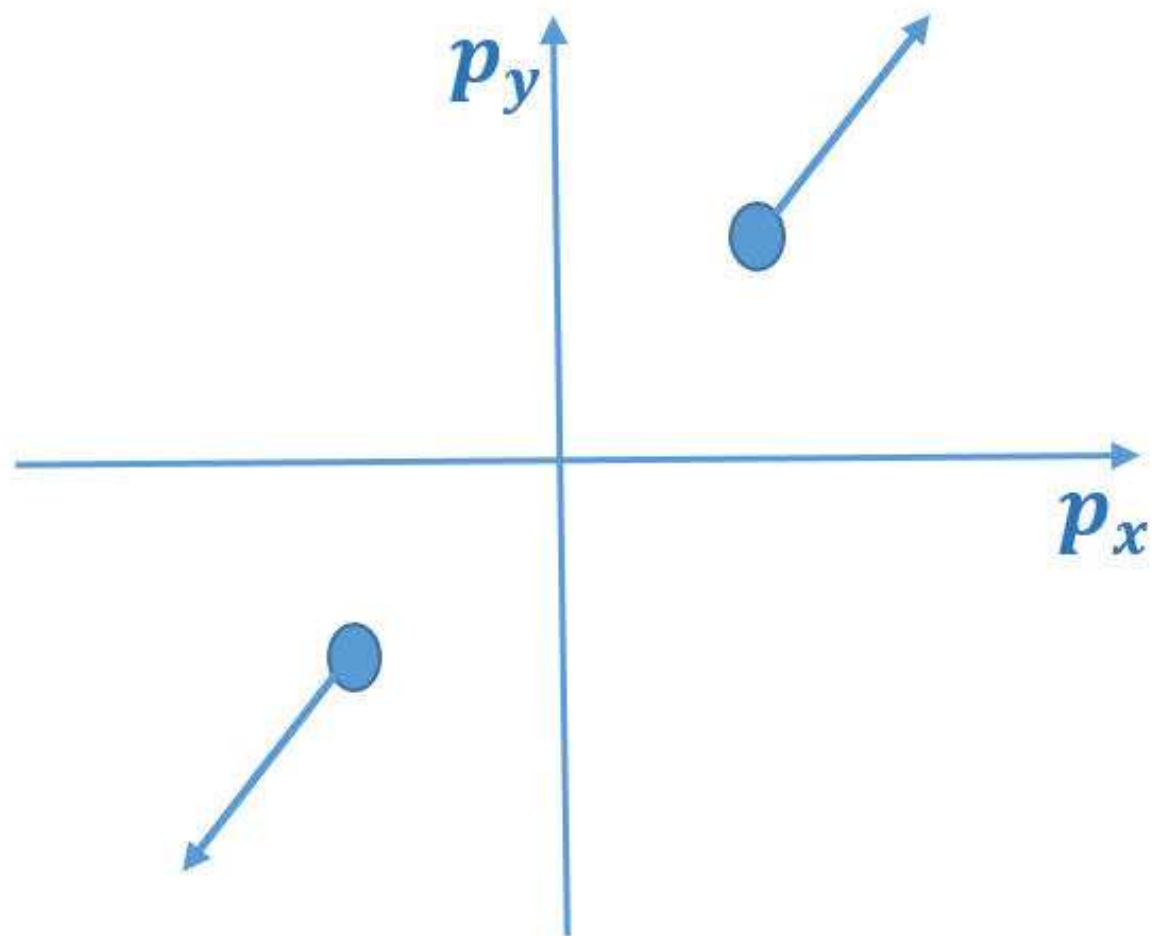
Central limit theorem



Sir Francis Galton (1822-1911)

- The bean machine demonstrates the central limit theorem, in particular that the normal distribution is approximate to the binomial distribution.

Multi-particle correlation due to TMC



$$f_k(\vec{p}_1, \dots, \vec{p}_k) = \frac{1}{A} f(\vec{p}_1) \cdots f(\vec{p}_k) \int_F \delta^2(\vec{p}_1 + \dots + \vec{p}_N) f(\vec{p}_{k+1}) \cdots f(\vec{p}_N) d^2 \vec{p}_{k+1} \cdots d^2 \vec{p}_N.$$

$\langle \mathbf{p} \rangle = 0$

$\sigma^2 = \langle \mathbf{p}^2 \rangle$

$$f_k(\vec{p}_1, \dots, \vec{p}_k) = f(\vec{p}_1) \cdots f(\vec{p}_k) \frac{N}{N - k} \exp \left(-\frac{(\vec{p}_1 + \dots + \vec{p}_k)^2}{(N - k) \langle \mathbf{p}^2 \rangle_F} \right)$$

c₂{2} from TMC

$$c_2\{2\} = \langle e^{i2(\phi_1 - \phi_2)} \rangle = \frac{\int_0^{2\pi} f_2(\vec{p}_1, \vec{p}_2) e^{i2(\phi_1 - \phi_2)} d\phi_1 d\phi_2}{\int_0^{2\pi} f_2(\vec{p}_1, \vec{p}_2) d\phi_1 d\phi_2}$$

$$f_2(\vec{p}_1, \vec{p}_2) = f(\vec{p}_1) f(\vec{p}_2) \frac{N}{N-2} \exp\left(-\frac{p_1^2 + p_2^2 + 2p_1 p_2 \cos(\phi_1 - \phi_2)}{(N-2) \langle p^2 \rangle_F}\right)$$

$$c_2\{2\}|_{p_1, p_2} = \frac{I_2(x)}{I_0(x)}, \quad x = \frac{2p_1 p_2}{(N-2) \langle p^2 \rangle_F}$$

($I_k(x)$ is the modified Bessel function of the 1st kind.)

$$c_2\{2\}|_{p_1, p_2} \approx \frac{p_1^2 p_2^2}{2(N-2)^2 \langle p^2 \rangle_F^2}, \quad \text{if } p_1 p_2 < \frac{1}{2}(N-2) \langle p^2 \rangle_F.$$

c₂{k} from TMC

$$c_2\{2\}|_{p_1,p_2} \approx \frac{p_1^2 p_2^2}{2(N-2)^2 \langle p^2 \rangle_F^2};$$

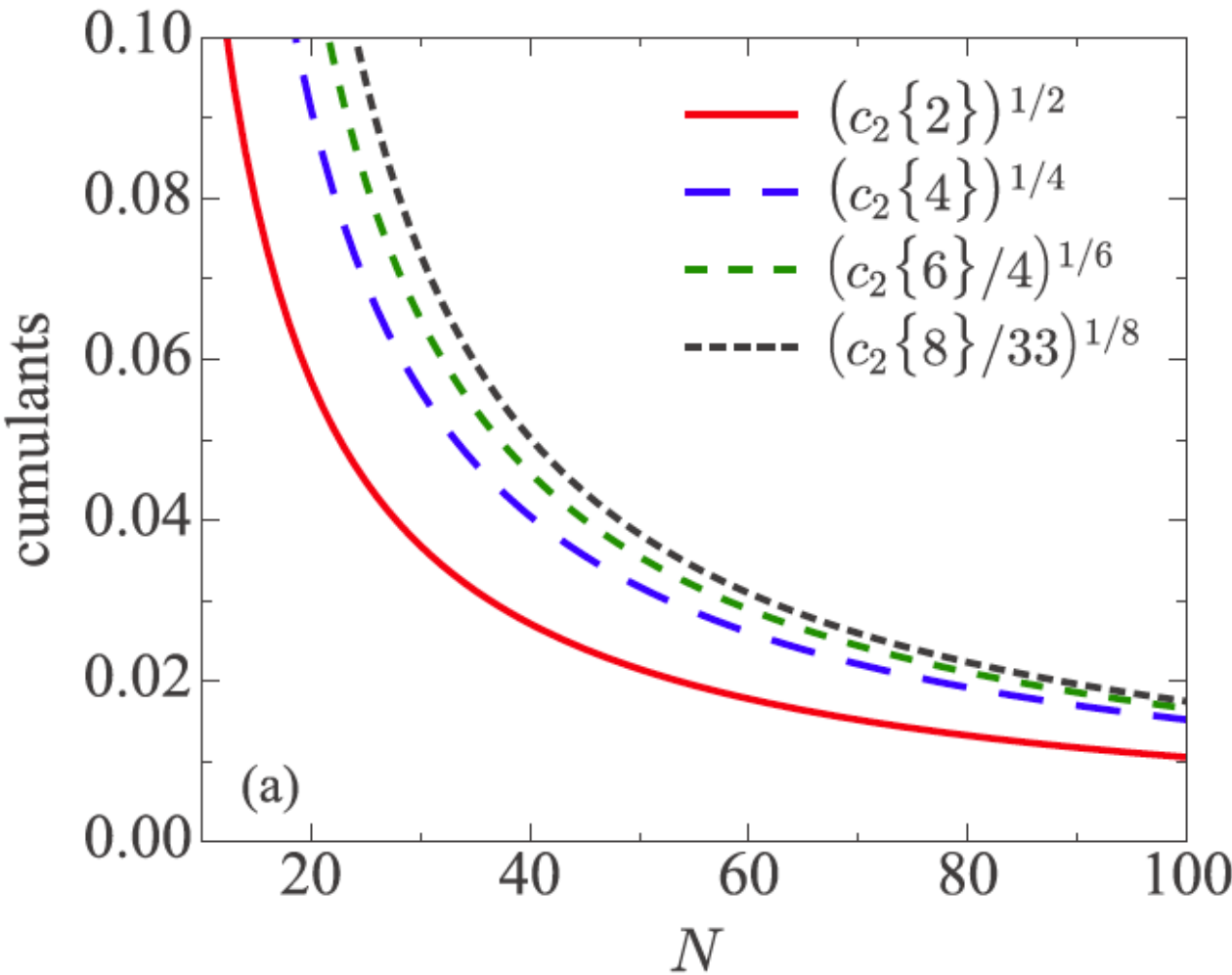
$$c_2\{4\}|_{p_1,p_2,p_3,p_4} \approx \frac{(p_1 p_2 p_3 p_4)^2}{(N-4)^4 \langle p^2 \rangle_F^4}.$$

$$\frac{1}{4} c_2\{6\}|_{p_1,\dots,p_6} \approx \frac{3}{2} \frac{(p_1 p_2 p_3 p_4 p_5 p_6)^2}{(N-6)^6 \langle p^2 \rangle_F^6}$$

$$\frac{1}{33} c_2\{8\}|_{p_1,\dots,p_8} \approx \frac{24}{11} \frac{(p_1 p_2 p_3 p_4 p_5 p_6 p_7 p_8)^2}{(N-8)^8 \langle p^2 \rangle_F^8}$$

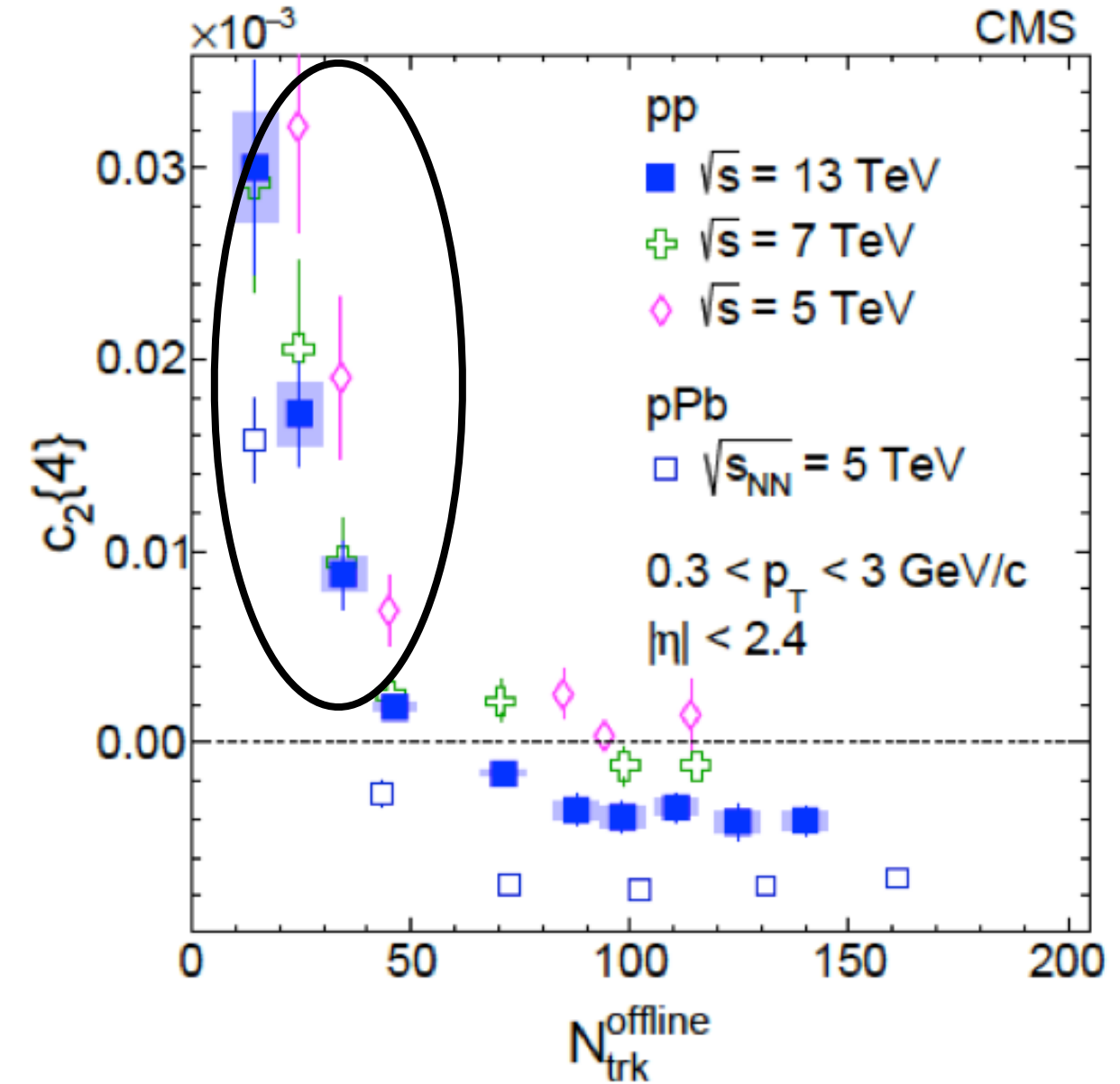
$c_2\{4\}$ from TMC vs the data

Our TMC results:



- Always $c_2\{k\} > 0$

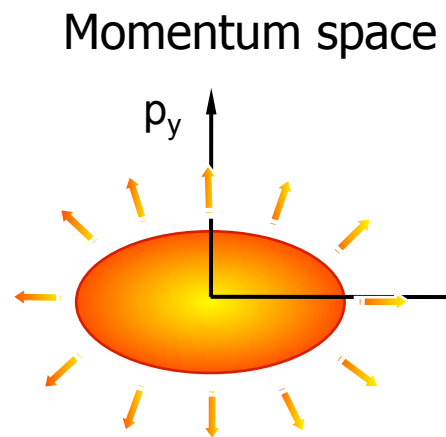
The data:



- $c_2\{4\}$ changes from positive to negative with N_{track} .

- => Data = TMC + negative part?

c₂{2} from TMC+hydro-like flow



$$f(p, \phi) = \frac{g(p)}{2\pi} [1 + 2v_2(p)\cos(2\phi - 2\Psi_2)],$$

CLT($\langle p \rangle = 0$, $\sigma_x^2 = \langle p_x^2 \rangle$, $\sigma_y^2 = \langle p_y^2 \rangle$)

$$f_2(p_1, \phi_1, p_2, \phi_2) = f(p_1, \phi_1)f(p_2, \phi_2) \frac{N}{N-2} \exp\left(-\frac{(p_{1,x} + p_{2,x})^2}{2(N-2)\langle p_x^2 \rangle_F} - \frac{(p_{1,y} + p_{2,y})^2}{2(N-2)\langle p_y^2 \rangle_F}\right)$$

$$\begin{aligned} \langle p_x^2 \rangle_F &= \frac{1}{2} \langle p^2 \rangle_F (1 + \bar{v}_{2,F}) \\ \langle p_y^2 \rangle_F &= \frac{1}{2} \langle p^2 \rangle_F (1 - \bar{v}_{2,F}) \end{aligned}$$

$$c_2\{2\} =$$

$$\langle e^{2i(\phi_1 - \phi_2)} \rangle|_{p_1, p_2} = \frac{\int_0^{2\pi} f_2(p_1, \phi_1; p_2, \phi_2) e^{2i(\phi_1 - \phi_2)} d\phi_1 d\phi_2}{\int_0^{2\pi} f_2(p_1, \phi_1; p_2, \phi_2) d\phi_1 d\phi_2}$$



$$c_2\{2\} \approx \boxed{(v_2(p))^2} - \frac{p^2 v_2(p) [2v_2(p) - \bar{v}_{2,F}]}{(N-2)\langle p^2 \rangle_F} + \boxed{\frac{p^4}{2(N-2)^2 \langle p^2 \rangle_F^2}}$$

Flow

TMC

c2{4} from TMC+hydro-like flow

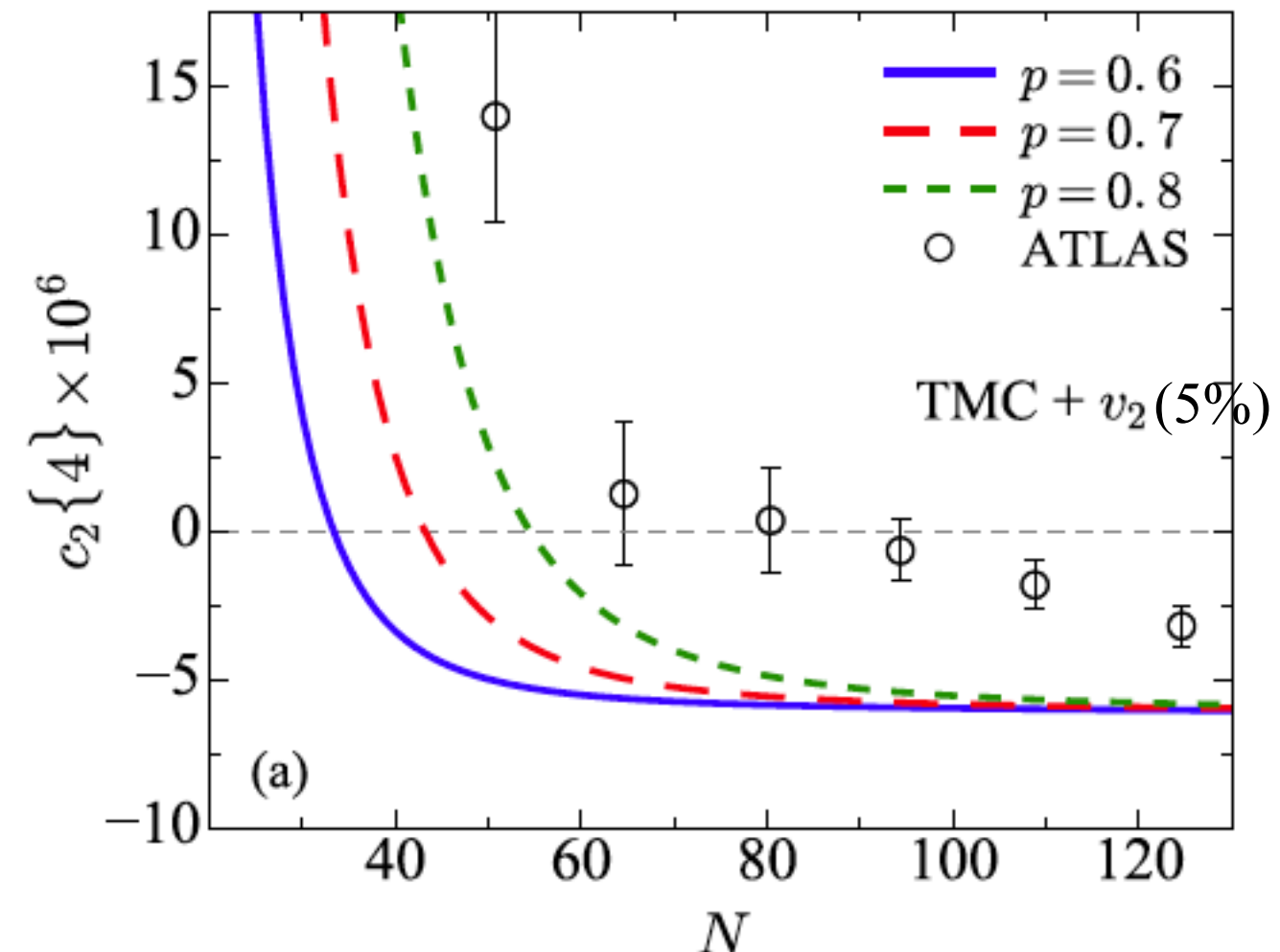
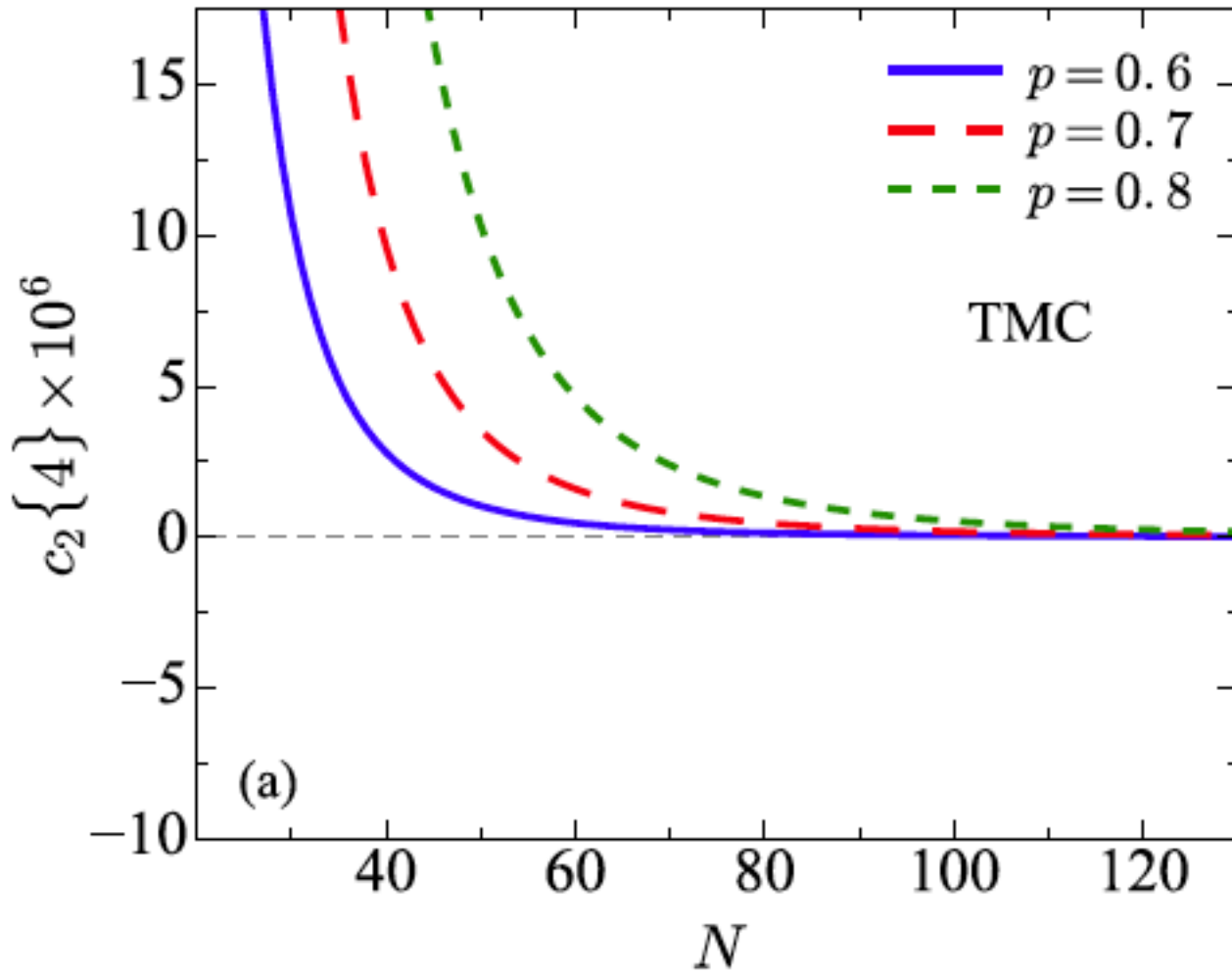
$$f_4(p_1, \phi_1, \dots, p_4, \phi_4) = f(p_1, \phi_1) \cdots f(p_4, \phi_4) \frac{N}{N-4} \times \\ \exp \left(-\frac{(p_{1,x} + \dots + p_{4,x})^2}{2(N-4) \langle p_x^2 \rangle_F} - \frac{(p_{1,y} + \dots + p_{4,y})^2}{2(N-4) \langle p_y^2 \rangle_F} \right)$$

$$\langle e^{2i(\phi_1 + \phi_2 - \phi_3 - \phi_4)} \rangle|_{p_1, p_2, p_3, p_4} = \frac{\int_0^{2\pi} f_4(p_1, \phi_1, \dots, p_4, \phi_4) e^{2i(\phi_1 + \phi_2 - \phi_3 - \phi_4)} d\phi_1 \cdots d\phi_4}{\int_0^{2\pi} f_4(p_1, \phi_1, \dots, p_4, \phi_4) d\phi_1 \cdots d\phi_4}$$

$$c_2\{4\} \approx (v_2(p))^4 - \frac{2p^2(v_2(p))^3[2v_2(p) - \bar{v}_{2,F}]}{(N-4) \langle p^2 \rangle_F} + \frac{2p^4(v_2(p))^2}{(N-4)^2 \langle p^2 \rangle_F^2} - \frac{2p^6v_2(p)[8v_2(p) - 3\bar{v}_{2,F}]}{(N-4)^3 \langle p^2 \rangle_F^3} \\ + \frac{p^8[442(v_2(p))^2 - 360v_2(p)\bar{v}_{2,F} + 27(\bar{v}_{2,F})^2]}{6(N-4)^4 \langle p^2 \rangle_F^4} + \frac{3p^8}{2(N-4)^4 \langle p^2 \rangle_F^4} - 2(c_2\{2\})^2,$$

$c_2\{4\}$ from TMC+hydro-like flow

Adam Bzdak and Guo-Liang Ma, Phys. Lett. B 781, 117 (2018)



- Transverse momentum conservation brings $c_2\{k\} \propto 1/N^k > 0$, resulting in a large positive non-flow at small N .
- $c_2\{4\}$, originating from TMC \oplus flow(v_2), qualitatively agrees with the observed sign change behavior of $c_2\{4\}$.

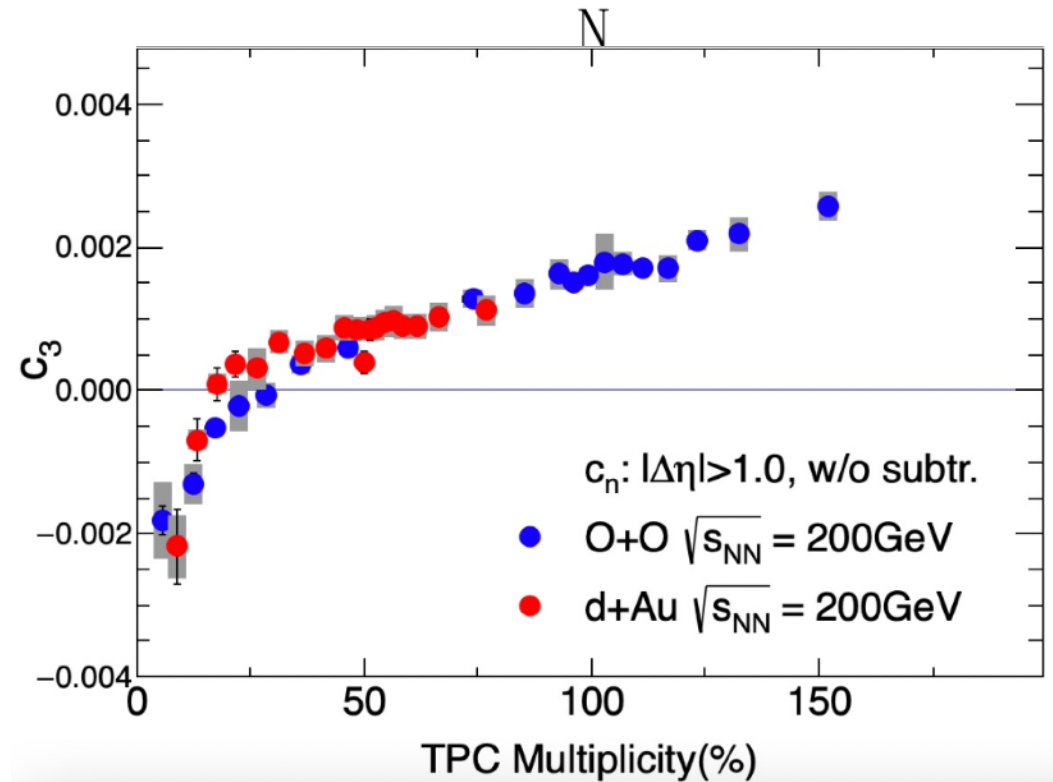
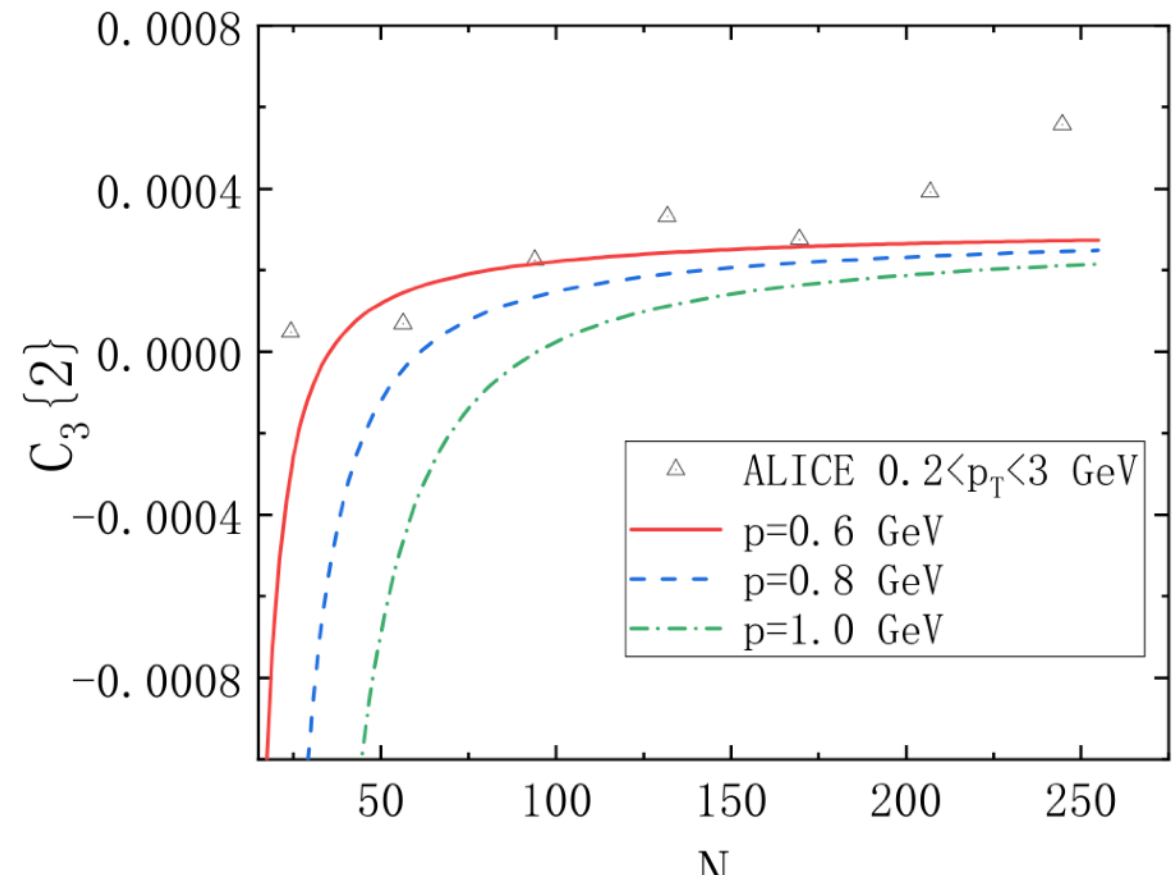
$c_3\{2\}$ from TMC+hydro-like flow

Mu-Ting Xie, Adam Bzdak and Guo-Liang Ma,
Phys. Rev. C 105, 054904 (2022)

TABLE I. The n th order $2k$ -particle cumulant $c_n\{2k\}$ from the global conservation of transverse momentum only.

n	$c_n\{2\}$	$c_n\{4\}$	$c_n\{6\}$	$c_n\{8\}$
2	$\frac{1}{2} \frac{p_1^2 p_2^2}{[(N-2)\langle p^2 \rangle_F]^2}$	$\frac{p_1^2 p_2^2 p_3^2 p_4^2}{[(N-4)\langle p^2 \rangle_F]^4}$	$6 \frac{p_1^2 p_2^2 \cdots p_6^2}{[(N-6)\langle p^2 \rangle_F]^6}$	$72 \frac{p_1^2 p_2^2 \cdots p_8^2}{[(N-8)\langle p^2 \rangle_F]^8}$
3	$-\frac{1}{6} \frac{p_1^3 p_2^3}{[(N-2)\langle p^2 \rangle_F]^3}$	$\frac{1}{2} \frac{p_1^3 p_2^3 p_3^3 p_4^3}{[(N-4)\langle p^2 \rangle_F]^6}$	$-7 \frac{p_1^3 p_2^3 \cdots p_6^3}{[(N-6)\langle p^2 \rangle_F]^9}$	$261 \frac{p_1^3 p_2^3 \cdots p_8^3}{[(N-8)\langle p^2 \rangle_F]^{12}}$
4	$\frac{1}{24} \frac{p_1^4 p_2^4}{[(N-2)\langle p^2 \rangle_F]^4}$	$\frac{17}{144} \frac{p_1^4 p_2^4 p_3^4 p_4^4}{[(N-4)\langle p^2 \rangle_F]^8}$	$\frac{709}{288} \frac{p_1^4 p_2^4 \cdots p_6^4}{[(N-6)\langle p^2 \rangle_F]^{12}}$	$\frac{54193}{288} \frac{p_1^4 p_2^4 \cdots p_8^4}{[(N-8)\langle p^2 \rangle_F]^{16}}$

- Transverse momentum conservation brings $c_3\{2\} \propto 1/N^3 < 0$, resulting in a negative non-flow to v_3 at small N .
- $c_3\{2\}$, originating from TMC \oplus flow, qualitatively agrees with the observed sign change behavior of $c_3\{2\}$.



Symmetric and asymmetric cumulants from TMC

$$sc_{2,4}\{4\} = \left\langle \left\langle e^{i2(\phi_1-\phi_2)+i4(\phi_3-\phi_4)} \right\rangle \right\rangle - \left\langle \left\langle e^{i2(\phi_1-\phi_2)} \right\rangle \right\rangle \left\langle \left\langle e^{i4(\phi_3-\phi_4)} \right\rangle \right\rangle \\ = \langle v_2^2 v_4^2 \rangle - \langle v_2^2 \rangle \langle v_4^2 \rangle$$

$$ac_2\{3\} = \left\langle \left\langle e^{i2(\phi_1+\phi_2-2\phi_3)} \right\rangle \right\rangle = \langle v_2^2 v_4 \cos 4(\Psi_2 - \Psi_4) \rangle$$

□ For 3-particle:

$$f(\vec{p}_1, \dots, \vec{p}_3) = f(\vec{p}_1) \cdots f(\vec{p}_3) \frac{N}{N-3} \exp\left(-\frac{p_1^2 + p_2^2 + p_3^2}{(N-3)\langle p^2 \rangle_F}\right) \exp(-\Phi)$$

where

$$\Phi = \frac{2}{(N-3)\langle p^2 \rangle_F} \sum_{i,j=1; i < j}^3 p_i p_j \cos(\phi_i - \phi_j)$$

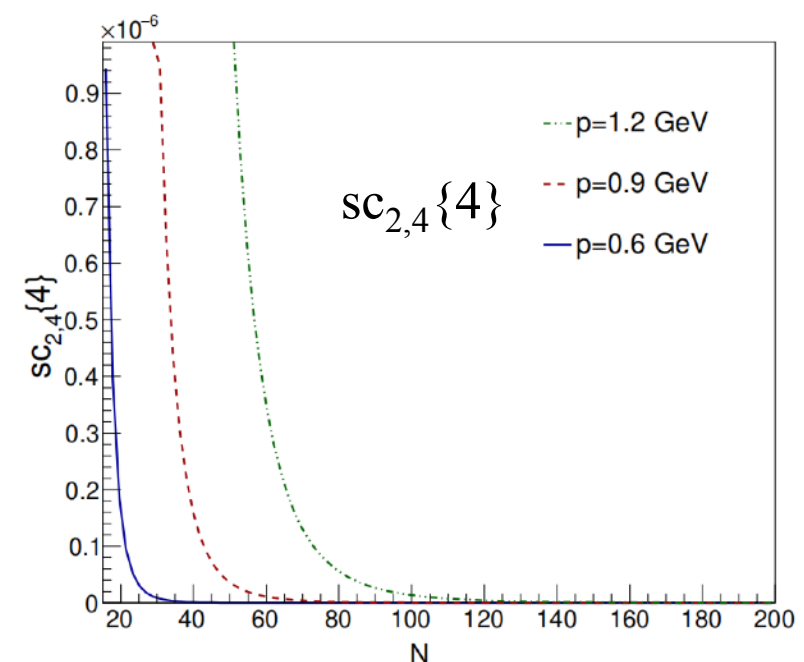
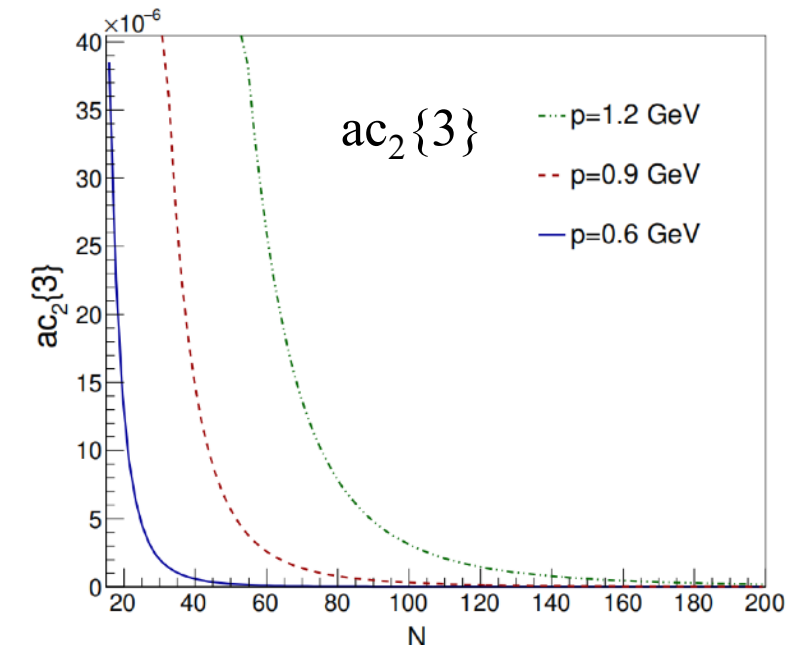
$$ac_2\{3\}|p = \frac{\int_0^{2\pi} e^{i2(\phi_1+\phi_2-2\phi_3)} \exp(-\Phi) d\phi_1 \cdots d\phi_4}{\int_0^{2\pi} \exp(-\Phi) d\phi_1 \cdots d\phi_4} \approx \frac{p^8}{4(N-3)^4 \langle p^2 \rangle_F^4}$$

□ For 4-particle:

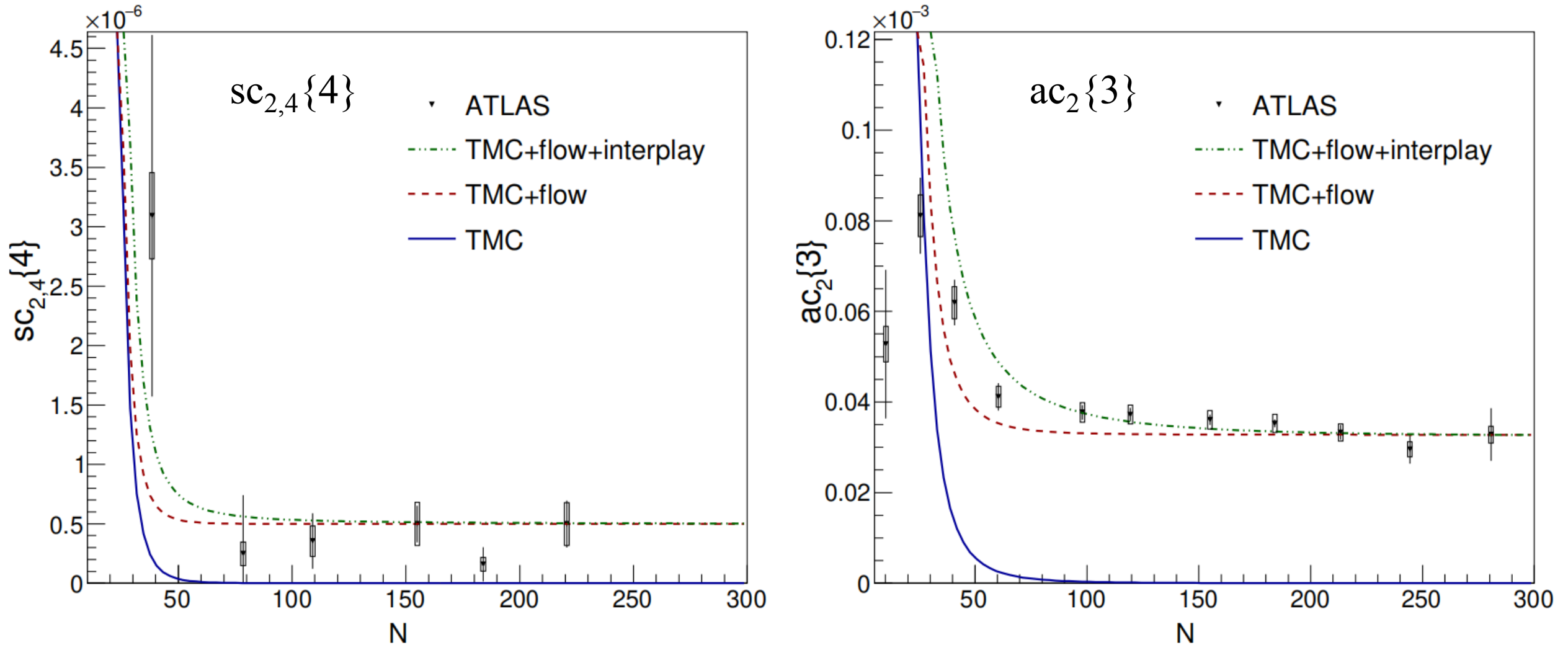
$$sc_{2,4}\{4\} = \left\langle e^{i2(\phi_1-\phi_2)+i4(\phi_3-\phi_4)} \right\rangle - \left\langle e^{i2(\phi_1-\phi_2)} \right\rangle \left\langle e^{i4(\phi_3-\phi_4)} \right\rangle \\ \approx \frac{5p^{12}}{16(N-4)^6 \langle p^2 \rangle_F^6} - \frac{p^{12}}{48(N-2)^6 \langle p^2 \rangle_F^6}$$

□ Decrease and tend to zero with increasing N and decreasing p

Jia-Lin Pei, Adam Bzdak and Guo-Liang Ma, Phys. Rev. C 110, 024901 (2024)



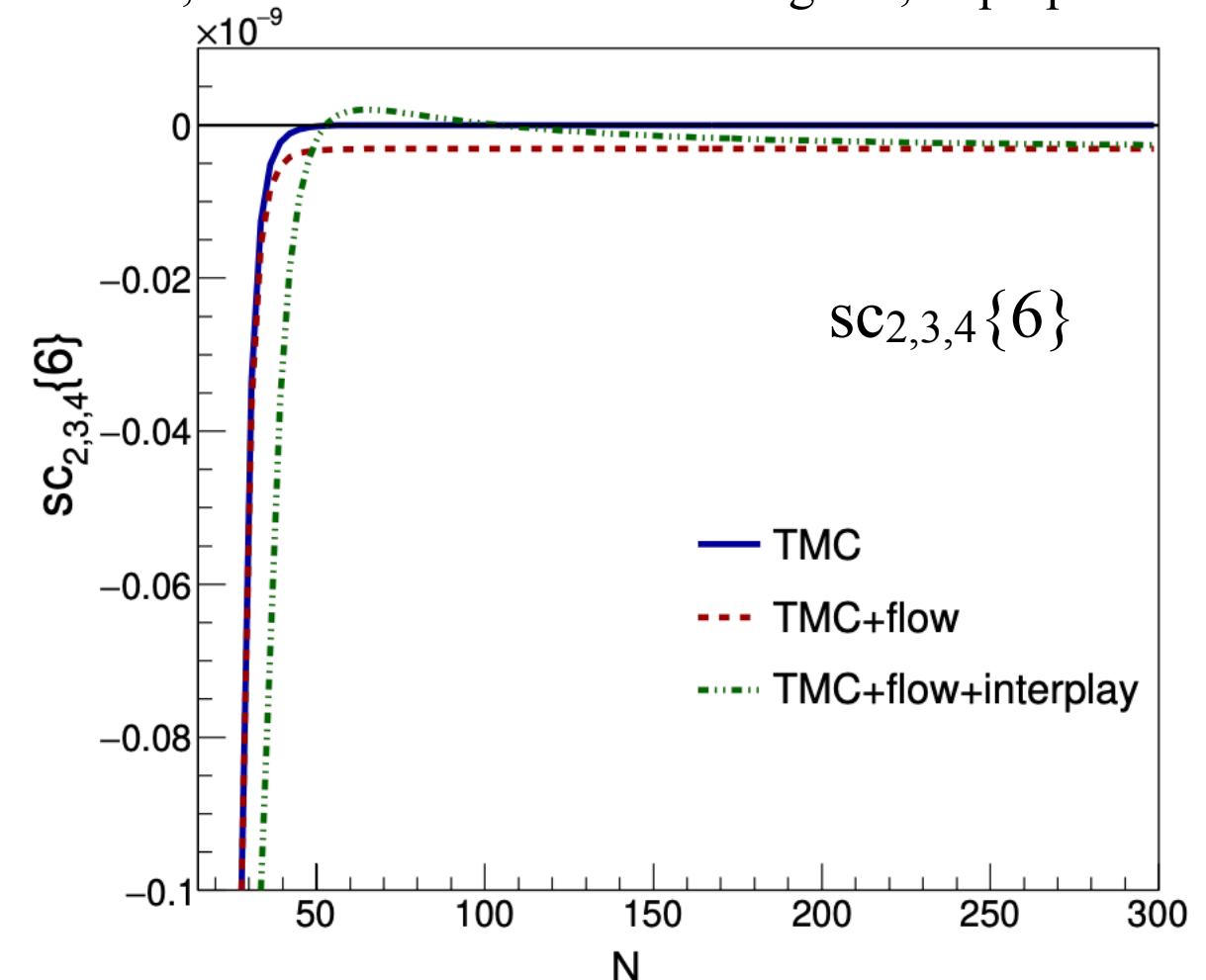
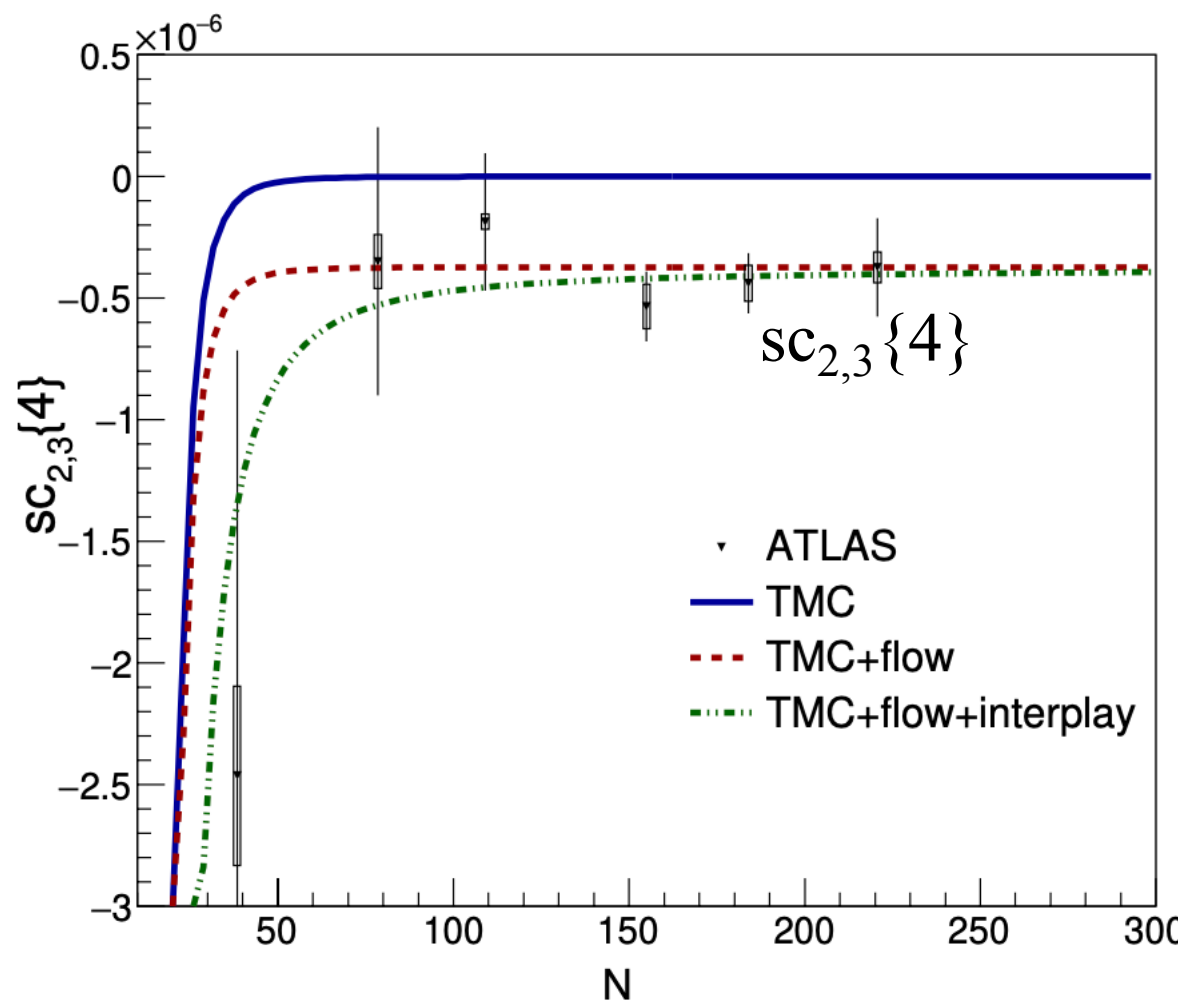
Symmetric and asymmetric cumulants from TMC and Flow



- Collective flow makes them higher
- The interplay is present when N is small, but almost negligible when N is large
- At small N , TMC dominates, and at large N , flow becomes significant

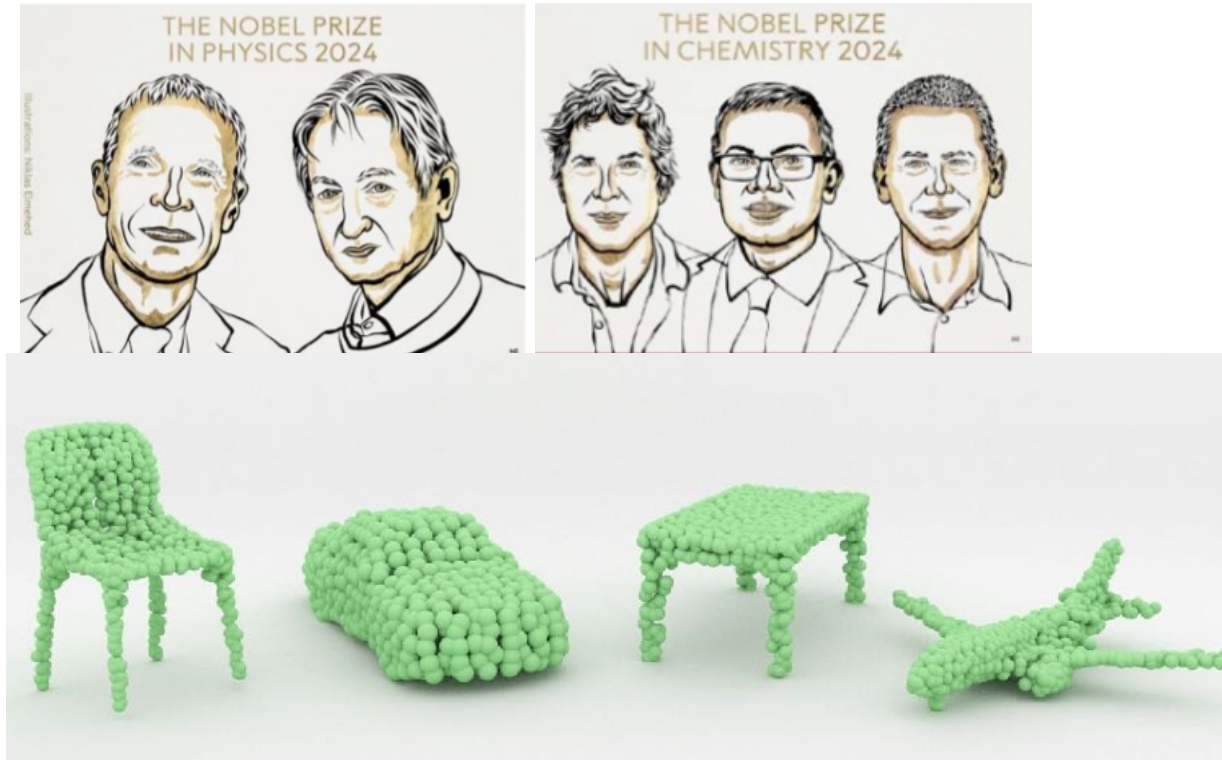
Symmetric and asymmetric cumulants from TMC and Flow

Jia-Lin Pei, Adam Bzdak and Guo-Liang Ma, in preparation



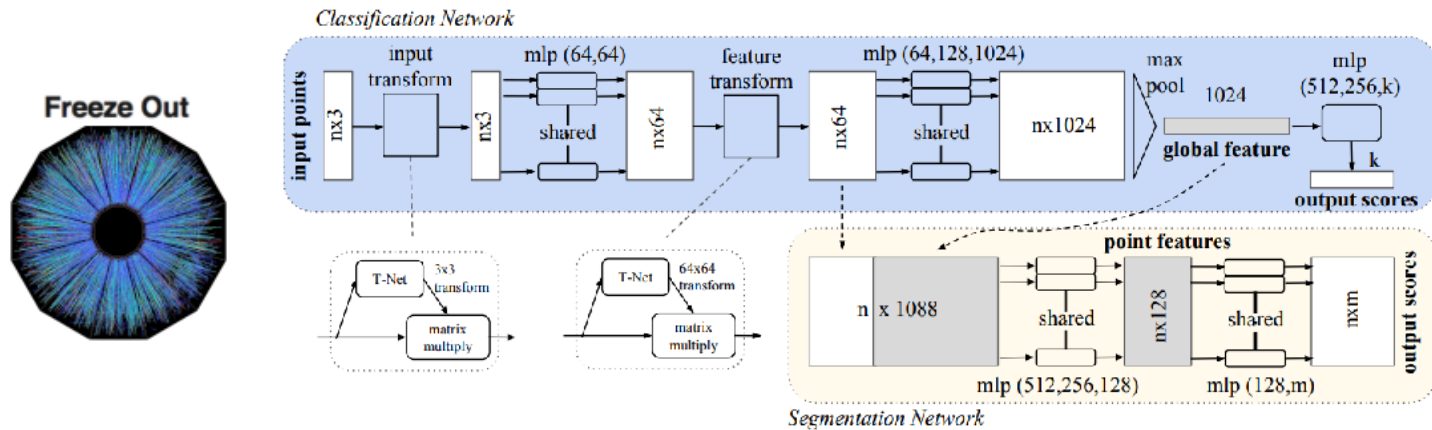
- Collective flow makes them lower
- The interplay is present when N is small, but almost negligible when N is large
- At small N , TMC dominates, and at large N , flow becomes significant

点云神经网络



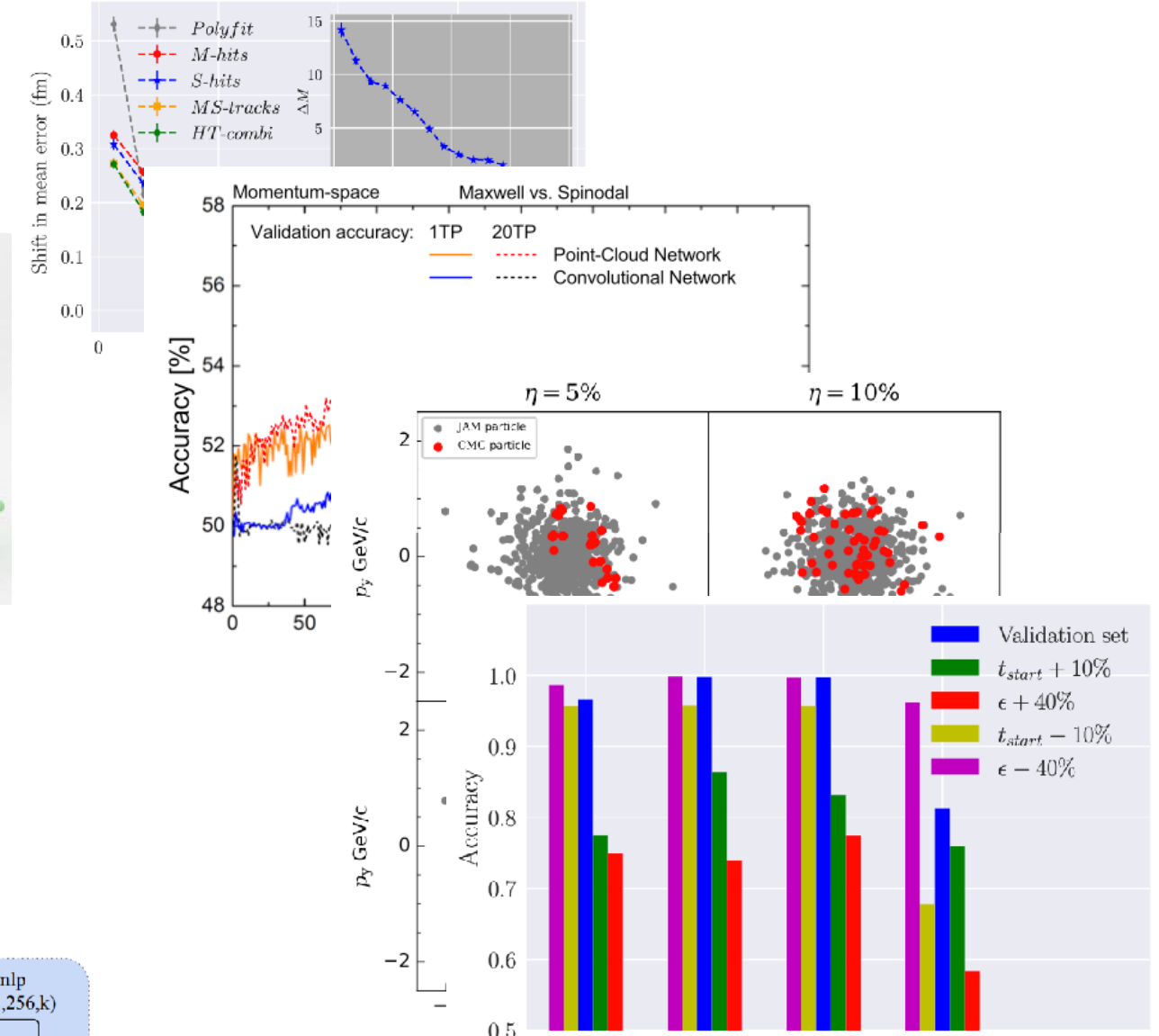
- Unordered
- Interaction among points
- Invariance under transformations

C. R. Qi, H. Su, K. Mo, and L. J. Guibas, arXiv:1612.00593, 2016.



Shuang Guo, Han-Sheng Wang, Kai Zhou, Guo-Liang Ma, Phys. Rev. C 110, 024910 (2024)

M. Omana Kuttan, et al, Phys. Lett. B 811, 135872 (2020),



M. Omana Kuttan, et al, Phys. Lett. B 811, 135872 (2020),
J. Steinheimer, et al, JHEP 12, 122 (2019),
Y. Huang, L.-G. Pang, X. Luo, and X.-N. Wang, Phys. Lett. B 827, 137001 (2022),
M. Omana Kuttan, ,et al, JHEP 21, 184 (2020),

模型数据类型特点

ampt.dat

Event#	Test#	Particle#	b(fm)	Npart1	Npart2						
1	1	4218	8.0000	84	84	2	82	1	83		
2112	0.000	0.000	99.996	0.940	6.00	-4.86	0.23	0.00			
2112	0.000	0.000	99.996	0.940	6.78	3.61	0.21	0.00			
2212	0.000	0.000	99.996	0.940	5.53	1.48	0.26	0.00			
2212	0.000	0.000	-99.996	0.940	-9.31	-2.75	-0.16	0.00			
111	0.071	-0.334	-0.376	0.135	1.81	-0.96	-1.18	7.00			

Diagram illustrating the structure of the ampt.dat file:

- Blue arrows point from the headers "Event#", "Test#", "Particle#", "b(fm)", "Npart1", and "Npart2" to their corresponding values in the data rows.
- Green arrows point from the labels "Particle ID (PYTHIA)", "Final momentum", "mass", and "Final position & time (at kinetic freeze-out)" to the columns 3, 4, 5, and 6 respectively.

将所有事件中的满足条件的粒子的动量集合为一个列表

$p_{1,x}$	$p_{1,y}$	$p_{1,z}$	E_1	$p_{2,x}$	$p_{2,y}$	$p_{2,z}$	E_2	$p_{N_{ch},x}$	$p_{N_{ch},y}$	$p_{N_{ch},z}$	$E_{N_{ch}}$
-----------	-----------	-----------	-------	-----------	-----------	-----------	-------	-------	----------------	----------------	----------------	--------------

机器学习数据变换

$p_{1,x}$	$p_{1,y}$	$p_{1,z}$	E_1	$p_{2,x}$	$p_{2,y}$	$p_{2,z}$	E_2	$p_{N_{ch},x}$	$p_{N_{ch},y}$	$p_{N_{ch},z}$	$E_{N_{ch}}$
-----------	-----------	-----------	-------	-----------	-----------	-----------	-------	-------	----------------	----------------	----------------	--------------

一维卷积

输入

1	2	3	4	5	6	7
---	---	---	---	---	---	---

卷积核

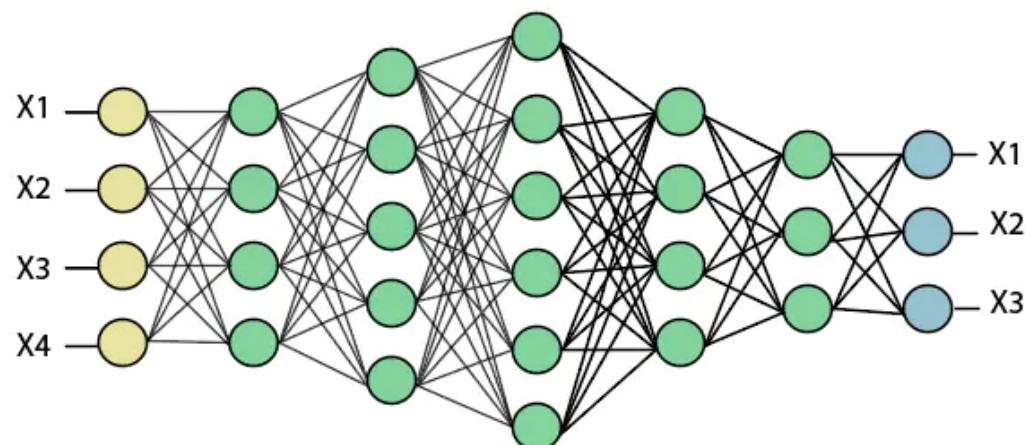
-1	2	1
----	---	---

输出

2	4	6	8	10
---	---	---	---	----

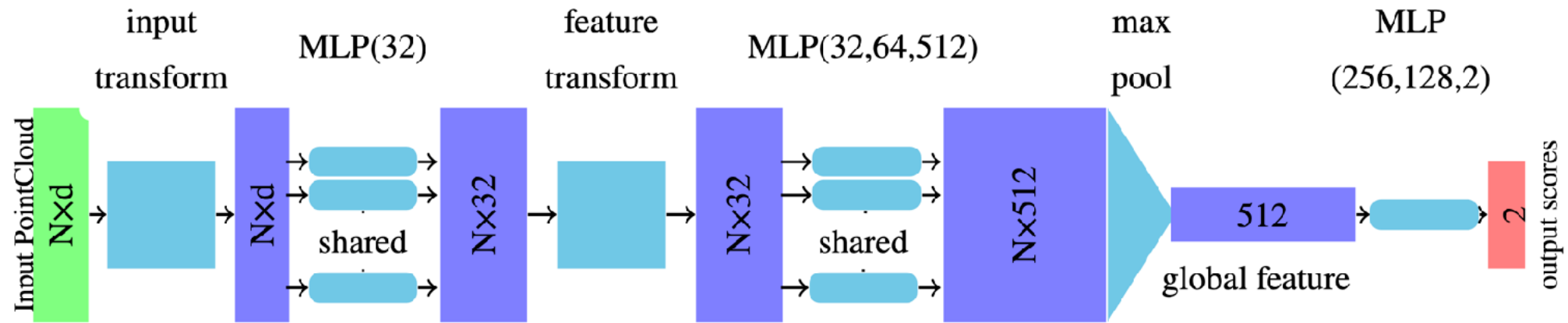
$$1 \times 1 + 2 \times 2 + 3 \times (-1) = 2$$

Fully Connected Layer

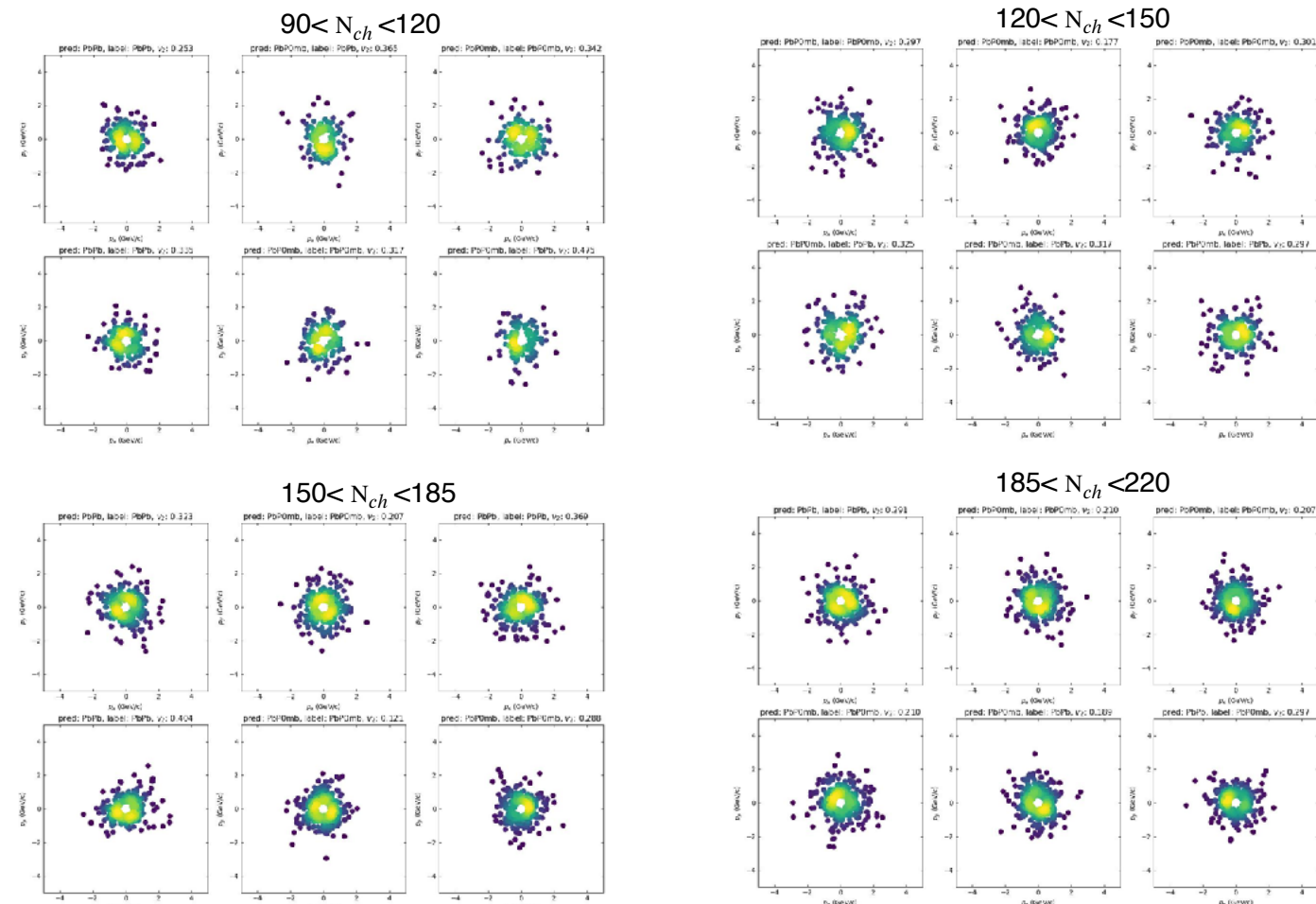
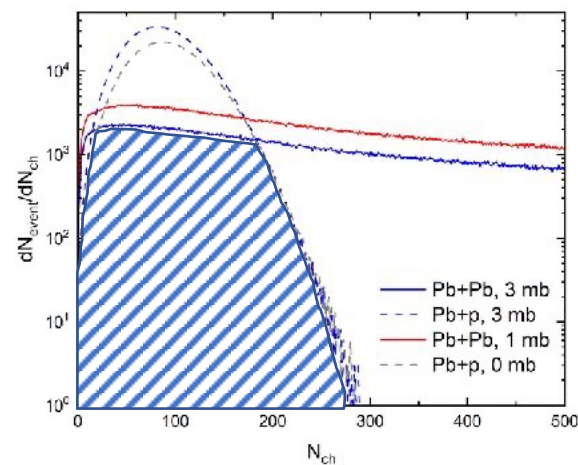


$$Y = W \cdot X + B$$

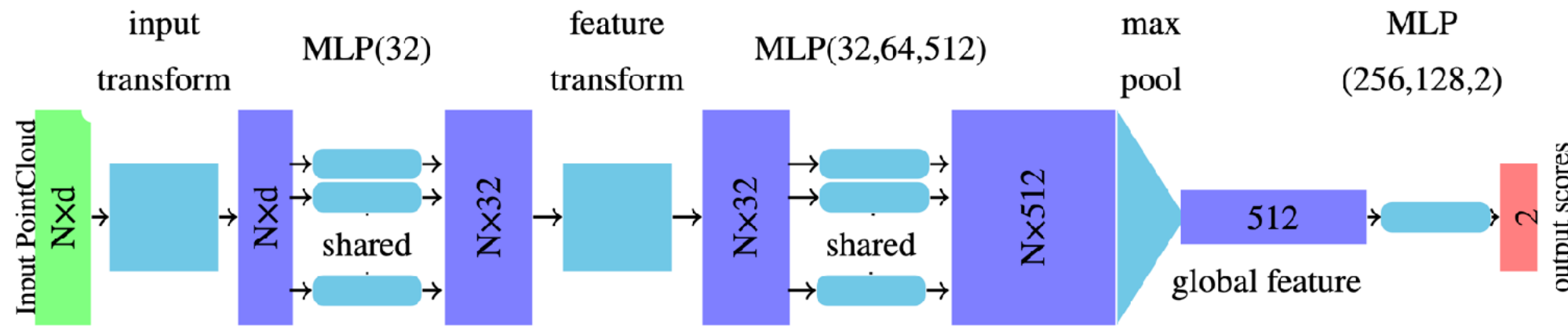
机器学习数据集



训练集/测试集=7/3，为了方便训练时两个系统每个多重数下都取相同事件数。



点云神经网络结构



定义一个模型：

```
model = keras.Model(inputs=inputs, outputs=outputs, name="pointnet")
```

定义一个训练过程：

```
model.compile()
```

损失函数：交叉熵
优化器
评估标准

$$\text{categorical_crossentropy}(y, \hat{y}) = - \sum_{i=1}^C y_i \log(\hat{y}_i)$$

0 log0 +1 log1

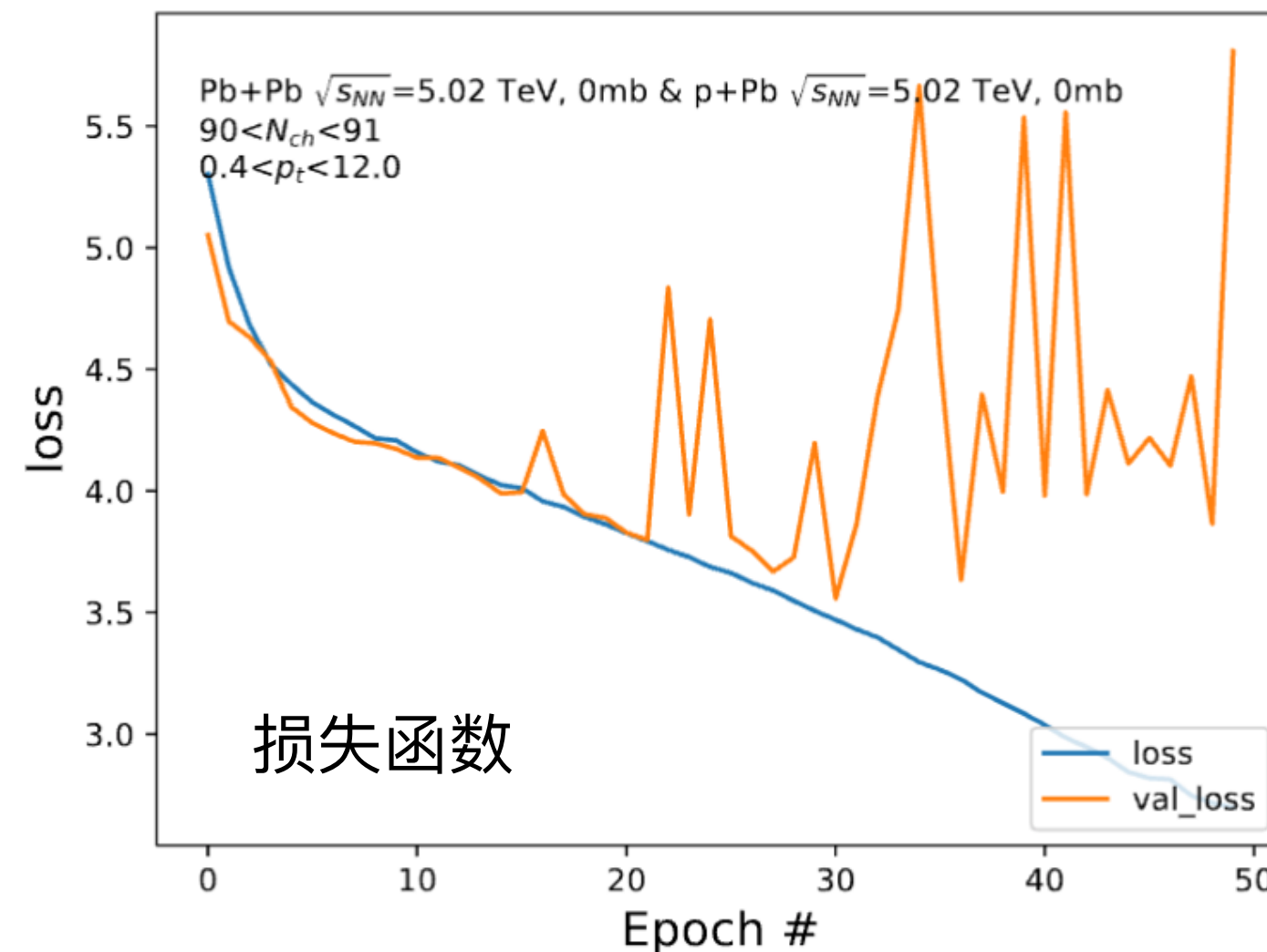
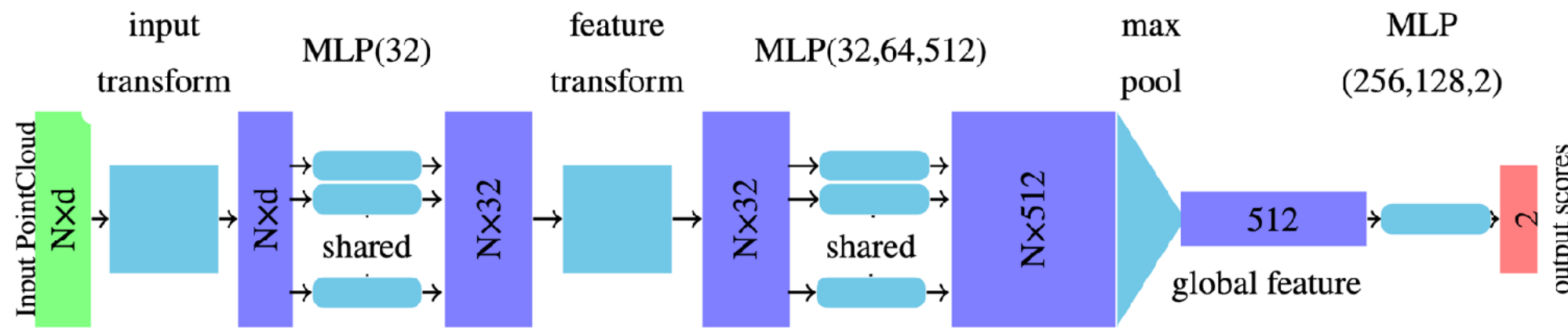
训练一个模型：

```
H=model.fit()
```

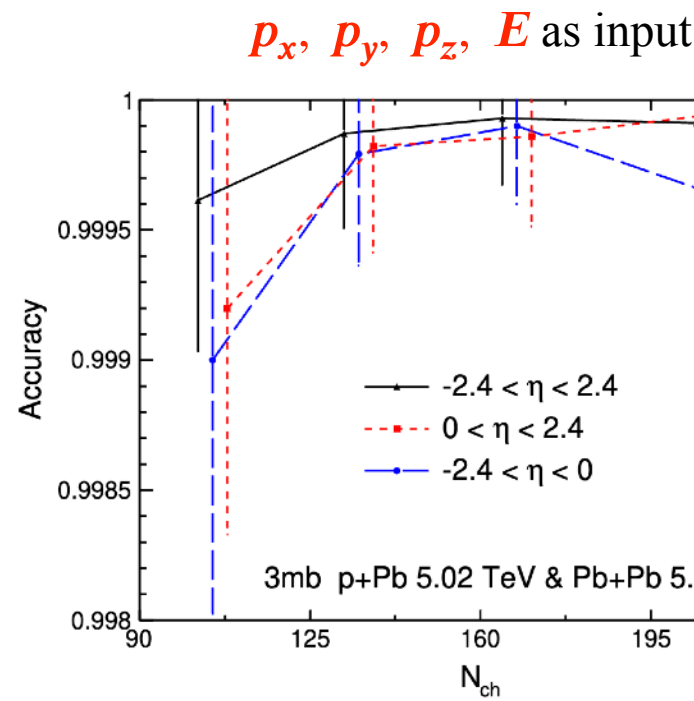
使用一个模型：

```
model.evaluate()
```

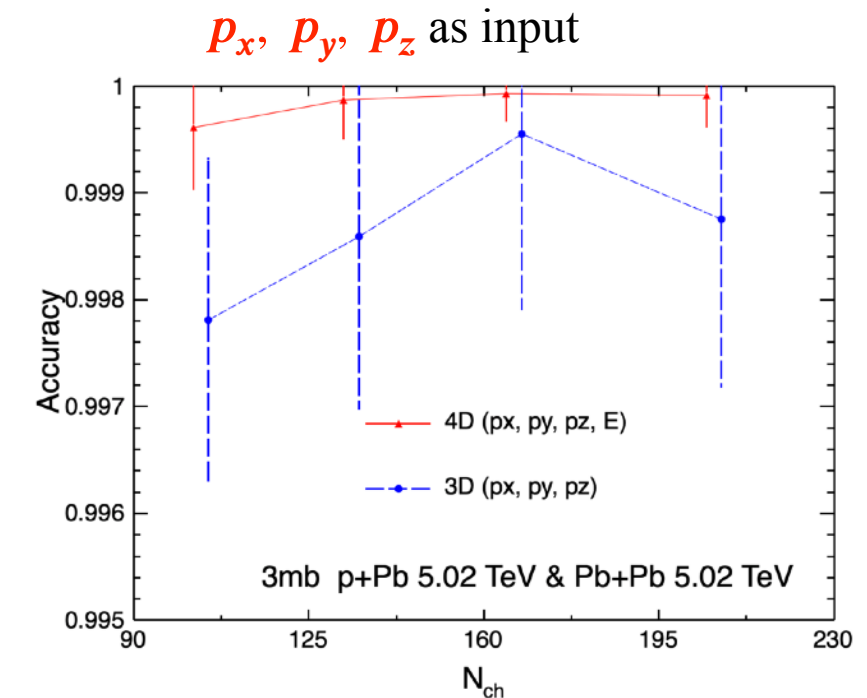
点云神经网络训练效果



机器学习3或4维动量

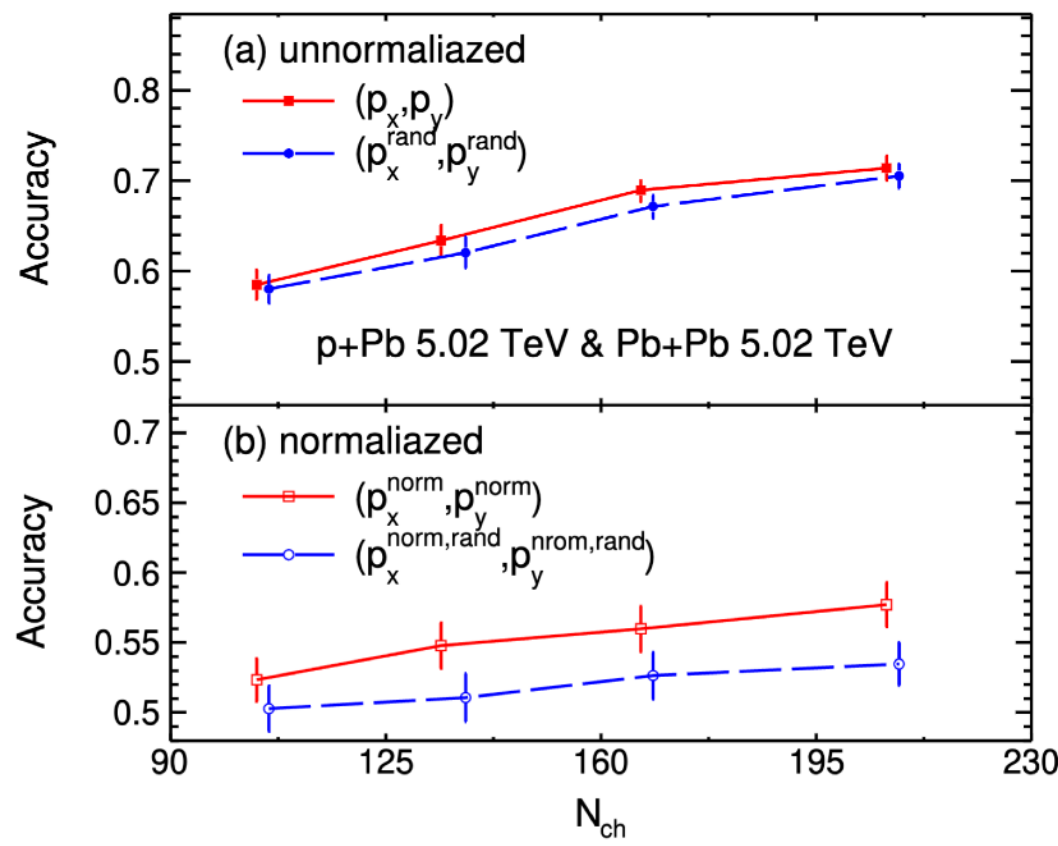


PCN can identify two systems
From what features?
Change different inputs
Remove or reduce some known features
Observe changes in accuracy
Infer which features the model has learned



- 使用 3 维或 4 维动量训练的 PCN 网络可以准确地区分这两种系统。为什么？

机器学习2维横动量



Eliminate the p_t value:

$$p_x^{norm} = \frac{p_x}{p_T}$$
$$p_y^{norm} = \frac{p_y}{p_T}$$

Eliminate azimuthal angle distribution:

$$p_x^{rand} = p_x \times \cos\phi_{rand} - p_y \times \sin\phi_{rand}$$

$$p_y^{rand} = p_x \times \sin\phi_{rand} - p_y \times \cos\phi_{rand}$$

$$p_x^{rand,norm} = \frac{(p_x \times \cos\phi_{rand} - p_y \times \sin\phi_{rand})}{p_T}$$
$$p_y^{rand,norm} = \frac{(p_z \times \sin\phi_{rand} - p_y \times \cos\phi_{rand})}{p_T}$$

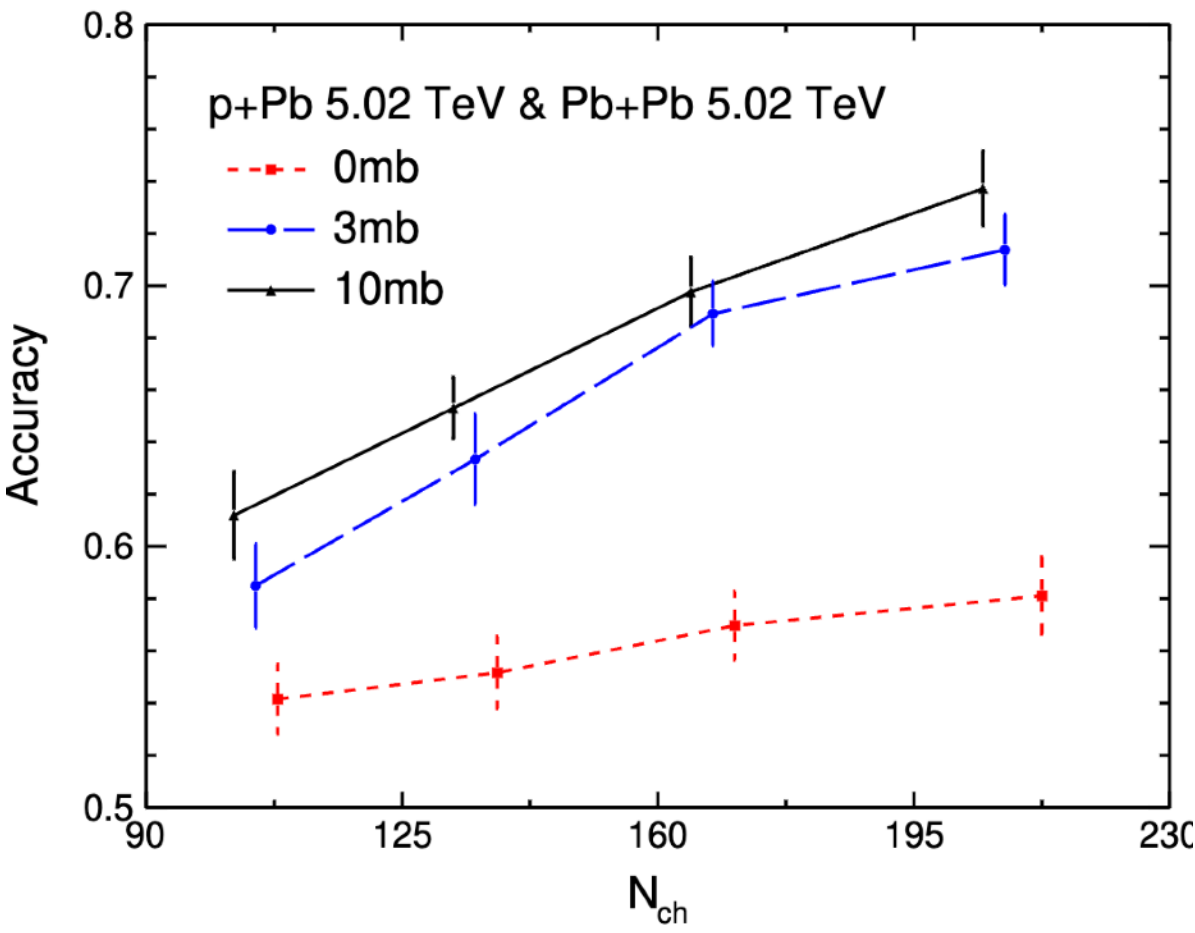
准确率：

- 从 3D 到 2D 后，陡降： p_z 起主要作用
- 随机旋转后，微降：集体流起极小作用
- 归一化后，再次陡降： p_T 起一定作用

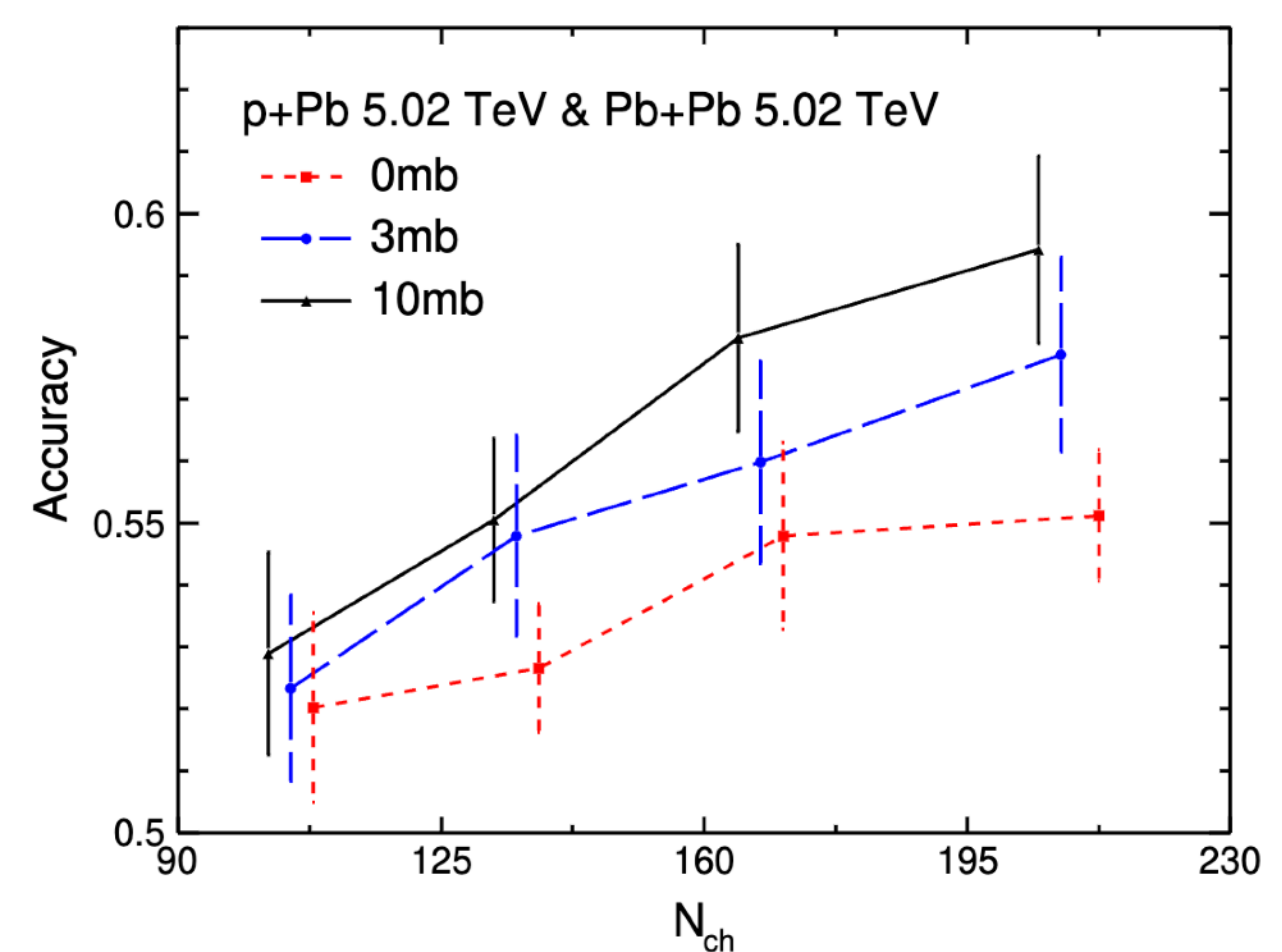
机器学习集体流

cross section of parton interaction → collective flow in different intensities

p_x, p_y as input

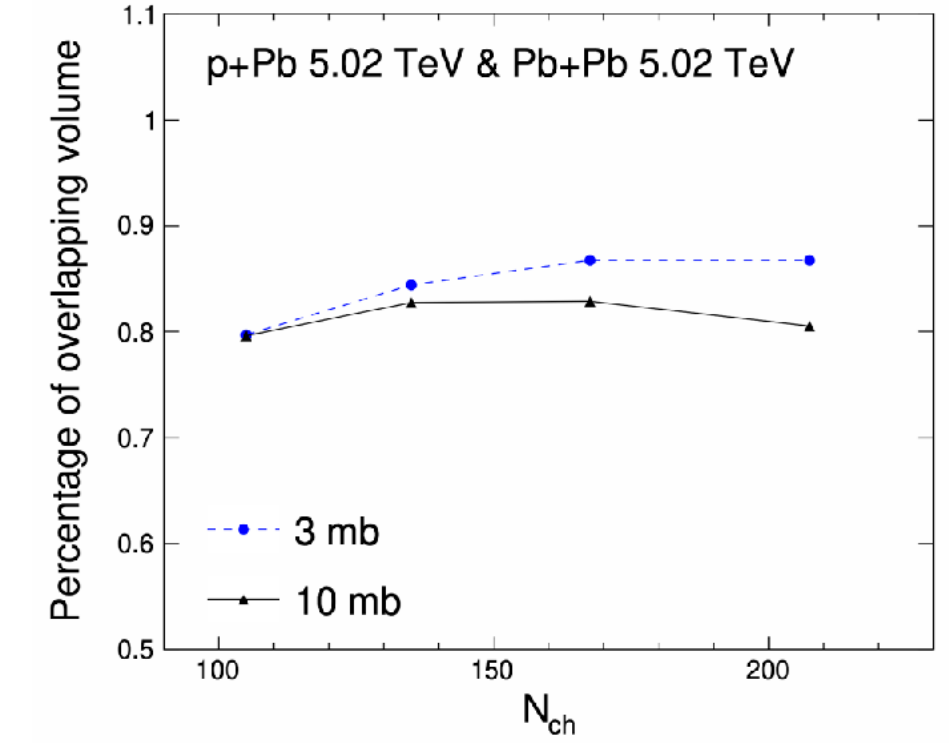
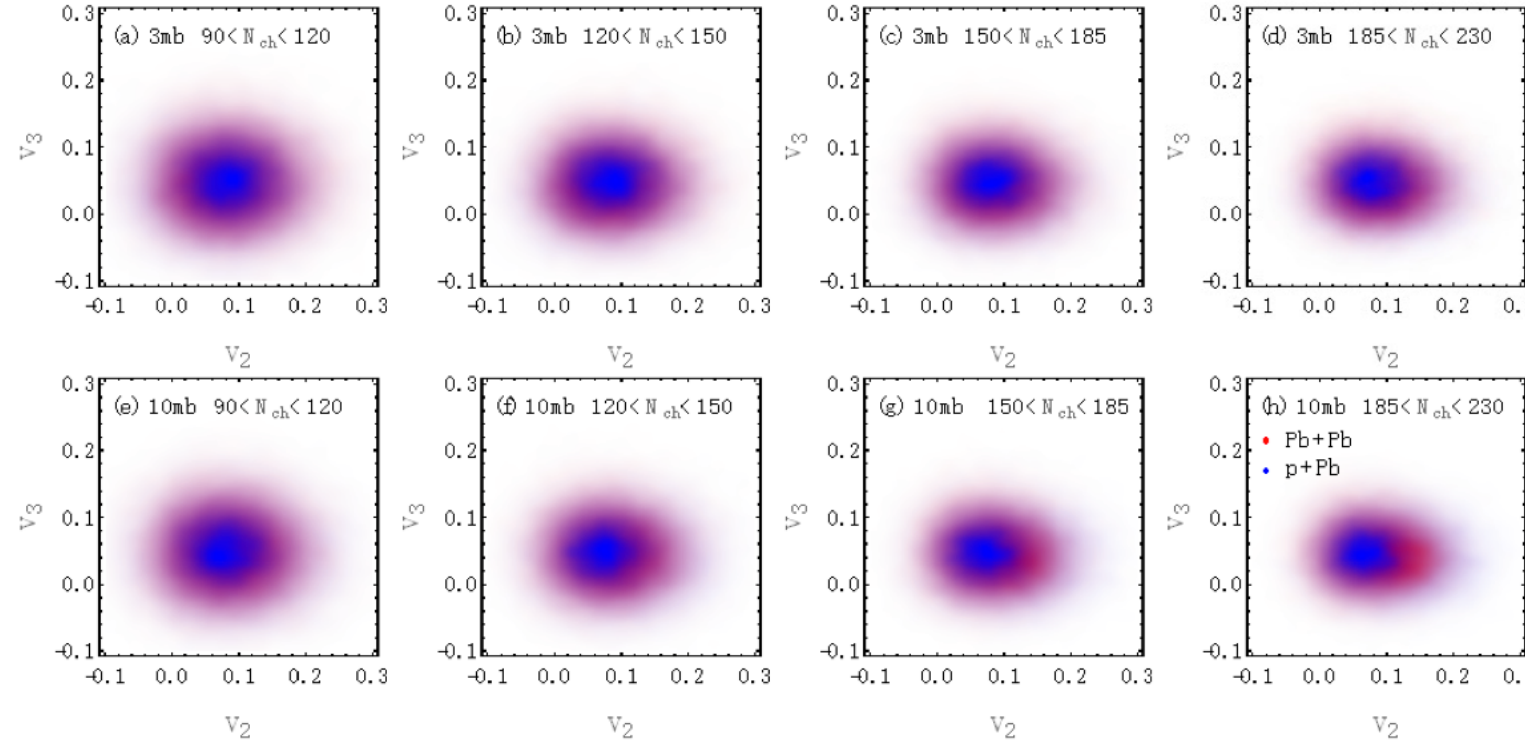


p_x^{norm}, p_y^{norm} as input



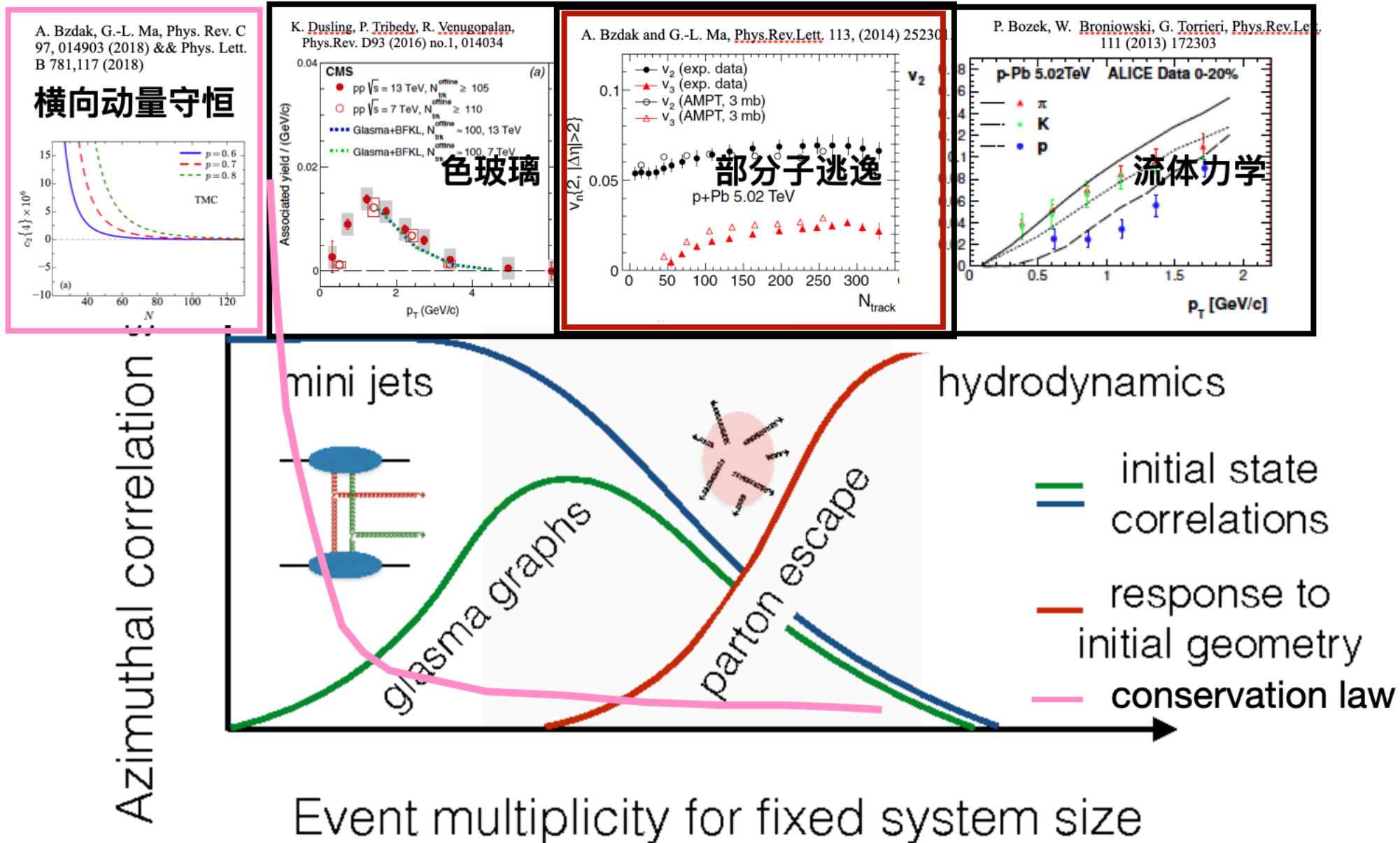
更大截面的预测准确率更高表明大集体流有助于提高准确率

机器学习集体流的难度



- 部分子散射截面越大，两个系统之间的 v_2 和 v_3 的差异越大
- 两系统间的 $P(v_2, v_3)$ 分布非常相似，以至于很难被点云神经网络识别

总结



- flow` = flow(escape ⊕ hydro ⊕ CGC) ⊕ non-flow(TMC+...)
- 输运模型+AI技术, 探索集体流产生之谜?

理论物理专款上海核物理研究中心



2023年4月14日，国家自然科学基金理论物理专款-上海核物理理论研究中心在复旦大学江湾校区交叉科学1号新楼启动揭牌，将为客座及青年学者来访、举办学术活动等提供优良会场和办公条件。欢迎您来交流访问！

谢谢！